

Monitoring and Control of the Cardiovascular System During Indoor Exercise

A thesis written by

Kaili Weng

under the supervision of

Dr. Steven Su

in fulfilment of the requirements of the degree of

Doctor of Philosophy

Faculty of Engineering and Information Technology

University of Technology Sydney, Australia

2012

CERTIFICATE OF AUTHORSHIP/ORIGINALITY

I certify that the work in this thesis has not previously been submitted for a degree nor has it been submitted as part of requirements for a degree except as fully acknowledged within the text.

I also certify that the thesis has been written by me. Any help that I have received in my research work and the preparation of the thesis itself has been acknowledged. In addition, I certify that all information sources and literature used are indicated in the thesis.

Production Note:

Signature removed prior to publication.

Kaili Weng

Abstract

The increase in obesity and diabetes is of great public health, social and economic concern worldwide. Modern treadmill systems can provide effective, safe and practical indoor exercise for the consumption of extra energy. However, an uncontrolled treadmill can cause excessive exertion on the cardiovascular system. To avoid excessive cardiovascular stress, an efficient way of monitoring and controlling of exercise strength is to regulate treadmill speed and/or gradient to stimulate the exerciser's heart rate following a predefined profile.

In this thesis, an automated treadmill system has been developed, which includes wireless portable ECG and tri-axial accelerometer sensors, and a Labview based control module. Based on this automated system, efficient rate detection techniques have been developed by using the pitch estimation method. Different types of multi-loop integral control configurations have been proposed and implemented to regulate the heart rate and/or step rate by manipulating treadmill speed and/or gradient. These control structures have been placed under real time testing which includes Single-Input Single-Output (SISO), Multiple-Input Single-Output (MISO) and Multiple-Input Multiple-Output (MIMO) control by using the established Labview module. It has been found that MISO control is the most efficient method, and would be effective in making the treadmill exercise more reliable and safer in rapidly tracking the heart rate profile to achieve desired exercising outcome. For this reason, this thesis also proposes the concept of Multi-loop Integral Controllability (MIC) and proves the existence of multi-loop integral controllers which can obtain unconditional multi-loop stability of the Two-Input Single-Output automated treadmill system.

The benefit of our automated control system includes assisting patients in post-cardiac attack rehabilitation and therapy to safely control the heart rate to follow a suitable profile. This reduces the need for supervision by medical professionals. Furthermore, in athletics and fitness applications, an automatic control system can allow users to optimize their training intensity.

Acknowledgements

First and foremost I would like to convey my many thanks to the remarkable people who provide support, motivation, knowledge, friendship and love on my journey to pursuit a Ph.D.

Special recognition must be given to my supervisor, Dr Steven Su for his expertise, supervision and unconditional encouragement throughout the course of this project. I am particularly grateful for his wisdom that has inspired me to be a life-long learner and a passionate seeker of knowledge, and for his always being the first subject to test our new setup instrumentations, even though some of them were quite tough. I thank him with the deepest of respect.

I would like to express tremendous gratitude towards my colleague Andrew Zhang for the great discussions about the research and help in many cases. I also acknowledge the support received by Sam Cheng and Sam Chui for taking time to give insights into my thesis, as well as give me some suggestions for the research.

I am indebted to all of the volunteer subjects, who have given their precious time to participate in the experiment and helped me to collect the data. Special thanks to Basil Turk and Luis Dolores who were always willing to help out when I needed subjects for testing.

I wish to acknowledge the important support from Australian Postgraduate Scholarship which enabled me to pursue my higher degree at University of Technology Sydney.

Finally and most importantly, I would like to thank my family - my mother Chunchun Zhang for her care and being backbone during this period of my life. Thanks also go to my relatives in China. Without their eternal love and support, I would not be who I am today.

Content

Abstract	i
Acknowledgements	ii
Contents	iii
List of Figures	viii
List of Tables	xii
Acronyms and Abbreviations	xiii
1. Introduction	1
1.1. HRC treadmill exercise	2
1.2. Research areas in HRC treadmill exercise development.....	3
1.3. Thesis objectives	4
1.4. Main contributions of the thesis	6
1.5. Publications	7
1.6. Structure of the thesis	8
2. Background	10
2.1. Regular physical activity	11
2.2. Cardiovascular physiology	12
2.2.1. Structure of the heart	12
2.2.2. Cardiac cycle	13
2.2.3. Electrocardiogram	14
2.3. Cardiovascular exercise.....	17
2.3.1. Cardiac rehabilitation	17
2.3.2. Fitness development.....	18

2.4. Walking pace.....	19
2.4.1. Step rate.....	20
2.5. Summary	21
3. Treadmill system design.....	23
3.1. Introduction	24
3.1.1. Trackmaster TMX425	25
3.1.2. National instruments Labview 8.6.....	26
3.1.3. Alive wireless monitor	26
3.1.4. ECG electrodes.....	28
3.1.5. Pedometers	29
3.1.6. Bluetooth	29
3.1.7. Serial protocol	30
3.2. Data acquisition VI.....	30
3.3. Communication protocol VI.....	32
3.3.1. Data transmission VI.....	33
3.3.2. Data storage VI.....	35
3.4. HR and SR signal detection.....	36
3.4.1. AMDF pitch detection algorithm	36
3.4.2. ACF pitch detection algorithm.	37
3.4.3. Detection methodology	38
3.4.4. Detection experimental results	41
3.5. Summary	43

4. Labview implementation.....	45
4.1. Introduction	46
4.2. Pan and Tompkins method.....	47
4.2.1. Band-pass filter.....	49
4.2.2. Derivative action.	50
4.2.3. Squaring.....	50
4.2.4. Moving window integrator.....	51
4.3. HR sensor	53
4.3.1. Peak detector block	53
4.3.2. BPM mean value block	55
4.4. SR sensor.....	57
4.4.1. SR sensor accuracy tests.....	60
4.5. Summary	62
5. Control configuration	64
5.1. PID control design introduction	65
5.1.1. Open loop modelling	66
5.2. Open loop HR response.....	67
5.2.1. HR open loop response with speed	67
5.2.2. HR open loop response with gradient	68
5.2.3. Open loop HR response discussion	68

5.3. Open loop SR response	69
5.3.1. SR open loop response with speed	69
5.3.2. SR open loop response with gradient	70
5.3.3. Open loop SR response discussion.....	71
5.4. Controller values	71
5.4.1. HR controller values.....	73
5.4.2. SR controller values	73
5.5. SISO modelling methodology	74
5.6. HR SISO control	76
5.6.1. HR SISO control with speed test results	77
5.6.2. HR SISO control with gradient test results	78
5.7. SR SISO control	79
5.7.1. SR SISO control with speed test results	79
5.7.2. SR SISO control with gradient test results.....	80
5.8. Summary	81
6. MISO control methodology	83
6.1. MISO control modelling	84
6.2. MISO control test results.....	86
6.3. SISO control and MISO control comparison	87

6.4. MISO control in exercise zones	88
6.4.1. Moderate Activity exercise zone	89
6.4.2. Weight control exercise zone	90
6.4.3. Aerobic cardio endurance exercise zone	92
6.5. Summary	94
7. MISO analysis.....	95
7.1. Introduction	96
7.2. Multi-loop integral controllability	97
7.2.1. Multi-loop integral controllability analysis for HR response.....	98
7.2.2. Experiment design.....	104
7.3. Illustrative simulation study	105
7.4. Summary	110
8. MIMO control methodology	112
8.1. MIMO control modelling	113
8.2. Test 1 results.....	115
8.3. Test 2 results.....	118
8.4. Summary	120
9. Conclusions and future work.....	122
9.1. Conclusions	123
9.2. Direction for future research	124
Bibliography	126

List of Figures

2.1:	The structure of the heart and its main components (Shirley, 2007).....	.13
2.2:	Chest leads: V1, V2, V3, V4, V5 and V6 (Shirley 2007)15
2.3:	Electrocardiogram (McGill, 2000)16
2.4:	Cardiovascular exercise (McGill, 2000).....	.17
3.1:	Hardware and software system design24
3.2:	Trackmaster FVX325 series treadmill.....	.25
3.3:	Alive technologies wireless monitor27
3.4:	The orientation of the x, y and z axes in build in Tri-Axial Accelerometer.....	.28
3.5:	ECG Electrodes28
3.6:	Pedometer29
3.7:	USB Bluetooth dongle.....	.29
3.8:	USB to RS-232 connector30
3.9:	ECG signal.....	.30
3.10:	Front panel of the treadmill initialisation31
3.11:	Block diagram of the data acquisition32
3.12:	Bluetooth open and close connection functions33
3.13:	Implementation of the open connection function33
3.14:	Packet layout from ECG alive technologies health monitor system33
3.15:	Verifying the validity of data packets.....	.34
3.16:	Separation of ECG and Accelerometer data.....	.34
3.17:	The data storage VI.....	.35
3.18:	Block diagram of the proposed approach.....	.39
3.19:	Description square wave matching approach39
3.20:	ECG signal with different thresholds40
3.21:	TA signal processing by using AMDF41
3.22:	TA signal processing by using ACF.....	.41

3.23:	Noise polluted TA signal processing by using $AMDF^2$42
3.24:	Noise polluted TA signal processing by using ACF^242
3.25:	Noise polluted TA signal processing by using $AMDF+ACF$42
3.26:	Heart rate detection.....	.43
4.1:	Sequence of events for the implementation of the HR detection VI.....	.46
4.2:	Communication to the Bluetooth protocol47
4.3:	Original ECG signal of a jogging test subject48
4.4:	Output from the band pass filter49
4.5:	Output from the derivative filter.....	.50
4.6:	Output from squaring operation50
4.7:	Output from moving window integrator.....	.51
4.8:	Example of the output of the moving window integrator.....	.52
4.9:	Pan and Tompkins method52
4.10:	Pan and Tompkins heart rate detection.....	.53
4.11:	Peak detector block.....	.54
4.12:	Peak detection.....	.54
4.13:	BPM testing55
4.14:	Mean value block.....	.56
4.15:	Comparison open loop BPM mean response vs. Instantaneous BPM.....	.57
4.16:	Overview of step rate sensor58
4.17:	Step rate sensor initialisation.....	.58
4.18:	Mean calculator in step rate sensor.....	.60
5.1:	HR open-loop response with speed67
5.2:	HR open-loop response with gradient68
5.3:	SR open-loop response with speed.....	.69
5.4:	SR open-loop response with gradient.....	.70
5.5:	SISO PI closed loop control using speed as controlling signal75

5.6:	Implementation of SISO PI controller in Labview.....	.75
5.7:	HR SISO control with speed control response77
5.8:	HR SISO control with gradient control response78
5.9:	SR SISO control with speed control response.....	.79
5.10:	SR SISO control with gradient control response.....	.80
6.1:	Block diagram of the MISO control system.....	.84
6.2:	Implementation of MISO controller in Labview.....	.85
6.3:	Comparison of SISO speed test with MISO control.....	.86
6.4:	Comparison of SISO gradient test with MISO control.....	.86
6.5:	SISO and MISO control comparison.....	.87
6.6:	Exercise zones for different exercise purpose88
6.7:	MISO control response in the warm up zone89
6.8:	MISO control - speed control effort in the warm up zone.....	.89
6.9:	MISO control - gradient control effort in the warm up zone.....	.90
6.10:	MISO control response in the weight control zone91
6.11:	MISO control - speed control effort in the weight control zone91
6.12:	MISO control - gradient control effort in the weight control zone ..	.91
6.13:	MISO control response in the areobic cardio endurance exercise zone.....	.92
6.14:	MISO control - speed control effort in the areobic cardio endurance exercise zone93
6.15:	MISO control - gradient control effort in the areobic cardio endurance exercise zone93
7.1:	Multi-loop integral controllability for a 2ISO system94
7.2:	The 2ISO Hammerstein system.....	.106
7.3:	Steady state response of heart rate.....	.107
7.4:	The function $u_1' = \phi(u_2')$108
7.5:	Simulation results - adjusting speed only109
7.6:	Simulation results - adjusting speed and gradient110

8.1:	The structure of the MIMO control113
8.2:	MIMO control - treadmill operating system.....	.114
8.3:	MIMO control - control algorithm115
8.4:	MIMO control test 1 - control response116
8.5:	MIMO control test 1 - HR controller control effort117
8.6:	MIMO control test 1 - SR controller control effort.....	.117
8.7:	MIMO control test 2 - control response119
8.8:	MIMO control test 2 - HR controller control effort120
8.9:	MIMO control test 2 - SR controller control effort.....	.120

List of Table

2.1:	Cardiac cycle of the human heart (Anonim 2000)14
3.1:	The treadmill specifications.....	.25
3.2:	The Alive wireless monitor specifications27
4.1:	Treadmill speed at 3km/h61
4.2:	Treadmill speed at 5km/h61
4.3:	Treadmill speed at 7km/h62
5.1:	Key open loop response parameters72
5.2:	Results of HR SISO control with speed77
5.3:	Results of HR SISO control with gradient78
5.4:	Results of SR SISO control with speed80
5.5:	Results of SR SISO control with gradient81
6.1:	SISO and MISO control comparison table87
6.2:	Performance results of MISO control in warm up zone90
6.3:	Performance results of MISO control in weight control exercise zone.....	.92
6.4:	Performance results of MISO control in aerobic cardio endurance zone93
7.1:	Subjects characteristics.....	.104
7.2:	Heart rate response at steady state105
8.1:	MIMO control test 1 HR controller performance.....	.116
8.2:	MIMO control test 1 SR controller performance116
8.3:	MIMO control test 2 HR controller performance.....	.119
8.4:	MIMO control test 2 SR controller performance119

Acronyms and Abbreviations

Units of Measure

hr	Hour(s)
km/h	Kilometres per hour
min	Minute(s)
m	Meter
sec	Second(s)

Acronyms

2ISO	Two Inputs and Single Output
ACF	Autocorrelation Function
AMDF	Average Magnitude Difference Function
BPM	Beats Per Minute
DAQ	Data Acquisition
DIC	Decentralized Integral Controllability
DUS	Decentralized Unconditional Stability
ECG	Electrocardiograph
GAS	Globally Asymptotically Stable
GUI	Graphical User Interface
HR	Heart Rate
HRC	Heart Rate Controlled
K_p	Proportional Gain
K_i	Integral Gain
K_d	Derivative Gain
LES	Locally Exponentially Stable
MISO	Multi-Input Single-Output

MIMO	Multi-Input Multi-Output
MIC	Multi-loop Integral Controllability
NI	National Instruments
PC	Personal Computer
PID	Proportional Integral Derivative
PPM	Paces per Minute
RMS	Root Mean Square
SISO	Single-Input Single-Output
SPM	Steps per Minute
SR	Step Rate
TA	Tri-axial Accelerometer
UTS	University of Technology Sydney
VI	Virtual Instrument

Chapter 1

Introduction

Regular exercises and physical activity is beneficial for long-term health and well-being. Treadmill exercise is a great way to maintain the human body and enhancing cardiovascular health. It helps to increase blood circulation, body temperature and improve the health of the heart. To obtain a positive outcome from treadmill exercise, a currently used method is to monitor and regulate exercise intensity (measured by a portable wireless heart rate sensor) throughout treadmill exercise. This will ensure that people are exercising within their personal heart rate training zones and hence achieving maximum efficiency. An overview of the research is given in this chapter.

In Section 1.1, a brief history of heart rate controlled (HRC) treadmill exercise is provided. Sections 1.2 and 1.3 introduce the research areas in the context of treadmill use, the focus of the thesis. Section 1.4 summarizes the main contributions of the research. Publications reporting this work are listed in Section 1.5. Finally, the structure of the thesis is given in section 1.6.

1.1. HRC treadmill exercise

In the rehabilitation area, HRC treadmill exercise is usually considered one of the most popular methods in examining cardiovascular condition. In cardiovascular training, it has been shown to be safe and effective regardless of the stage of stroke recovery in a supervised treadmill walking exercise program (Bouchard 1994). On the other hand, for fitness training, monitoring heart rate (HR) has been recommended by selecting appropriate intensities of treadmill exercise to improve or maintain the cardio respiratory fitness (ACSM 2000).

Over the last several decades, many efforts have been made in HRC treadmill exercise development. In 1952, Dr. Robert Bruce at University of Washington applied treadmill technology to his evaluation of patients' cardiovascular condition, monitoring their heart rates through an escalating series of treadmill exercises. This can be considered as the first major development in the HRC treadmill exercise field (Rose 2011). Medical treadmills are designed to be active measuring devices, of which one of the functions is to measure the HR of the subject. When a treadmill is connected to interface with an electrocardiograph (ECG) or ergospirometry or blood pressure monitor (BPM), it can become a new medical system (e.g. stress test system or cardiopulmonary rehab system) and measure the subject's ECG, breath volumes, blood pressure, muscle activity and various other vital functions.

A HR monitor is an important part of HRC treadmill exercise. The convenience of a treadmill HR monitor allows the user to gain a real time measurement of their heart beat. Users can accurately gauge the intensity of the workload. For optimal cardiovascular fitness, the exerciser should exercise within 50 to 75 percent of exerciser's maximum HR, as recommended by the University of Maryland Medical Center (Rogers 2011). An early development for the HR wireless monitor was made for the Finnish National Cross Country Ski team in 1977. The ECG signal can be a simple radio pulse or a unique coded signal from the chest strap (Mary 2011). Nowadays, HR monitors are becoming more portable and practical for HRC treadmill exercise.

Because of the shrinking size requirements of chip-based memory, most modern HR monitors also record HR workout data and allow users to transfer their information to software in order to track performance throughout the course of the routine and compare it to previous treadmill training sessions. The latest developed technologies, such as the Alive technologies, produces a wireless health monitoring system for screening, diagnosis and management of chronic diseases, and for consumer health and fitness. Applications include the management of atrial fibrillation and heart failure, cardiac rehabilitation and fitness monitoring (Alive 2008). Based on the real time feedback on intensity and performance, it also can be easily applied to the HRC treadmill exercise to transmit ECG and accelerometer data to customized programs in the computer or mobile phone.

1.2 Research areas in HRC treadmill exercise development

It has been pointed out in (Su 2005) that commercial treadmills are already available which offer HRC modules. However, these normally use very simple control strategies, their control performance is poor and they have no mechanism for setting a desired HR profile. Therefore, it is important to design exercise protocols for patients with cardiovascular disease, training protocols for athletes and more efficient weight loss protocols for the obese, and rehabilitation exercises to aid patients recovering from cardiothoracic surgery.

An early development for the HRC treadmill exercise in (Saito 1991) has shown that HRC treadmill exercise test is an effective method of examining circulatory and respiratory functions under load. There are many different protocols by which the workload is increased gradually or in a stepwise manner by varying the walking speed and/or the slope. Previously, no exercise workload protocol could generate a reproducible linear increase in HR. In order to increase the effectiveness and safety of treadmill exercise, the authors attempted to control workload and realize a linear increase in heart rate. They found that a workload protocol, in which walking speed

is increased logarithmically, satisfied this requirement (Saito 1992). In Janos' study (Porszasz 2003), a novel approach is explained for applying an increase in work rate on the treadmill to yield a protocol equivalent to that which continues to be widely used for clinical-diagnostic purposes. The linearly increasing work rate profile is achieved by a linear increase in walking speed. The time course of treadmill inclination is also calculated to provide a linear increase in work rate.

A control of the Hammerstein system (Bernotéas 1986) is designed for the approximated linear model to achieve robust tracking performance. This approach is applied to the design of a computer-controlled treadmill system for the regulation of HR during treadmill exercise. Minimizing deviations of the heart rate from a preset profile is achieved by controlling the speed of the treadmill. Both conventional Proportional Integral Derivative (PID) control and the hammerstein model have been employed for the controller design to estimate the HR tracking performance (Su 2006). Recently, in a control design for tracking HR during treadmill exercise based on a nonlinear exercise HR model, an output feedback tracking controller was constructed by using the guaranteed cost control technique, and is researched by (Cheng 2008).

1.3 Thesis objectives

The aim of this research is to develop an automated treadmill system for the purpose of safe training and rehabilitation exercises. This is achieved by monitoring and control of simple physiological parameters such as HR and body movement signals such as step rate (SR) of the individual exercisers. We have established control-oriented models for HR and SR for the regulation of treadmill exercises. These identified models will provide a better understanding of the human cardiovascular system response to exercise and have been incorporated in the control system design.

This thesis focuses on the speed and gradient of the treadmill. In particular, it develops an automated treadmill system, wireless communication and control module which can monitor the automatic regulation of exercise intensity by manipulating treadmill speed and gradient. In addition, reliable and efficient rate detection approaches and Pan Tompkins QRS detection technique have been designed for HR and SR detection. This module is for the implementation of feedback control of cardio-respiratory responses to treadmill exercises. Finally, all detection approaches and control algorithms are integrated into a Labview based system which enables designers to test HR and SR related to the treadmill speed and gradient.

The whole Labview based system consists of a treadmill system module, wireless communication module, HR and SR detector module with noise filtering functions and controller module, which needs to be robust enough to achieve stable results from dynamic performance. In this case, important variables are required to be controlled strictly. Firstly, the HR and SR detector must minimise random noise, which can result in faulty analysis of the body's condition and can cause injuries when jogging on the treadmill. On the other hand, the controller should produce minimum overshoots and a fast rise time is always an essential requirement for control systems for these variables. In addition, robustness to uncertainties is required to overcome the nonlinearities, disturbance, and model errors.

The response of the treadmill is determined by the HR and SR when exerciser is jogging. To understand this relationship, comprehensive real time investigation of applying different control approaches for the regulation of HR and SR is required. Given the reference HR and SR, control parameters and the treadmill configuration, this model of system will manipulate the treadmill's speed and gradient automatically in SISO, MISO and MIMO control structures to achieve desired HR and/or SR.

1.4. Main contributions of the thesis

The highlights of the main contributions of this thesis are the development of efficient control methods for the regulation of treadmill exercises. These include both rate detection and multivariable control to increase the value of the treadmill efficiency. The main contributions of this thesis are as follows:

- **Rate detection:** The aim of rate detection is to design proper approaches for SR and HR signals respectively. For the detection of HR and SR, this study developed a novel rate detection approach based on pitch estimation method. The pitch estimation has two types, the integral type and differential type. It is found that the integral type approaches (the short-time average magnitude difference function (AMDF) and short-term autocorrelation function (ACF)) are particularly suitable for SR signal detection. The differential type approaches are found to be very efficient for HR signal detection.
- **MISO control in treadmill:** In this thesis, the multi-loop integral controller is designed to simultaneously adjust both the treadmill speed and its gradient in order to fast track a designed HR profile. As far as the author is aware, there is no report for such a closed loop configuration for HR tracking in literature. It is found that MISO control is very effective for fast tracking the HR profile and produces better results than when only speed or gradient are used individually to track the HR. We believe the newly developed system can improve both effectiveness and flexibility of treadmill exercises.
- **MIMO control in treadmill:** The aim of the MIMO control is to automatically adjust the treadmill's speed and gradient simultaneously to control both HR and SR to maintain the rates at reference levels. This work is partly based on the system developed for MISO control. For MIMO control configuration, the final aim is to synchronize HR and SR, which has been reported to improve

performance for the training of athletes. Despite the novel concept, the MIMO controller produced an acceptable performance in this study, and is still under the improvement at this stage.

- **Nonlinear multi-loop integral controllability:** In this thesis, it has been experimentally demonstrated that using two actuators and multi-loop control structure for the control of single output variable has great potential to handle system failures so as to improve the reliability of treadmill based training and rehabilitation. This thesis provides theoretical analyses to show the benefits of using redundant actuators based on the examination of the steady state characteristics of heart rate response. It extends nonlinear Decentralized Integral Controllability (DIC) analysis to the non-square process, and provides sufficient condition for heart rate tracking under multi-loop integral control. This is the most significant contribution of this thesis.

1.5. Publications

Paper published:

Kaili Weng, Nghia Nguyen, Hung T.Nguyen, and Steven Su, "Rate estimation for the monitoring of rehabilitation exercises," *the 31st IEEE Engineering in Medicine and Biology Society*, Minneapolis, USA, pp 6267-6270, Sep 3-6, 2009.

Kaili Weng, Basil Turk, Louis Dolores, Tuan N. Nguyen, Branko Celler, Steven Su, and Hung T.Nguyen" Fast tracking of a given heart rate profile in treadmill exercise," *the 32nd IEEE Engineering in Medicine and Biology Society*, Buenos Aires, Argentina, pp 2569-2572, Aug. 31-Sep. 4, 2010.

Kaili Weng, Yi Zhang, Tuan N. Nguyen, Azzam Haddad, Branko Celler, Steven Su, Ying Guo, and Hung Nguyen, "Multi-loop integral control by using redundant control inputs for passive fault tolerant implementation," *the 2nd International*

Conference on Measurement and Control Engineering, Puerto Rico, USA, pp C004-C009, October 22-23, 2011.

Felician More, Kaili Weng, Mclean Peter, Su Steven, “Analysis of nonlinear and linear behaviors of heart rate for running exercise,” *the 4th IEEE Conference on Industrial Electronics and Applications*, Xi’an, China, pp 3920-3925, May 25-27, 2009.

Steven W. Su, H Nguyen, R Jarman, Joe Zhu, D Lowe, P McLean, S Huang, N T. Nguyen, R Nicholson, and Kaili Weng, “Model Predictive Control of Gantry Crane with Input Nonlinearity Compensation,” *the IEEE International conference on Control Automation and Systems Engineering*, Bangalore, India, pp 312-316, Aug. 22-25, 2009.

Paper submitted:

Kaili Weng, Yi Zhang, Tuan N. Nguyen, Ying Guo, Branko G. Celler, Steven W. Su, and Hung T. Nguyen, “Reliable heart rate regulation for treadmill exercise by manipulating both speed and gradient,” will be submitted for a journal.

1.6. Structure of the thesis

The thesis is made up of five main parts.

Part I introduces the general background of the research and literature review in the related research areas. Chapter 2 gives a brief introduction of cardiovascular and exercise physiology. The main methods of measuring HR and the SR are also described. The literature that provides the motivation for this research is reviewed and the approach to complete this study have been shown in the related chapters.

Part II encompasses the design and analysis of the measurement system. Chapter 3 describes the details of system hardware and software design. In order to better understand the measurement system and gauge the accuracy of the results, the rate detection method is implemented. The reliable HR and SR detection results can be found in the experiment. Chapter 4 develops a Labview program based on Pan-Tompkins method to filter the Electrocardiogram (ECG) data from a wireless ECG Monitor. This program can also obtain ECG and Tri-axial Accelerometer (TA) signals by using Bluetooth wireless communication.

Part III provides a detailed description of the system modelling, controller design and experiments of simple control algorithms. Chapter 5 provides the results of the open loop experiment for HR and SR controllers, which determined the initial values of K_p and K_i , the methodology of SISO control that includes the four experiments: HR control with speed (SISO control of HR by manipulating treadmill speed), HR control with gradient, SR control with speed and SR control with gradient have been tested in this chapter.

Part IV highlights the multivariable control in treadmill exercise. Chapter 6 discusses a new and efficient MISO (speed and gradient as inputs and HR as an output) control method. The MISO design is implemented by incorporating two SISO control systems to adjust either the treadmill speed or its gradient automatically in order to achieve a desired HR. The MISO control in different exercise zones have also analysed. Chapter 7 analyses the possibility of using a multi-loop integral controller to unconditionally stabilize the system from nonlinear control point of view. Chapter 8 introduces the MIMO control to regulate HR and SR by adjusting treadmill's speed and gradient simultaneously.

Part V summarises the whole research findings. It also provides recommendations for further research in Chapter 9.

Chapter 2

Background

This chapter presents the relevant background of cardiovascular exercise. The key concept is the exercise physiological basis of HR and SR. Secondly, a broad overview of walking pace is explained. In the available literature, there are not many discoveries regarding estimation of SR. By analysing SR, we can be better understand the regulation of treadmill exercises. This chapter is organised as follows. Section 2.1 investigates the importance of regular physical activity. Cardiovascular Physiology is explained in Section 2.2. The Cardiac Rehabilitation and Fitness Development designed for Cardiovascular Exercise in Section 2.3. The studies of walking pace will be introduced in Section 2.4.

2.1. Regular physical activity

Regular physical activity is undertaken by many people in the community and for many reasons. The purpose of physical activity is to improve their health and fitness. One the other hand, regular physical activity is an important part of effective weight loss and weight maintenance. It also can help prevent several diseases and improve the overall health. Studies show that even the most inactive people can gain significant health benefits if they accumulate 30 minutes or more of physical activity per day. Based on these findings, the U.S. Public Health Service has identified increased physical activity as a priority in (Healthy People 2020).

The research has shown that regular physical activity can significantly reduce the risk for several diseases and conditions, and improve the overall quality of life. Meanwhile, regular physical activity also help people to prevent from the following health problems (Niddk 2010):

- Heart Disease and Stroke. Daily physical activity can help prevent heart disease and stroke by strengthening your heart muscle, lowering your blood pressure, raising your high-density lipoprotein (HDL) levels (good cholesterol) and lowering low-density lipoprotein (LDL) levels (bad cholesterol), improving blood flow, and increasing your heart's working capacity.
- High Blood Pressure. Regular physical activity can reduce blood pressure in those with high blood pressure levels. Physical activity also reduces body fatness, which is associated with high blood pressure.
- No insulin-Dependent Diabetes. By reducing body fatness, physical activity can help to prevent and control this type of diabetes.
- Obesity. Physical activity helps to reduce body fat by building or preserving muscle mass and improving the body's ability to use calories. When physical activity is combined with proper nutrition, it can help control weight and prevent obesity, a major risk factor for many diseases.

- **Back Pain.** By increasing muscle strength and endurance and improving flexibility and posture, regular exercise helps to prevent back pain.
- **Osteoporosis.** Regular treadmill exercise promotes bone formation and may prevent many forms of bone loss associated with aging.

The health benefits gained from moderate physical activity are significant, especially for improving an individual's cardiovascular fitness. The Australian Institute of Health and Welfare reported in the year 1999 that an estimated physical inactivity in adult Australians is responsible for 7% of the total burden of all the diseases in Australia. With the greatest health problem in Australia being cardiovascular disease, representing 36% of all deaths and more deaths than any other disease, promoting physical activity could not be more important (Mathers 1999).

2.2. Cardiovascular physiology

The cardiovascular system can be thought of as the transport system of the body. This system has three main components: the heart, the blood vessels and the blood itself. The heart is the system's pump and the blood vessels are like the delivery routes. The following information describes the structure and function of the heart and the cardiovascular system as a whole.

2.2.1. Structure of the heart

Figure 2.1 presents a general diagram of the structure of the human heart. The human heart is composed mainly of four chambers. The upper chambers are called the atria, while the lower chambers are called the ventricles. The upper and lower atria and ventricles are separated by valves to prevent blood from backflow. The Tricuspid valve separates the right atrium from the right ventricle, while the Mitral valve separates the left atrium from the left ventricle (Hic 2011).

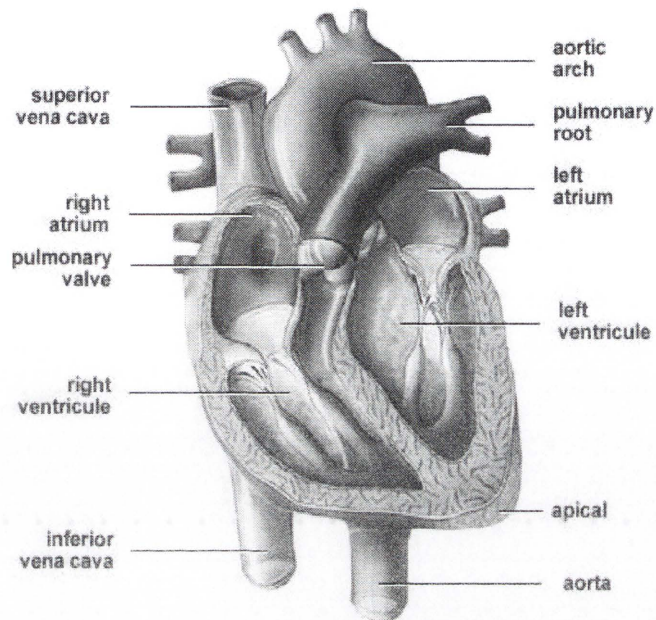


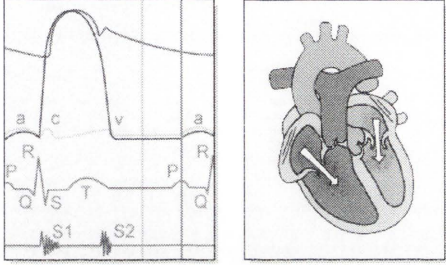
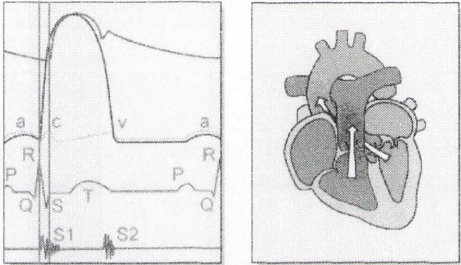
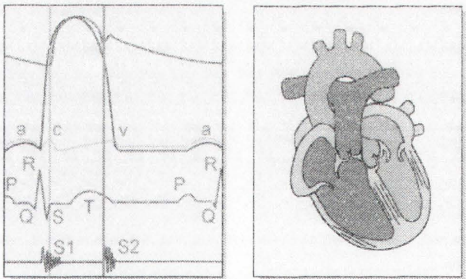
Figure 2.1 The structure of the heart and its main components (Shirley, 2007)

The pulmonary root separates the two vascular systems in left and right sections (left and right are referenced on human body orientation). The right section of the heart is fed by the superior and inferior vena cava, while the aorta is the main medium of delivering clean blood to the rest of the body. The pulmonary valve is in charge of preventing backflow to the right section of the heart, while the aortic valve prevents backflow to the left chambers (Jones 2007).

2.2.2. Cardiac cycle

The following table and diagrams present the sequence of events of the cardiac cycle in the human body. The three section of the graph indicate the period of duration of ventricular systole, while the turquoise section indicates the diastole duration.

Table 2.1 Cardiac cycle of the human heart (Anonim 2000)

Event	Description
<p style="text-align: center;">Ventricular Diastole</p>  <p style="text-align: center;">Atrial Systole</p>	<ul style="list-style-type: none"> • Blood flows from the superior and inferior vena cava. • Both atria contract, Tricuspid and Mitral valves open. • Blood flows from atria to ventricles
<p style="text-align: center;">Ventricular Systole</p>  <p style="text-align: center;">Atrial Diastole</p>	<ul style="list-style-type: none"> • Atria relax. • Right ventricle contracts, sending blood through the pulmonary veins to the lungs. • Right atrium contracts sending clean blood through the aorta to the rest of the body. • Tricuspid and Mitral valves close. • Pulmonary and Aortic valves open
<p style="text-align: center;">Ventricular Systole – Diastole</p>  <p style="text-align: center;">Aortic & Pulmonic Valves Close/Isovolumic Relaxation</p>	<ul style="list-style-type: none"> • All muscles in the heart relax • Pulmonary and Aortic valves shut • Cycle starts again

2.2.3. Electrocardiogram

The ability of heart is to generate an electric signal to pump blood into the human body. This natural signal has become a very important signal in order to determine the level of heart healthiness amongst patients. The signal's characteristics can be

used to monitor closely the steps of the heart beat and therefore isolate the stage where the heart is not performing appropriately.

An ECG is a medical test that records the heart electrical activity. With each beat, the electric current produced by the “pacemaker” signals travels. In order to detect a display these signals, special sensors called electrodes are placed in several positions in order to detect a variety of difference of potentials (Jones 2007). The performance of ECG has made possible to monitor the heart activity and physical conditions of patients worldwide. A standard medical ECG exam is performed with 12 leads; the placement configuration is shown in Figure 2.2 below. However, acquiring the heart signal is possible with as few as 6, 3, or 2 leads. In this project a 2-lead configuration is used. Electrodes are placed in locations V1 and V2 depicted.

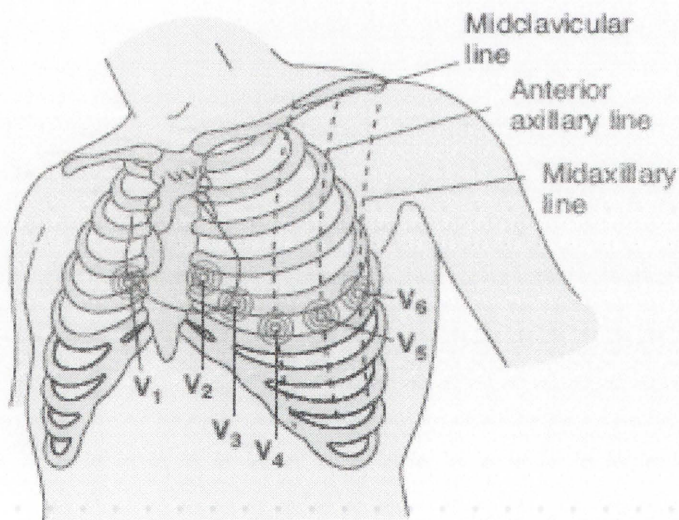


Figure 2.2 Chest leads: V1, V2, V3, V4, V5 and V6 (Shirley, 2007)

The ECG is composed of waves and complexes. Waves and complexes in the normal sinus rhythm are the P wave, PR interval, PR segment, QRS complex, ST segment, QT interval and T wave are shown in Figure 2.3.

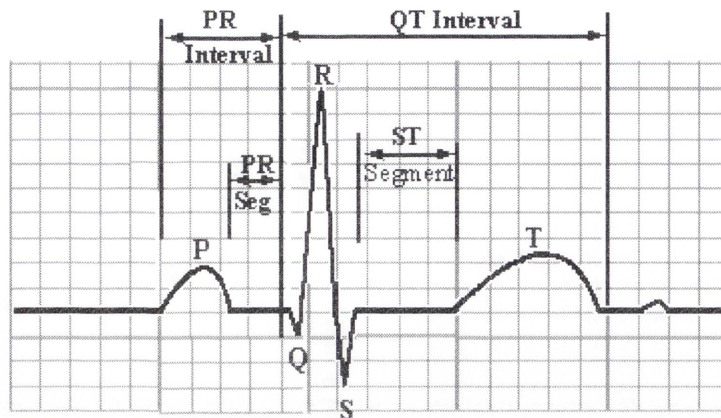


Figure 2.3 Electrocardiogram (McGill, 2000)

The P wave is caused by atrial depolarization. It is usually smooth and positive. Its duration is normally less than 0.12 sec.

The PR interval is the portion of the ECG wave from the beginning of the P wave (onset of atrial depolarization) to the beginning of the QRS complex (onset of ventricular depolarization). It is around 0.12 sec - 0.20 sec.

The PR segment is the portion on the ECG wave from the end of the P wave to the beginning of the QRS complex. The PR segment corresponds to the time between the ends of atrial depolarization to the onset of ventricular depolarization. It is an isoelectric segment, during which the impulse travels from the AV node through the conducting tissue (bundle branches, and Purkinje fibres) towards the ventricles.

The QRS complex represents the time it takes for depolarization of the ventricles. The normal QRS interval range is from 0.04 sec - 0.12 sec measured from the first deflection to the end of the QRS complex.

The ST segment represents the period of ventricular muscle contraction before repolarization. It is normally isoelectric (no electrical activity is recorded). However, the ventricles are contracting.

The QT interval begins at the onset of the QRS complex and to the end of the T wave. It represents the time of ventricular depolarization until ventricular repolarization. The T wave is normally rounded and positive due to ventricular repolarization.

2.3. Cardiovascular exercise

Both cardiac rehabilitation and fitness development program include counselling to help people achieve lifestyle changes (give up smoking, lose weight, change diet, learn to reduce stress, cope with depression, anger and stress during recovery). It provides support and training to help people manage their personal heart condition. It also includes supervised and monitored treadmill sessions to improve the patient's cardiovascular fitness.



Figure 2.4 Cardiovascular exercise (McGill, 2000)

2.3.1. Cardiac rehabilitation

Today, exercise-based cardiac rehabilitation has been shown to provide a 20-24%

reduction in cardiovascular mortality and has now become the 'standard of care' within the medical community by which a broad spectrum of patients are restored to their optimum physical, medical and psychosocial status after an acute cardiac event (Franklin 1998).

A concept called 'target HR' has been developed in treating cardiac patients where they are prescribed a target HR and are able to exercise or perform physical activities up to the target HR. (Franklin 1998) outlines that this concept has important advantages for controlling the exercise intensity. This is due to the built-in regulator for changes in fitness. As the patient becomes more fit over time they are able to increase the walking speed of a treadmill without an increase in their HR. As a result, the target HR set originally that is achievable at a lower level of effort is only achievable through greater exertion.

(Hiatt 1994) observed that treadmill is superior to strength training, as strength training did not increase walking time to claudication onset and resulted in a lower improvement in peak walking time. Furthermore, previous research has shown that combining treadmill and strength training does not result in larger improvements than treadmill training alone. According to (Kraus 2007), treadmill walking protocols, with and without an inclined treadmill, and stair climbing protocols have very similar values for onset of claudication, time to maximal claudication pain. Both constant-intensity protocols and graded exercise tests, where the intensity is progressively increased through increases in treadmill speed and/or grade, have been utilized for this population.

2.3.2. Fitness development

HR has traditionally been used to prescribe appropriate intensities of aerobic exercise for individuals exercising to improve or maintain cardio respiratory fitness. Based on the results of an exercise test, the American College of Sports Medicine (ACSM 2000) recommends that exercise intensity be defined as a percentage of HR reserve

or maximal HR. Target HR zones are used to assure an appropriate and safe exercise intensity.

The main aim of fitness development is to improve cardiovascular fitness and upgrade performance. A fitness development that lacks high intensity training will not improve aerobic fitness (Gilman 1996). Therefore, the essential part of any fitness coaching program is to be able to monitor the intensity of exercise at which the athlete trained (Stannard 1998). According to (King 1996):

Maximal Heart Rate = $220 - \text{age}$

Resting Heart Rate = Standing Resting Heart Rate

Maximal Heart Rate – Resting Heart Rate = Heart Rate Reserve

Heart Rate Reserve x (50% to 85%) + Resting Heart Rate = Target Heart Rate

This general guideline would be used as reference to set up the personal target HR. It not only applies to the cardio training subjects, but also provides information in calculating the formula for the weight control subjects and the maximum effort subjects.

2.4. Walking pace

Walking is a form of locomotion used by humans, where the legs move similar to a double pendulum in which a leg leaves the ground, moves forward swinging from the hip, resumes contact with the ground at the heel and as the body moves forward the toes resume contact with the ground. This is one step in walking, the other leg then moves forward in the same motion beyond the original leg and then the process repeats. The rate at which a person walks is termed walking pace. By monitoring the walking pace of an exerciser; the intensity of the exercise is able to be determined.

In a study assessing the impact of exercise and the risk of coronary heart disease among men, researchers found that men who train with weights, jog or row show the most significantly reduced risk of chronic heart disease compared to those who do not do those forms of exercise (Tanasescu 2002).

In assessing the walking pace, the study found that men who walked at a quick pace were found to have an 18% reduction in risk of chronic heart disease compared to non-walkers. Overall it is found that walking pace is independent of the hours spent walking had an important impact on reducing the risk of chronic heart disease (Hu 2002).

2.4.1. Step rate

SR is a parameter of locomotion that is sometimes chosen to maximize metabolic economy at preferred locomotory speeds. Humans have previously been shown to have the ability to choose movement patterns that minimize metabolic energy expenditure, a process that has been referred to as self-optimization (Holt 1995). Self-organizing systems tend to choose preferred states that show the most stable coordination and the least energy requirements. When SR is varied above and below preferred, metabolic cost forms an inverted U-shape curve with the minimum at the preferred (Holt 1995). Self-organizing human systems tend to choose preferred states that show the most stable coordination and the least energy requirements. The respiratory system has, as its primary task, maintenance of adequate ventilation in order to supply the necessary amount of oxygen to and remove metabolic by products from the circulatory system.

SR is one of the key factors in running injury. Many running injuries are caused or aggravated by repetitive eccentric action. An eccentric contraction of a muscle involves lengthening of the muscle while it is under tension. Fast running will intensify eccentric contractions and the risk of injury.

To avoid over striding, the step rate should reach 2.5-3 step/sec regardless of the treadmill speed. This may require shorter, faster steps in the treadmill exercise. A high SR encourages exerciser running smoothly and efficiently which minimizes excessive forces on the injured body. Depending on the type of injury, many injuries respond positively to inclined treadmill running because it keeps the speed down, lessens the impact forces and builds strength. The amount of incline will vary with the type of injury and individual running biomechanics. Typically 2%-8% is the recommended range.

The pedometers could provide great insights into treadmill exercise. A pedometer is a device, usually portable and electronic or electromechanical, that counts each step a person takes by detecting the motion of the person's hips. Because the distance of each person's step varies, an informal calibration, performed by the user, is required if presentation of the distance covered in a unit of length (such as in kilometres or miles) is desired.

The study has shown the relationship between HR intensity and pedometer SR counts in adolescents. To determine cardio respiratory fitness, 106 participants (47 boys, 59 girls, mean age 14.2 years, $s = 0.8$) completed the step test and were classified as having low, moderate or high cardio respiratory fitness. Adolescents also completed a 10-min treadmill trial while wearing a pedometer and HR monitor. The participants were instructed to maintain their heart rate between 65 and 75% of their maximum HR while running or walking on a treadmill. A HR of 65-75% maximum is associated with 146 steps per minute in boys and 137 steps per minute in girls. The results from this study suggest that a SR of 130 steps per minute is equal to 65-75% maximum heart rate in low-fit adolescents and achieving 130 steps per minute could be used as an initial goal to improve fitness (Lubans 2009).

2.5. Summary

This chapter investigates the importance of physical activity in maintaining good physical and mental health, the guidelines on physical activity, and how energy expenditure relates to physical activity. The importance of regulating HR during physical activity to maintain desired exercise intensity is explored through an explanation of the cardiovascular system. Meanwhile, the concept of SR is introduced as there is growing popularity in the research of walking pace area. The purpose of analysing SR is that it is an efficient way to track the body motion in the exercise and prevent the running injuries. This study also investigates the relationship between HR intensity and SR in the treadmill exercise. Detailed descriptions including the main themes of the thesis will appear in the relevant subsequent chapters.

Every effort has been made in this literature review to provide a comprehensive research background for the work performed in this thesis. Each of the references has been cited is selected discriminatingly based on their direct contribution to the body of knowledge, their approach to the topic and the analysis and methodology used in the study.

Additionally, this review has helped to enforce certain principles which have provided the study with a stronger background as a result. Consequently, the experimental method and analysis described later in this thesis reflect the knowledge and methodology acquired from the research into the studies covered in this literature review, and have contributed in part to the development of the ideas included in the scope of this work.

Chapter 3

Treadmill system design

This chapter introduces the system that is the setup for our experiments. The main steps for designing and implementing data acquisition system have been described, particularly from signal acquisition, transmission and storage. Meanwhile, the pitch estimation methods are also described to improve the quality of ECG and TA signals. An overview of Section 3.1 introduces the basic process of communication in both hardware and software. It also gives the detailed description and specifications of each component. Data Acquisition VI provides a platform to analyse the HR and SR signals for the wireless Alive Monitor, which will be explained in Section 3.2. The communication protocol between Bluetooth and Labview connection which includes data transmission and storage, will be described in Section 3.3. Section 3.4 presents the HR and SR detection which include pitch estimation approaches, the average magnitude difference function (AMDF) and autocorrelation function (ACF) detection algorithm, followed by the summary in Section 3.5.

3.1. Introduction

The following section intends to describe the hardware and software components used in the experiments.

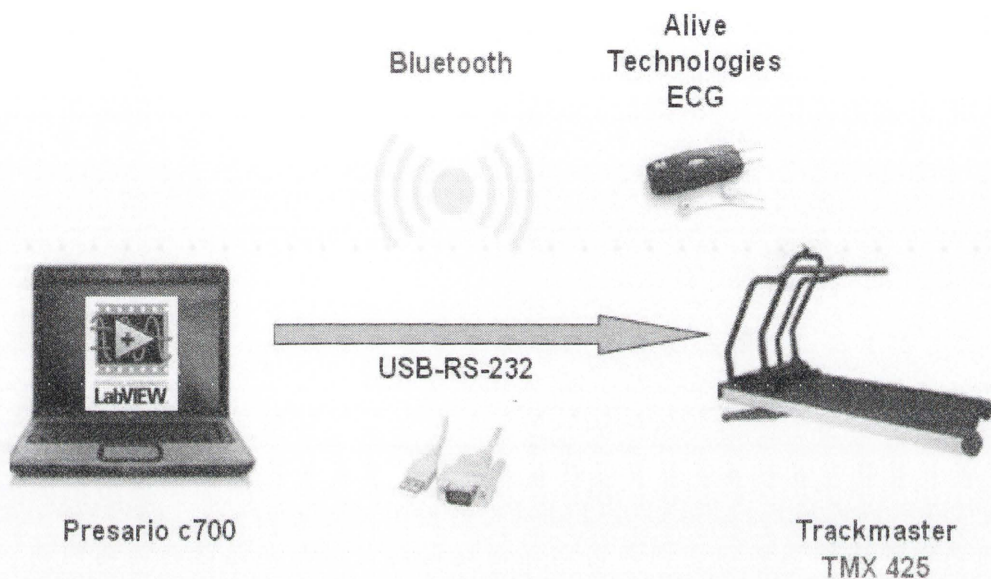


Figure 3.1 Hardware and software system design

Figure 3.1 shows the setup of the project. It consists of a wireless Bluetooth ECG device which attaches to the individual by two electrodes. The electrodes sense the electric signals produced in the heart and transmit the data to the ECG device which is resting around the volunteer's chest zone. The packets of data are transmitted via a Bluetooth connection to the computer. A Labview VI is used to establish a communication protocol in order to receive the packets and extract the information necessary to perform either HR or SR detection. A wired USB to RS-232 connection links the computer with the treadmill. This connection allows speed and gradient commands to be sent from the computer to the treadmill which will end up modifying the HR of the exerciser.

3.1.1. Trackmaster TMX425

The treadmill used in this project is the Track master TMX425. The model belongs to a series of heavy duty medical treadmills designed to be interfaced with and controlled via computer with a serial RS-232 connection. The speed and the gradient of inclination of the treadmill can be varied by commands sent through RS-232. The speed of the treadmill can be varied from 1-19 km/h, while the gradient of the treadmill can be changed from 0-25%.



Figure 3.2 Trackmaster FVX325 series treadmill

The treadmill technical specifications are as follows:

Table 3.1 The treadmill specifications

Specifications	
User weight capacity	227kg
Distance from ground	190mm
Running surface size	559mm x 1244mm
Floor surface requirements	838mm x 1626mm
Drive System	Heavy-Duty 2.2HP AC inverter drive
Rated Voltage	208-240V, 50/60Hz
Speed Range	Zero start, 0.8 – 19kmh
Elevation Range	0 – 25%

Since one of the most important aspects in the experiment is the safety of the test subject, determining safe working ranges is imperative. The safety workable ranges are determined by the level of comfort of each individual. Therefore a unique comfort range for every individual is necessary.

Initial tests were performed to determine both the maximum speed and gradient that could be set while not exceeding the comfort limits of the individual. After some trials, and by obtaining the feedback of the test subject, the following ranges were determined:

- Speed: 3-7 km/h.
- Gradient 0-25%.

3.1.2. National instruments Labview 8.6

Labview is the main software application used in the experiment. It allows hardware to communicate with software by means of communication protocols such as Bluetooth and RS-232 serial communication. Labview allows the user to process and utilize the input signals by means of Virtual Instrument (VI). Labview is a very user friendly application which allows programming in a graphical interface. The treadmill communication protocol, HR and SR detector, and the controller loops were all implemented in Labview.

3.1.3. Alive wireless monitor

The monitor used in the project is a wireless monitor developed by Alive Technologies. The device allows screening and monitoring HR performance which enables the user to monitor and diagnose not only HR related diseases and irregularities but also fitness performance if desired. Additionally, the unit includes a tri-axial accelerometer which can be used in a variety of applications such as pace detection, falling detection, etc.

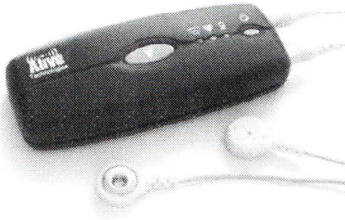


Figure 3.3 Alive technologies wireless monitor

The Alive wireless monitor technical specifications are as follows:

Table 3.2 The Alive wireless monitor specifications

Specifications	
ECG channels	Single channel, two electrodes
ECG sampling rate	300 samples/sec
Accelerometer axis	3 axes
Accelerometer sampling rate	75 samples/sec
Dimensions	90mm x 40mm x 16mm
Weight	55g (including battery)
Power Source	NP20 3.7 volt removable and rechargeable lithium-ion battery
Operating	48hrs – continuous wireless transmission
Bluetooth Compliance	Version 1.2 compliant
Bluetooth Classification	Class 1 (up to 100 meter range)
Bluetooth Profile	Serial Port Profile
Bluetooth Operation	Slave Point-to-Point

The wireless monitor is used to measure the HR and SR of the runner during exercise. The wireless transmission feature made it efficient to monitor the runner without interrupting their natural running style. The wireless monitor is attached to the runner using two ECG electrode pads. The wireless monitor readings will be transmitted to computer via a Bluetooth USB module, from which Labview is used to implement an

ECG protocol which analyses the readings and provided ECG and accelerometer information.

An accelerometer is a device for measuring acceleration and measures the motion of the body attached to the accelerometer. The SR sensor in the treadmill control system utilises a tri-axial accelerometer (TA) to measure the motion of the walker in the XYZ axis and the walking pace is calculated from motion in the XYZ axis.

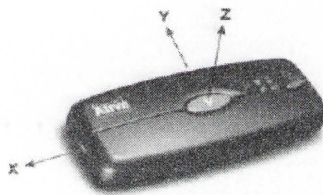


Figure 3.4 The orientation of the x, y, and z axes in build in tri-axial accelerometer

The TA consists of three axes and the recording sampling rate is 75 samples/sec which is designed to respond well to acceleration due to movement and gravitational acceleration.

The accelerometer has a range of $\pm 2.7g$ on each axis, a frequency range of 0 - 20Hz, noise estimate of $4.33 \times 10^{-3}g$ and a peak to peak noise estimate of $17.2 \times 10^{-3}g$.

3.1.4. ECG electrodes

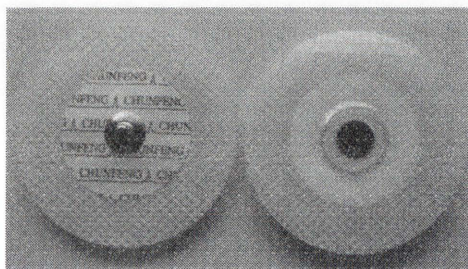


Figure 3.5 ECG Electrodes

The ECG electrodes are used, in conjunction with the wireless monitor, to measure ECG signal. The electrodes are placed on the surface of the chest and provided leads, from which the wireless module could attach to and measure ECG signal.

3.1.5. Pedometers



Figure 3.6 Pedometer

The pedometers are devices which can be used to detect the number of steps taken, while running or walking. The pedometers are used in the SR sensor accuracy test, as a comparison to the SR sensor readings.

3.1.6. Bluetooth



Figure 3.7 USB Bluetooth dongle

Bluetooth is a standard of radio technology that makes it possible to transmit signals over short distances between telephones, computers and other devices. The signal operates at frequencies of 2.4 GHz. Communication between the Alive Technologies ECG and the computer is done via wireless Bluetooth connection. The range of the Bluetooth connection is 100m. The data is received by a USB Bluetooth dongle.

3.1.7. Serial protocol

Communication between the computer and the treadmill is transmitted via serial port communication. The PC does not have a standard serial port socket available. Therefore a USB to RS-232 is used in order to establish this type of connection. RS-232 is a common serial communication electrical standard used by computers with data rates up to 20 kbps. It is suitable for both synchronous and asynchronous communications.

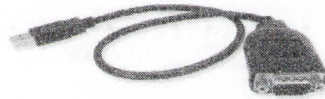


Figure 3.8 USB to RS-232 connector

3.2. Data acquisition VI

The Data acquisition VI is designed to acquire the HR and SR signals from the wireless Bluetooth data to a file for later analysis in Labview. The VI is outputted to the serial port with a constant gradient and varied speed as specified by the user.

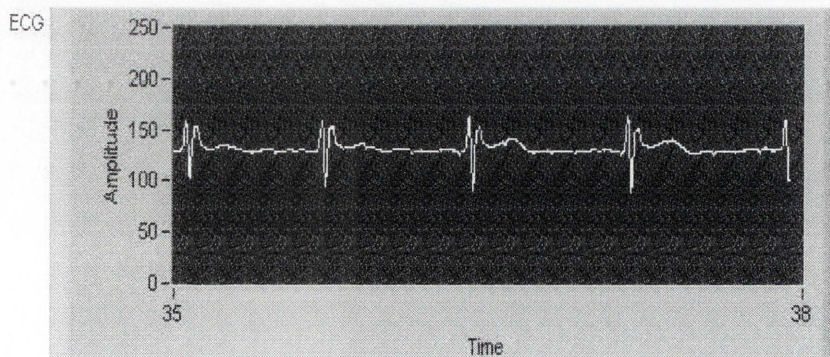


Figure 3.9 ECG signal

The front panel of the data acquisition VI as shown in Figure 3.9 displays the user's ECG signal. The VI allows the user to monitor the HR period and later implements PID control to adjust the treadmill speed and/or gradient.

The front panel which is initialised the treadmill via RS-232 from the PC to the treadmill. Figure 3.10 shows us the options available to choose the corresponding I/O port, baud rate, data bits, parity, stop bits and flow control.

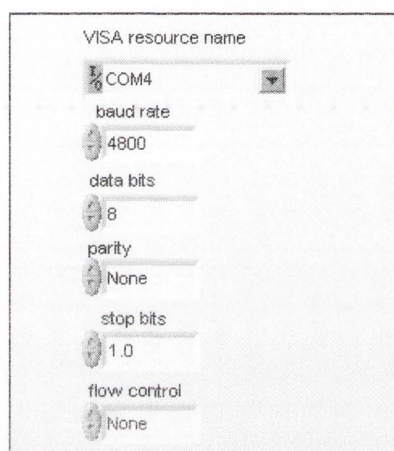


Figure 3.10 Front panel of the treadmill initialisation

In terms of the ECG monitor Bluetooth protocol instruction displayed in Figure 3.11, the ECG signal data range should be from 11 to 88 and the TA signal data range is between 88 and 143. By implementing the string subset function, the ECG signal data will start from 11 and we setup the length to 72 which make up the period from 11 to 88. And the same method is applied in TA.

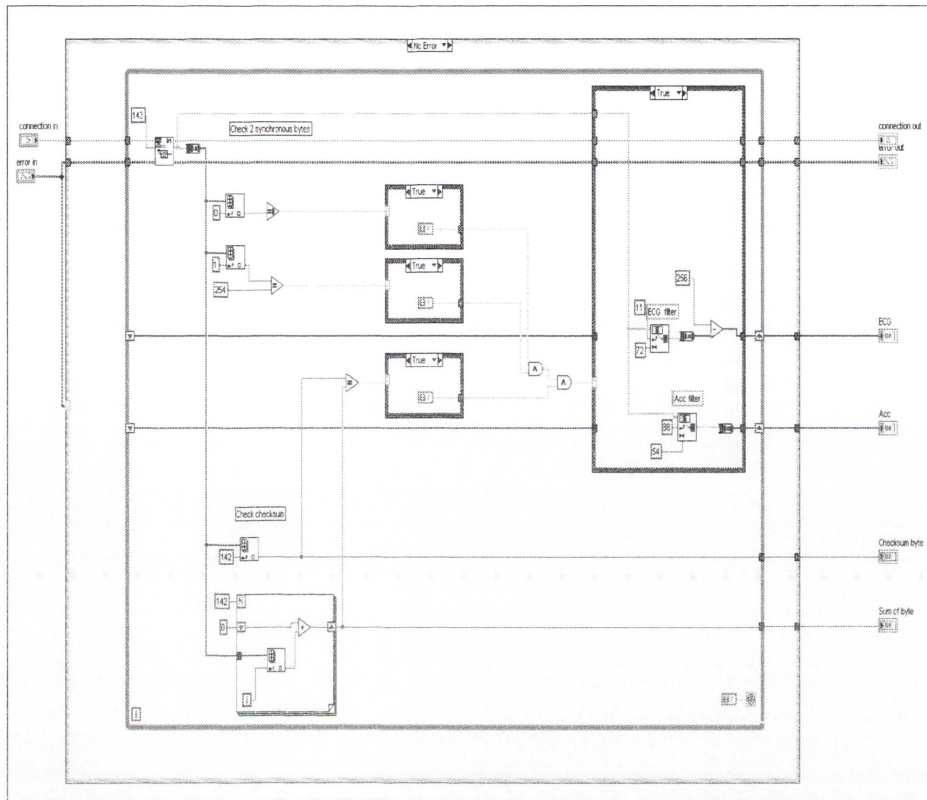


Figure 3.11 Block diagram of the data acquisition

3.3. Communication protocol VI

In order to receive and decompose the data packets in Labview, a communication function needs to be added to the VI. Labview contains a customize function called Bluetooth open connection function which will allow Labview to receive data from a Bluetooth server.

This block will allow the computer to act as a client and pick up the signals and data that is being transmitted. The connection needs to be closed at the end once transmission has finished.

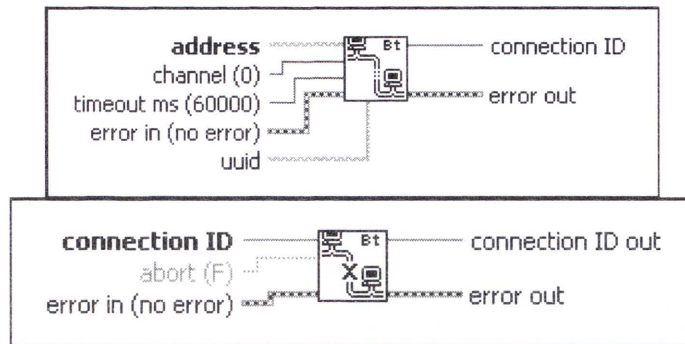


Figure 3.12 Bluetooth open and close connection functions

The inputs that need to be specified for the Bluetooth server to be recognized are the UUID and the address. The UUID is the unique identifier of the service. The address is the address of the Bluetooth server. Figure 3.13 below shows the implementation of the open connection function in the peak detector VI.

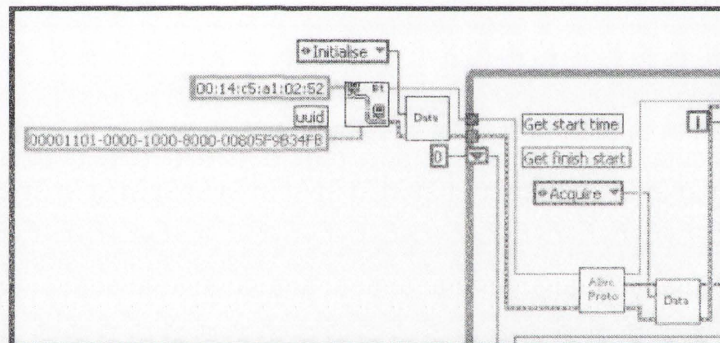


Figure 3.13 Implementation of the open connection function

3.3.1. Data transmission VI

The packets sent by the ECG monitor comprise of 143 bytes of data. The packet is divided in the following way:

Packet Structure

Packet Header	ECG Header	ECG Data	Acc Header	Acc Data	Checksum
6 Bytes	5 Bytes	n Bytes	5 Bytes	r Bytes	1 Byte

Figure 3.14 Packet layout from ECG alive technologies health monitor system

From the 143 bytes available in each packet, 17 bytes are allocated for the data headers, and the remainder 126 contain the data. From these 126 data bytes, 72 bytes represent the ECG signal while the remainder 54 bytes contain the data information of the TA.

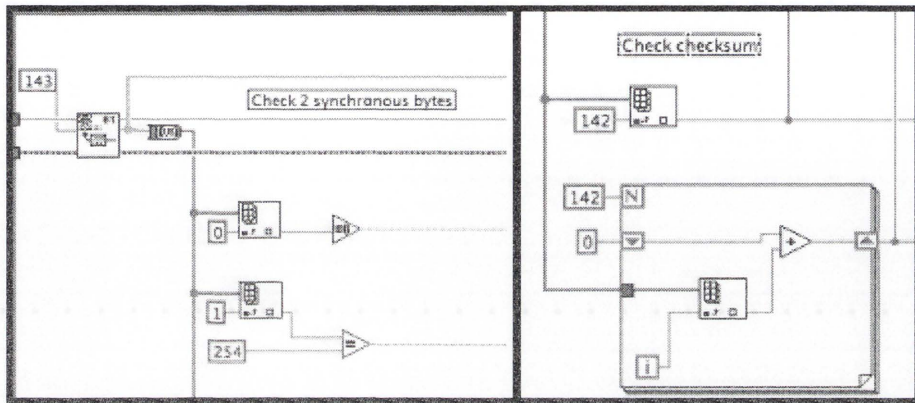


Figure 3.15 Verifying the validity of data packets

The ECG protocol VI accepts the 143 bytes of data and proceeds to verify the validity of the packet by checking the value of its synchronizing bytes and the checksum. This could be done simply in Labview by using the indexing array function.

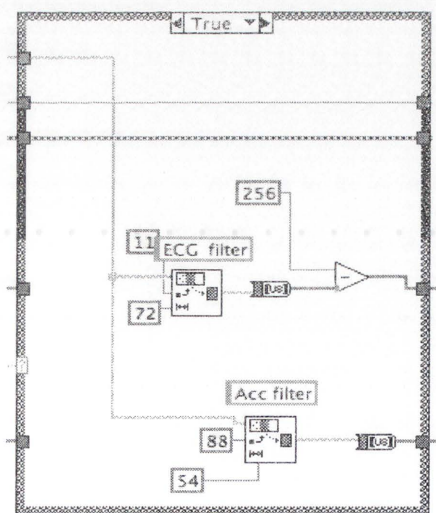


Figure 3.16 Separation of ECG and Accelerometer data

In order to separate the data bytes, the array subset function is implemented. The ECG data is extracted by separating the set of 72 bytes starting from the 11th byte. The Acceleration data is extracted by removing 54 bytes of data starting from the 88th byte.

3.3.2. Data storage VI

In order to successfully detect peaks, enough packets of data need to be obtained so that there is enough time for at least two RR peaks to occur. It is determined that 2 seconds of data is an acceptable period of time in order for the minimum number of RR peaks to occur. Packets of 72 bytes are received (or 72 samples, each sample represented by 1 byte), with a sampling rate of 300 Hz, 9 x 72 packets are needed to approximate 2 seconds of data.

This is implemented in Labview by using shift registers and the build array function. Each packet of 72 samples is received and shifted until 9 packets are received. The newest packet is received and placed in the build array, while the oldest is discarded.

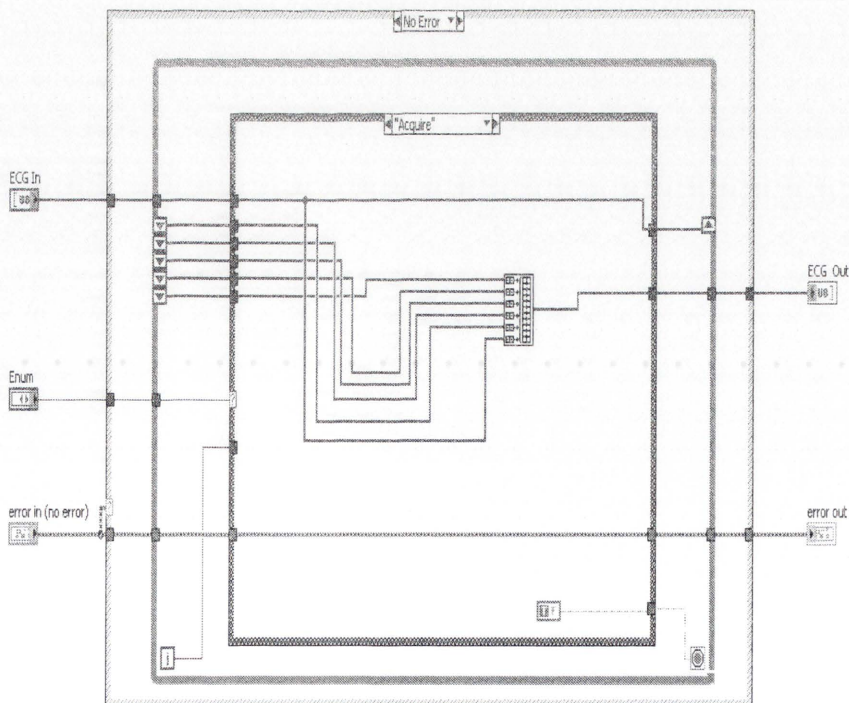


Figure 3.17 The data storage VI

3.4. HR and SR signals detection

In practice, a typical ECG recorder in the treadmill exercise may be corrupted by (1) electrical interference from surrounding equipment such as the effect of the electrical mains supply; (2) analog-to-digital conversion and (3) movement and muscle artifacts. In order to employ the ECG signal for facilitating medical diagnosis and fitness exercise record, filtering techniques may be employed to remove the distortions caused by these various sources of noise.

The pitch estimation plays a very important role in speech compression, speech coding, speech recognition and synthesis, as well as in voice translation. A good estimation of the pitch period is crucial to improving the performance of speech analysis and synthesis systems (Tan 2003). There are many pitch detection algorithms such as the short-time average magnitude difference function (AMDF), short-term autocorrelation function (ACF), spectrum, cepstrum, neural networks and wavelet transform algorithms. Although many pitch detection methods have been proposed, few of them have been built in special-purpose digital hardware capable of real-time operation (Hui 2006).

3.4.1. AMDF pitch detection algorithm

For periodic signal $s(n)$ of period T , the difference function $x(m)=s(n+m)-s(n)$ will be approximately zero for $m=0, \pm T, \pm 2T, \dots$, because the voiced speech signals are quasiperiodic, the difference function $x(m)=s(n+m)-s(n)$ will be small if $m=0, \pm T, \pm 2T, \dots$. Based on the reason, the AMDF function of a frame of speech signal is defined as:

$$x_w(m) = \frac{1}{N-m-1} \sum_{n=0}^{N-m-1} |s_w(n+m) - s_w(n)| \quad (3.1)$$

Where $s_w(n)$ is speech signal. N is the length of a frame of speech signal. The range of m is between 0 and N . When a frame of speech signal is quasi-periodic, the values of the AMDF function of a frame of speech signal are quasi-periodic.

$x_w(m)$ has the minimum value in the position of the integer times of the pitch period. The position of the minimum value is found and the distance between the position and origin point is calculated. And then the pitch period can be obtained. The position of the minimum value may not match the pitch period because of the effect of the amplitude, noise and formant of speech signal.

3.4.2. ACF pitch detection algorithm

An important guide to the persistence in a time series is given by the series of quantities called the sample ACF coefficients, which measure the correlation between observations at different times. The set of ACF coefficients arranged as a function of separation in time is the sample ACF. An analogy can be drawn between the ACF coefficient and the product-moment correlation coefficient.

$$r_k = \frac{\sum_{i=1}^{N-k} (x_i - \bar{x})(x_{i+k} - \bar{x})}{\sum_{i=1}^N (x_i - \bar{x})^2} \quad (3.2)$$

The quantity r_k is called the ACF coefficient at lag k . The plot of the ACF function as a function of lag is also called the correlogram. The correlation coefficients for the lagged scatter plots at lags $k = 1, 2, \dots, 8$ are equivalent to the ACF values at lags 1, 2, ..., 8. By analogy the auto-covariance of a time series is defined as the average product of departures at times t and $t+k$:

$$c_k = \frac{1}{N} \sum_{t=1}^{N-k} (x_t - \bar{x})(x_{t+k} - \bar{x}) \quad (3.3)$$

Where c_k is the auto-covariance coefficient at lag k . The auto-covariance at lag zero c_0 is the variance. By combining equations (3.2) and (3.3), the auto-correlation at lag k can be written in terms of the auto-covariance:

$$r_k = c_k / c_0 \quad (3.4)$$

Equation (3.3) is a biased (though asymptotically unbiased) estimator of the population covariance. The ACF is sometimes computed with the alternative equation:

$$c_k = \frac{1}{(N-k)} \sum_{t=1}^{N-k} (x_t - \bar{x})(x_{t+k} - \bar{x}) \quad (3.5)$$

3.4.3. Detection methodology

AMDF and ACF are frequently used to analyze the fundamental frequency of a regular periodic signal. We applied these two methods in the preprocessing of TA signal. A real-time algorithm has been developed based on AMDF and ACF. We prepare the signals found that under strong random noise background and then adopt AMDF, ACF, the combination of ACF and AMDF and the repeat usage of ACF and AMDF in the experiment to find out the effective approach for SR detection.

On the other hand, after being tested, the integral type approaches are not suitable for the pre-processing of ECG as they may reduce some high frequency signals, such as

the R peak. Based on this consideration, the differential type function combined with a square wave matching detection algorithm has been developed (see Figure 3.18), which uses a square wave to match an ECG signal.

Even if ECG signal is not well represented by the device, HR can still be detected accurately by the square wave matching method.

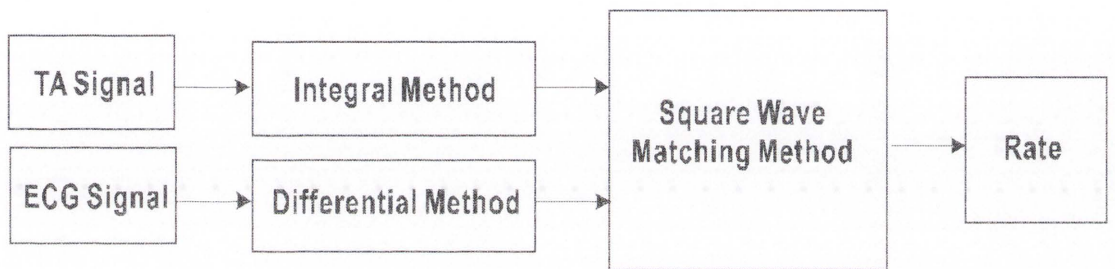


Figure 3.18 Block diagram of the proposed approach

The choice between ACF and AMDF depends on the level of noise in the TA signal. For the white random noise, the ACF and AMDF can be used to detect the SR. If the noise is strong, after ACF or AMDF are used once, the noise will be reduced, but the signal may still not be uniformly smooth. Therefore we can attempt to apply double ACF, double AMDF or ACF+AMDF. These two integral methods will be compared and presented. Meanwhile, the differential method is optimal for the weak noise in ECG signal. The developed square wave matching approach is illustrated in Figure 3.19.

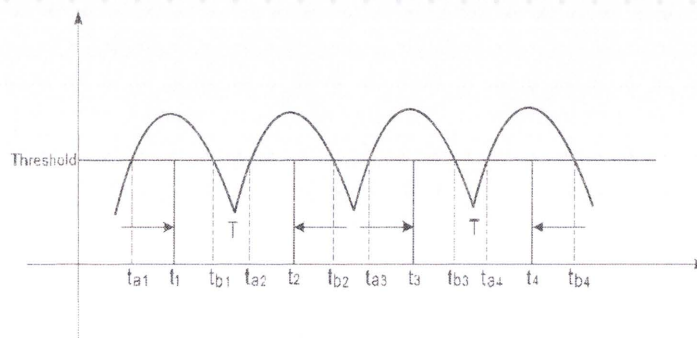


Figure 3.19 Description square wave matching approach

To apply the square wave matching method in the TA or ECG signal, an appropriate threshold need to be selected. Assume the input signal is $x(k)$, then the generate square wave $y(k)$ can be described:

$$y(k) = \begin{cases} 1, & x(k) \geq \text{threshold} \\ 0, & x(k) < \text{threshold} \end{cases} \quad (3.6)$$

The integers t_{ai} and t_{bi} can be estimated by using the following conditions:

For t_{ai} and t_{bi} , $i = 1, 2, 3, \dots, k$:

$$\begin{cases} y(t_{ai}) - y(t_{ai} - 1) = 1 \\ y(t_{bi} + 1) - y(t_{bi}) = 1 \end{cases} \quad (3.7)$$

The next step is to calculate the t_i by using the following equation:

$$t_i = \frac{t_{ai} + t_{bi}}{2} \quad (3.8)$$

The period T can be calculated as:

$$T = \frac{1}{n} \sum_{i=1}^n t_i \quad (3.9)$$

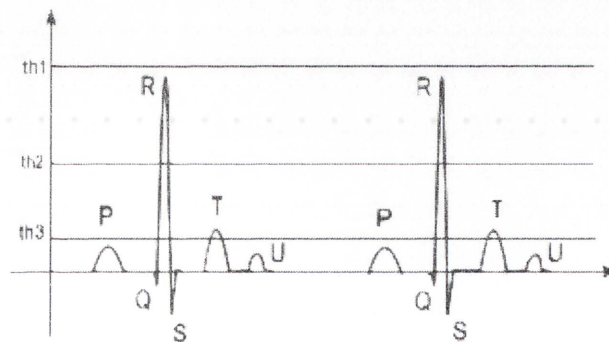


Figure 3.20 ECG signal with different thresholds

It is noticed that the estimated HR from using the proposed square wave matching method may be affected by the threshold values selected. In Figure 3.20, if the selected threshold value is $th1$, we can not detect the HR properly because there is no peak in the piece of ECG signal which can reach this threshold level. On the other hand, for the threshold $th3$, both P and T peaks will be counted. Therefore, the estimated rate should be divided by 2. The threshold $th2$ is a proper selection because only R peak can be detected by this threshold. To reduce threshold sensitivity, we pre-process the ECG signal by differentiation and obtained desired results.

3.4.4. Detection experimental results

According to Equations (3.1) and (3.2), both ACF and AMDF have the advantage of being simple and effective for random noise reduction. The rate can be detected from TA signal by using the integral type of approach (see Figure 3.21 and 3.22).

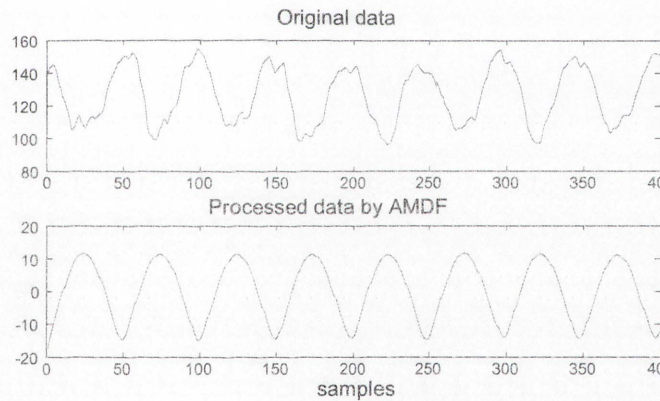


Figure 3.21 TA signal processing by using AMDF

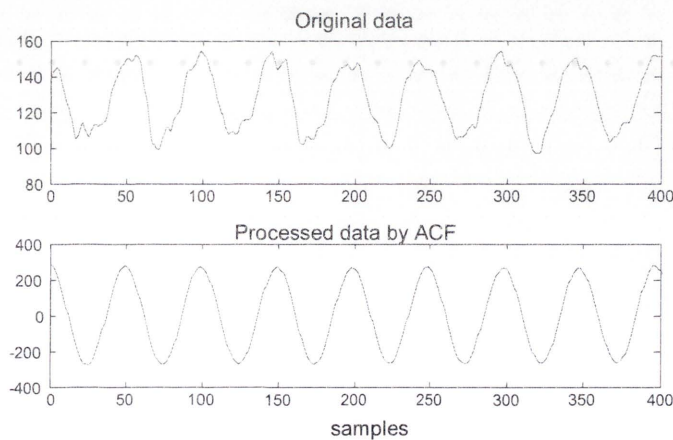


Figure 3.22 TA signal processing by using ACF

However, when noise is relatively high, the $AMDF^2$, ACF^2 or $AMDF+ACF$ method should be applied (see Figure 3.23, 3.24 and 3.25).

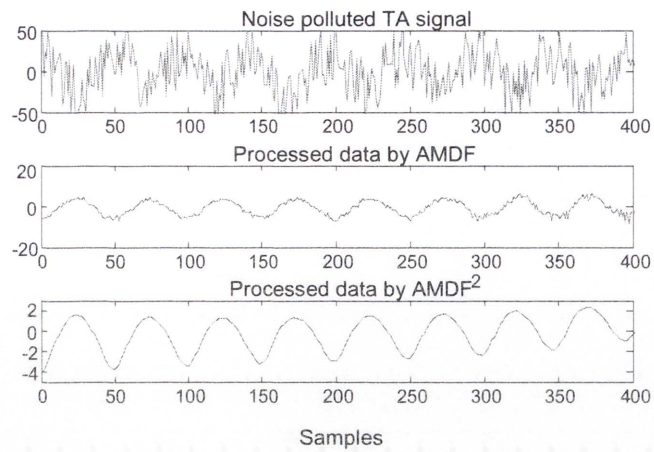


Figure 3.23 Noise polluted TA signal processing by using $AMDF^2$

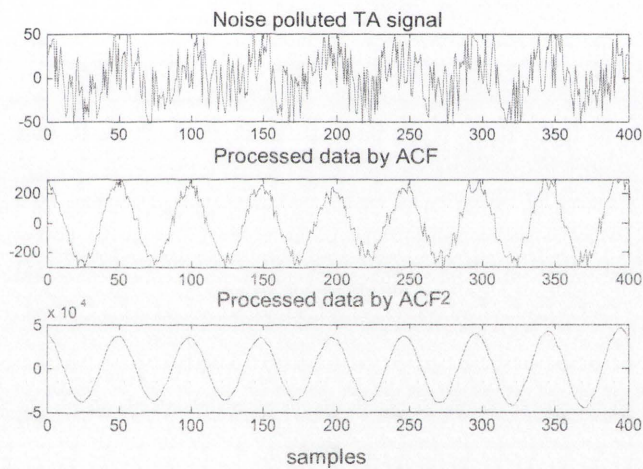


Figure 3.24 Noise polluted TA signal processing by using ACF^2

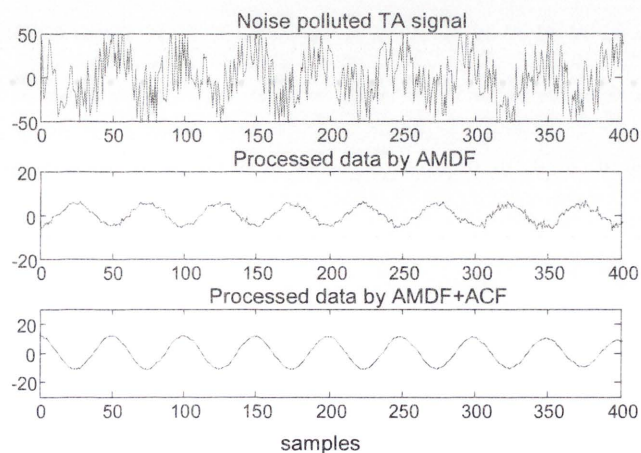


Figure 3.25 Noise polluted TA signal processing by using $AMDF+ACF$

As we could see in Figure 3.23 and Figure 3.24, either the ACF^2 or $AMDF^2$ method, in contrast to the integral ACF or $AMDF$, has the advantage of making the TA signal smoother. Meanwhile, the ECG signal can not be pre-processed by the integral method.

As discussed before, the square wave matching method is sensitive to the selected threshold level. To minimize the sensitivity, the differential method has been implemented to pre-process the ECG signal. The proposed square wave matching method has been used to determine the HR from the pre-processed ECG signal as shown in Figure 3.26.

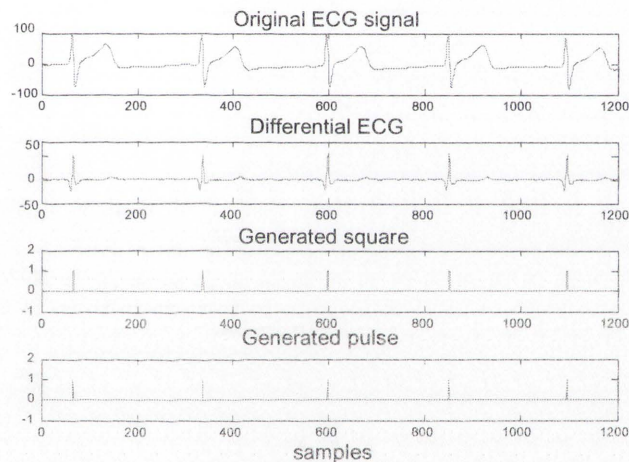


Figure 3.26 Heart rate detection

3.5. Summary

This chapter is intended as a brief introduction to the hardware and software systems used in the experiment. With this setup, an accurate reading of the HR and SR would be obtained. If we do not have such a hardware selection, it would be difficult to achieve reliable HR and SR readings from the hardware and software. Therefore, there are two major issues concerning this setup. The primary concern is the health and safety of the exerciser. If the equipment is not stable or connected properly, this would present an obvious risk to them. Second is the accuracy and reliability of the produced results. Any improperly functioning component of the system could cause

an error in the results. In the end, the pitch detection method has been implemented to filter the proper ECG and TA signal. It was found that the repeat or combination usage of ACF and AMDF are very effective for TA signal processing. Experimental results have shown that repeat ACF obtains a better result in contrast with AMDF and simple ACF and their combination. Simulation and experiments also show that the differential type algorithm is suitable for ECG signal pre-processing. We developed a real time square wave matching method to detect the rate of pre-processed signals. Experimental results indicate that the proposed methods can effectively detect HR from ECG signal and remove undesirable spikes.

Chapter 4

Labview implementation

The use of Labview and data acquisition in biomedical industry makes the real time monitors systems more reliable and flexible. In this chapter, we develop a Labview program based on the Pan-Tompkins method to filter the ECG data from the wireless ECG monitor. The BPM calculation and SR sensor will also be designed and explained. Section 4.1 gives a brief overview of the Labview interface. Section 4.2 explains each function in the Pan-Tompkins method. After filtering the ECG signal, BPM calculation block is presented in Section 4.3. The other part of the program, the SR sensor, is introduced in Section 4.4 and accuracy tests will be applied to the SR sensor. Finally, conclusions are drawn in the last section.

4.1. Introduction

The aim of this section is to determine the HR in a real time environment. Labview contains the function Mathscript which allows the user to enter mathematical commands that are available in Matlab. The following section describes the virtual interface designed for Labview.

The following section will describe the implementation of the HR detector in Labview. In order to implement the detector successfully, several steps need to be carried out. The following block diagram explains the sequence of events that occur in the VI.

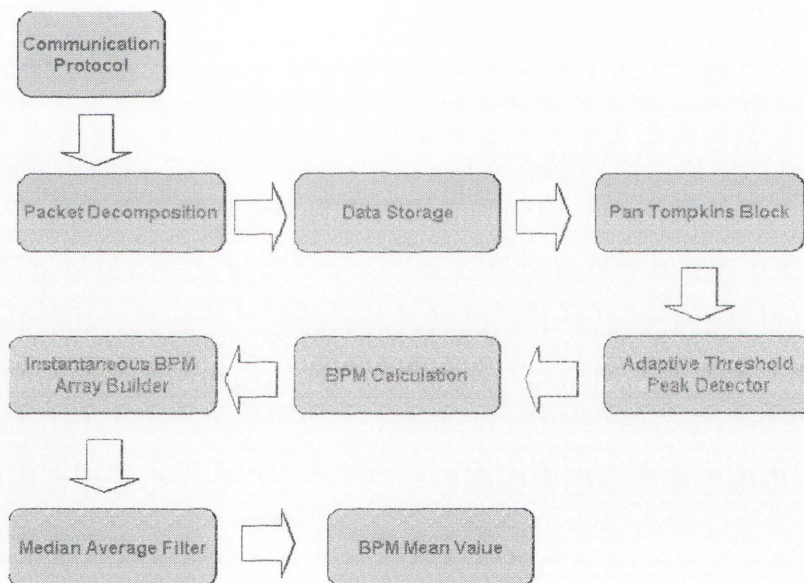


Figure 4.1 Sequence of events for the implementation of the HR detection VI

As the communication protocol, the data transmission and data storage modules have been mentioned in Chapter 3. The following figure shows the open and close procedure for acquiring packets via Bluetooth.

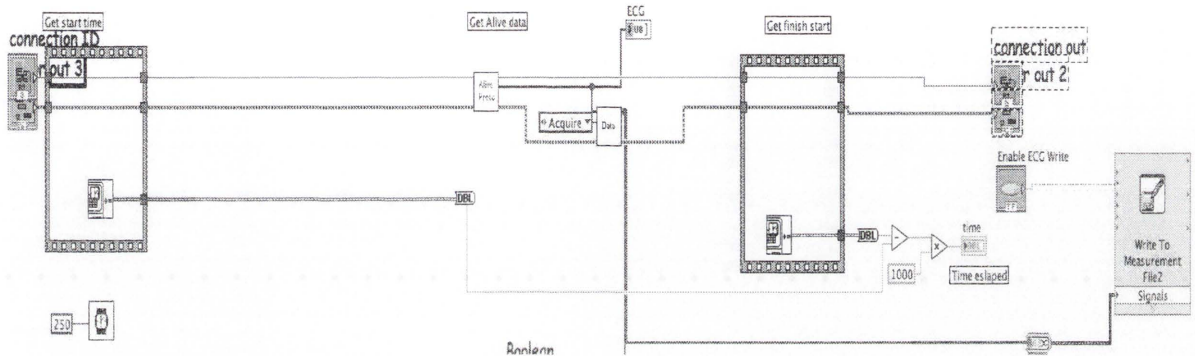


Figure 4.2 Communication to the Bluetooth protocol

4.2. Pan and Tompkins method

To provide considerable flexibility and efficiency in changing speed and gradient, accurate ECG signal is required. The Pan-Tompkins algorithm (Pan 1985) is the most well-known method consisting of several filtering stages in order to achieve R-peak detection. It comprises of a band-pass filter, differentiator, a squaring operation and a moving window integrator. The band-pass filter consists of a cascaded low pass and high pass filter in order to reduce noise in the ECG signal. This is done by matching the spectrum of the average QRS complex. After the signal has been filtered, it is differentiated through a five point derivative function in order to obtain information on the high frequency components. When the signal is differentiated, it accentuates the components with high slopes. This is possible because the QRS complex contains the highest slopes of the signal. The purpose of the squaring function is to ensure that every point in the filtered-differentiated signal is positive.

It assists the derivative function by suppressing P and T waves and further enhances the higher frequency QRS complexes. The final stage of the processing is the moving window integrator which is used to obtain a wave-form feature of the input. The output of a derivative base function will reveal multiple peaks within the duration of a QRS complex. The moving window integrator performs smoothing of the output and provides a single peak output for each QRS complex. After implementing these steps and by implementing an adaptive threshold algorithm with false peak detection capabilities, the proper ECG signal can be detected accurately.

The next steps will be involved in the Pan and Tompkins ECG detection process. It presents the output result of each stage involved for a sample ECG signal captured in real time. An example of a real time ECG signal is captured by the Alive Technologies ECG and is shown below. In this scenario, the exerciser is jogging at a low speed. From this example, it is clear that a threshold algorithm applied directly to the original signal would be difficult to implement due to the variability of the signals. Another obstacle to a direct threshold approach is the low frequency baseline wandering in the captured ECG data. Furthermore, it is important to notice that the R wave is the only ECG signal component that is easily identifiable in the waveform.

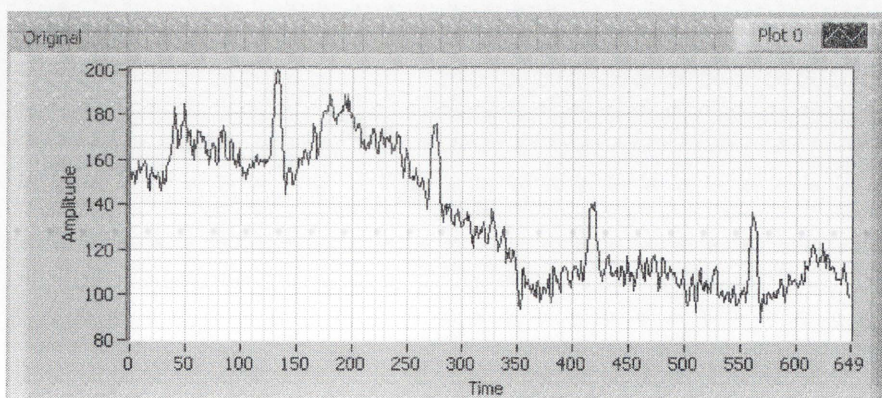


Figure 4.3 Original ECG signal of a jogging test subject

4.2.1. Band-pass filtering

The ECG signal is affected by noise coming from power line interference, exerciser muscle movement, baseline wandering, etc. The QRS complex which is of interest lies within 5-15 Hz. In order to reduce computational complexity, a filter with integer coefficients is required. In order to achieve this, a recursive filter in which poles are placed to cancel zeroes in the unit circle of the z-plane is necessary. The band pass filter is implemented by cascading a low pass filter of a cut-off frequency around 11Hz and a high pass filter of frequency around 5Hz. This pass band is close enough to the deal requirements.

The output of the band pass filter with cut-off frequency 5~11Hz is shown in the figure below. Notice that the waveform is free of low frequency baseline wandering thanks to the low cut-off frequency of 5Hz. Moreover, notice that the QRS complex has been emphasized because the high frequency noise has been removed from the original signal. The T wave component of the waveform has been attenuated.

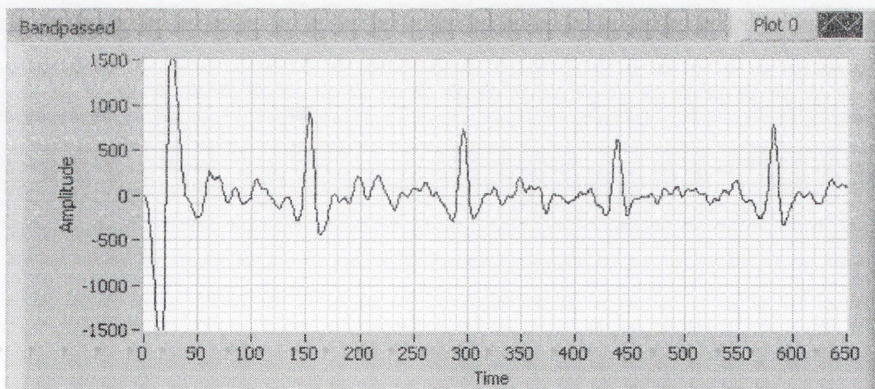


Figure 4.4 Output from the band pass filter

4.2.2. Derivative action

The Figure 4.5 shows the output of the derivative filter. The filter has emphasised the steep slopes present in the high frequency components of the QRS complex. This step helps in differentiating the low-slope P and T waves from the high-slope QRS waves.

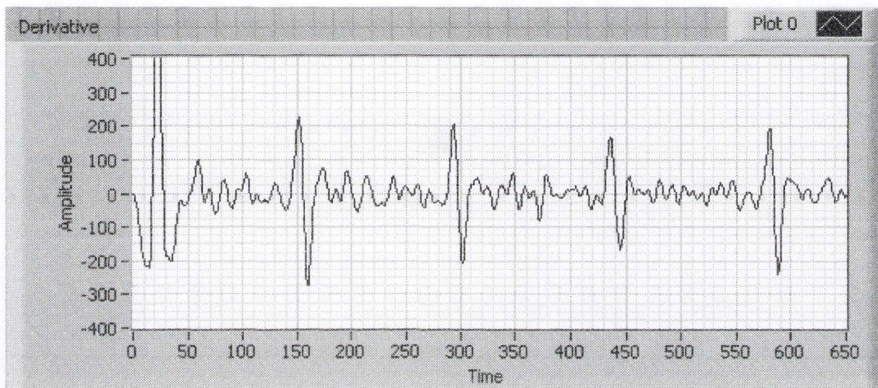


Figure 4.5 Output from the derivative filter

4.2.3. Squaring

Figure 4.6 below demonstrates the output of the derivative filter after being squared. This step converts all the sampled data to a positive value while maximizing the value. This step isolates the QRS complex form the rest of the signals even further.

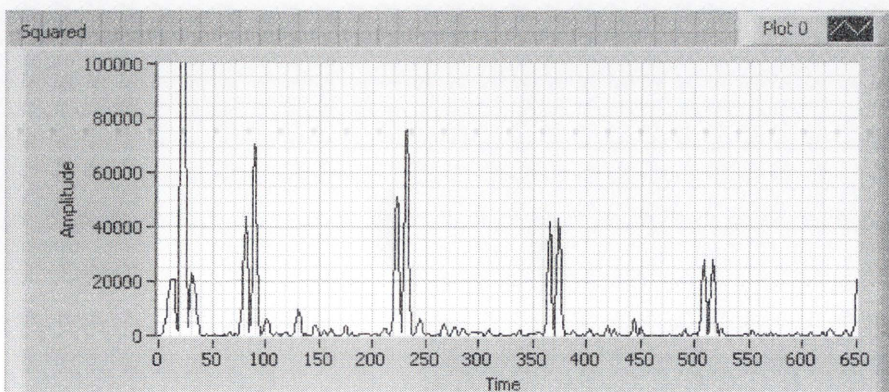


Figure 4.6 Output from squaring operation

4.2.4. Moving window integrator

The MWI is an important step since the slope information about the QRS complex alone is not sufficient. This is because some abnormal QRS components may have large amplitudes and duration with slopes that may not be too steep. The MWI helps extract additional features from the output signal of the derivative filter. This is implemented with the following differential equation:

$$y(nT) = \frac{1}{W} (x[nT - (W - 1)T] + x[nT - (W - 2)T] + \dots + x[nT]) \quad (4.1)$$

The value of W is an important parameter since it represents the width of the integration window. As a guideline, this width should be approximately the same size as the widest QRS complex. However, if the window is too wide, the window will merge the QRS and T complexes. The value of W is determined empirically to be 32.

The MWI will sum the area under the curve for an interval of 100 ms (30 samples). This is determined empirically to be a suitable value to include the width of the QRS complex coming from the squaring function. This sample width is long enough to include any abnormal QRS complexes and short enough so it does not overlap over the T waves or QRS complexes nearby. A false transient component is always present at beginning of the output of the MWI.

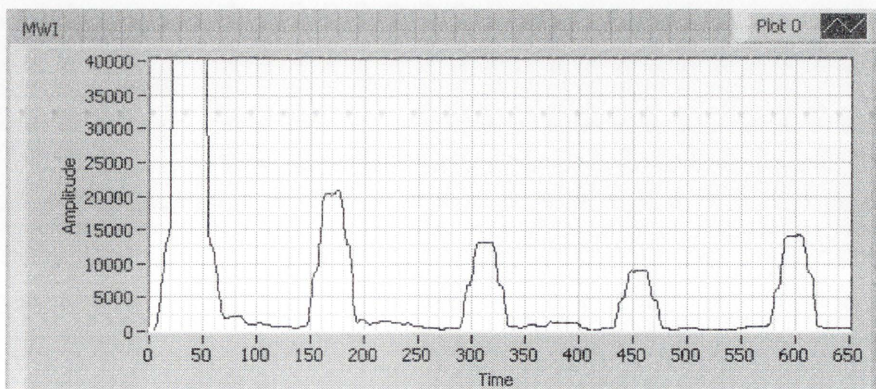


Figure 4.7 Output from moving window integrator

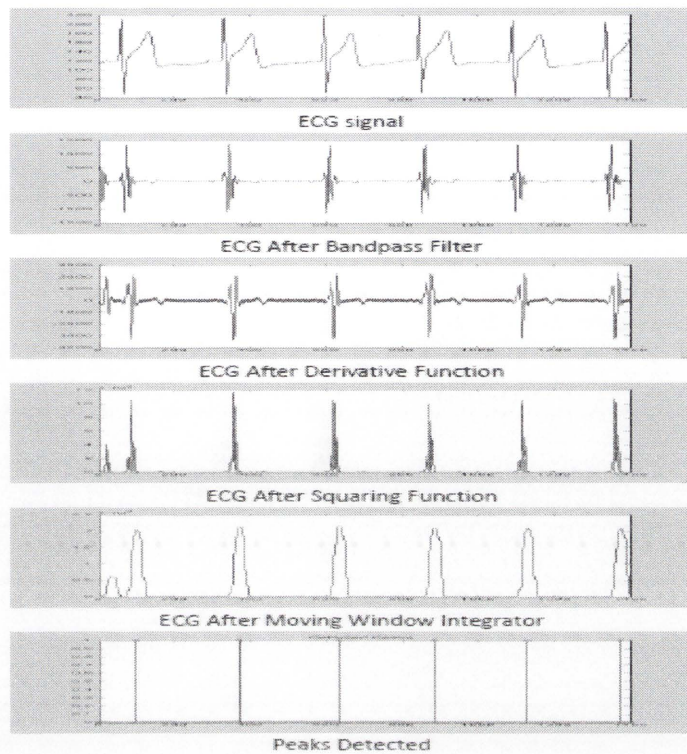


Figure 4.10 Pan and Tompkins heart rate detection

4.3. HR sensor

Calculating BPM is necessary in order to monitor the HR. In HR sensor, it converts the real time ECG signal to beats per minute in the Labview. The proposed BPM calculation model consists of two stages. In the first stage, the peak detection block is designed to select the suitable peaks in ECG signal. After that, the data storage we mentioned in chapter three uses shift registers and arrays to convert the two peak distance to BPM. In the second stage, BPM mean value block is introduced to minimize the random errors from the ECG signal.

4.3.1. Peak detector block

The peak detector block is used to detect the locations of peaks from the smoothed wave output of the moving wave integrator. In order to correctly identify peaks in the signal, key variables like width of the peak and the threshold need to be set.

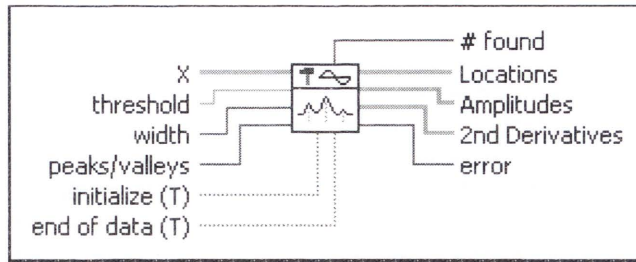


Figure 4.11 Peak detector block

The amount of samples for the moving wave integrator determines the width of the peak detector as this describes the width of the QRS. If we were to choose a lower value over a higher value, multiple peaks could be falsely detected within the signal. Likewise if we were to choose lower values than higher ones, we run the risk of missing QRS peaks. The other variable threshold is determined by the height of the smoothed QRS wave. This value is determined by the peaks of the wave and is largely determined by observing the signal and selecting a suitable peak. As HR tend to be nonlinear and vary in both rate and power spectrum, it is very difficult to estimate a single value that would work for all cases. It is therefore recommended that the value should be put in after initial observations of the wave. A good rule of thumb is to choose a value that is half the value of the average peak, rides on top of the noise and still is capable of detection from the peak detector.

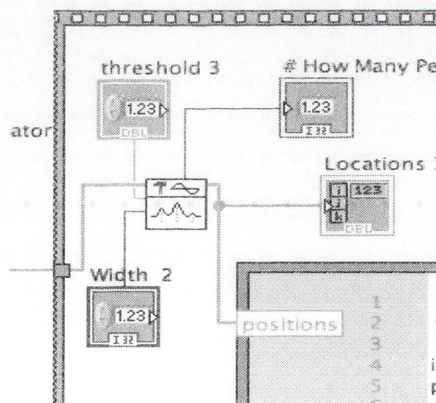


Figure 4.12 Peak detection

Once the peak detector has identified the locations of the peaks, the BPM can be calculated by applying the formula.

$$BPM = \frac{\text{sample rate of HR monitor} * \text{distance}}{60} \quad (4.2)$$

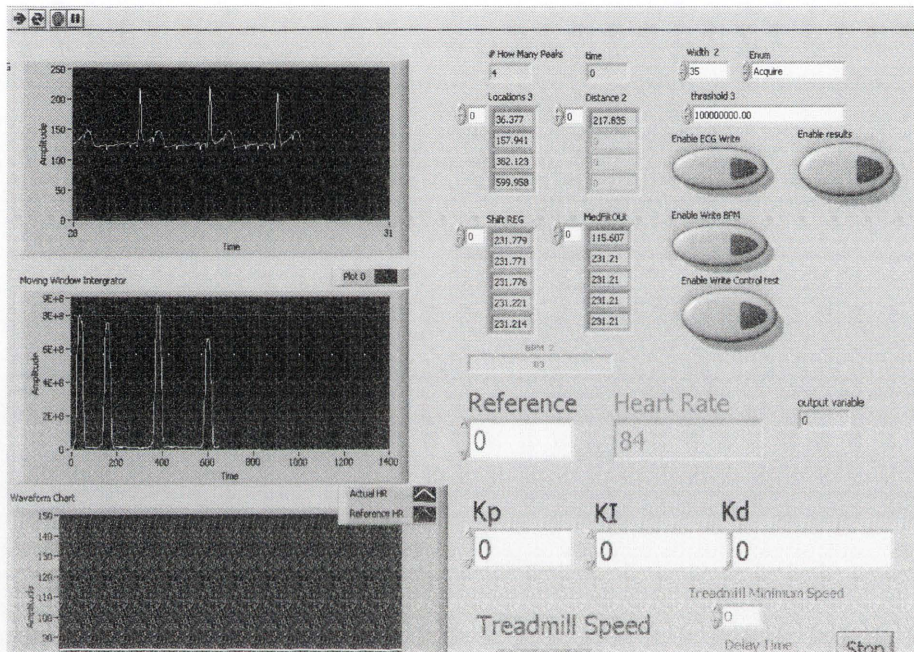


Figure 4.13 BPM testing

4.3.2. BPM mean value block

An array of instantaneous values that lie within $\pm 20\%$ of the previous mean value is constructed in the array builder. It is necessary to build an array of values with small variance in order to obtain stable mean values. The value of 20% error margin is determined empirically to be a range that is big enough to allow the BPM to increase naturally without

exceeding these limits, and small enough so as to reject any excessively large values of instantaneous BPMs. If this range is too narrow, a valid BPM value produced by the individual changing the running speed to a higher speed could go out of this limit. Since the HR is increasing, the value will not go back again to be within this range. If this 20% error margin is not applied, the instantaneous BPM values to form part of the array could create a difference of 60% in the previous mean value. This 60% limitation is implemented in the peak detector block in order to detect false peaks. Taking the mean of a set of values having large variance leads to sudden changes in the BPM mean. Limiting the values used to compute the mean to 20% error margin lead to acceptable mean results.

The initial approach towards obtaining a mean BPM value is simply to obtain the array of 8 instantaneous BPM values and take the mean of this set. This is implemented in Labview by using the mean block (this will also be referred to as the mean filter). The mean array builder and the mean block form a moving average filter which averages the latest 8 instantaneous values. A moving average filter is a type of smoothing filter.

NI_AALBase.lvlib:Mean.vi

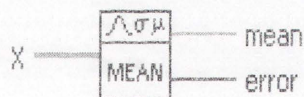


Figure 4.14 Mean value block

Taking the mean of instantaneous values that are within 20% of the mean significantly improved the response of the signals. The following moving mean response is recorded

simultaneously as the instantaneous HR response that is presented in Figure 4.15. The reduction of HR variability is clearly noticed.

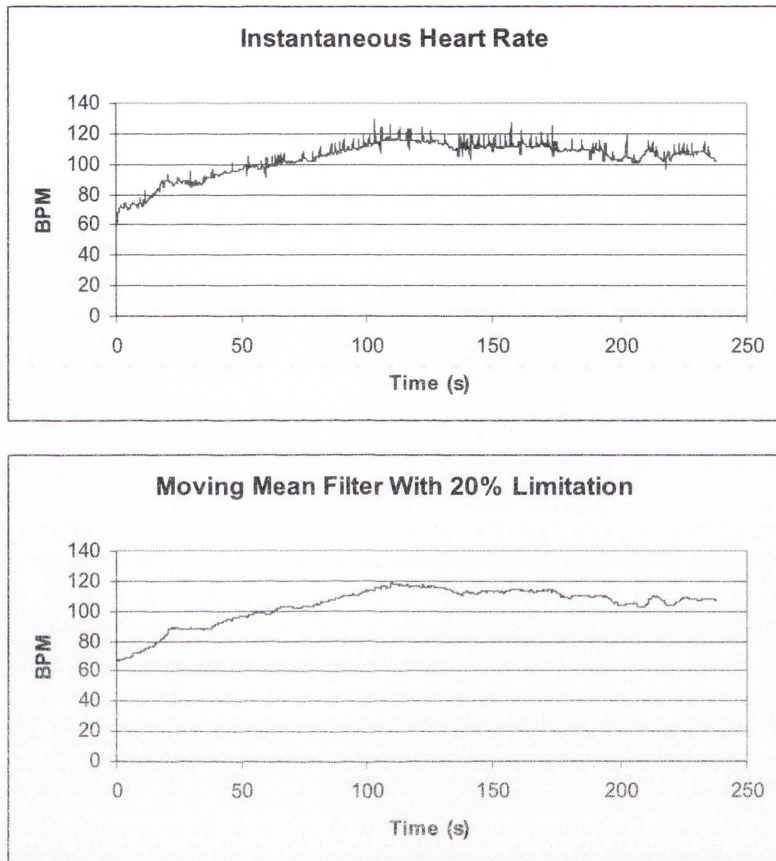


Figure 4.15 Comparison open loop BPM mean response vs. Instantaneous BPM

4.4. SR sensor

The SR sensor receives information from the wireless monitor via the USB Bluetooth module. From this information, it extracts accelerometer data which is used to detect when the test subject has taken a step. It then calculates the amount of steps the subject takes per minute. The following is an overall view of the SR sensor:

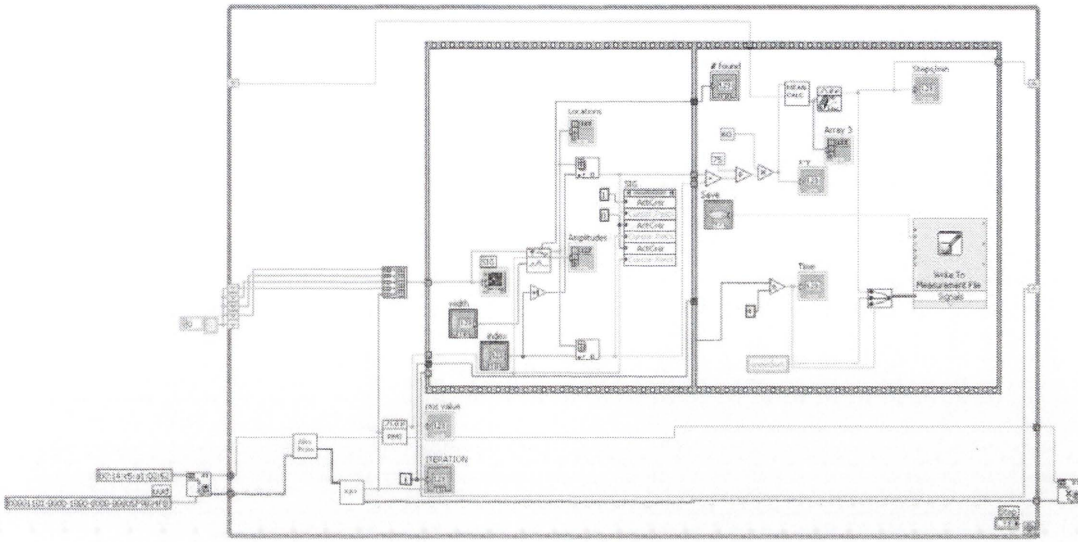


Figure 4.16 Overview of step rate sensor

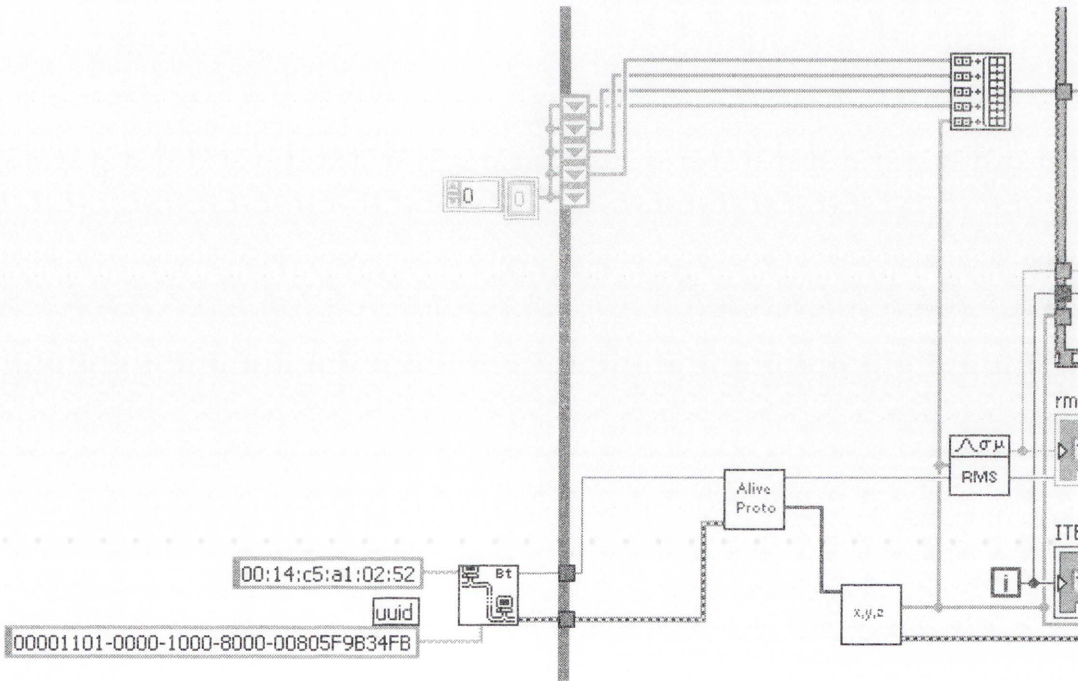


Figure 4.17 Step rate sensor initialisation

The first section of the SR sensor works similarly to the HR sensor. The USB Bluetooth module is initialised and data is read in from the wireless monitor. After this point, accelerometer data is extracted from the Alive ECG monitor protocol and sent to the XYZ block.

The XYZ block processes the accelerometer data and separates it into its three axis readings. For the purpose of the SR sensor, only the readings from the Y-axis are required. Since the test subject is running on a treadmill, the readings from the X-axis and Z-axis will be minimal and of no use. The Y-axis readings will provide the information on the vertical movement of the test subject which can be analysed to determine when a step occurs. The Y-axis reading is then sent to an array builder, to build up a signal consisting of current and previous Y-axis readings. The root mean square (RMS) value of the Y-axis reading is also taken and is used in the next section.

The second section is where steps are detected in the Y-axis accelerometer readings. The array of Y-axis readings are sent to the peak detector block, similar to the one used in the HR sensor. When the Y-axis readings are displayed on a graph, the signal looks similar to that of a sine wave. The steps occur during the rising peaks of the sine wave. This is when maximum positive vertical acceleration is measured by the accelerometer. The peak detector block will determine the time at which a peak occurs. An array consisting of these times becomes the output of the peak detector block. The output of the peak detector block will be sent to two separate index array blocks. The index array block receives an array and an index number and outputs the value in the array location which matches the index number. One of the index array block has an index number equal to the current index, while the other block has an index number equal to the previous index. In effect, these two blocks have extracted the time of the current and previous peak from the array. The information later will be graphed, before moving to the next section. The purpose of this section is to process the information received from the previous section to determine the SR. By receiving the time of the current peak and previous peak, it can be calculated the difference between the two times and then converts them into steps/min. The value will sent to the mean calculator

block to filters out any false values and adds correct values to an array. This array will shift to the median average filter block, to provide an instantaneous value for SR.

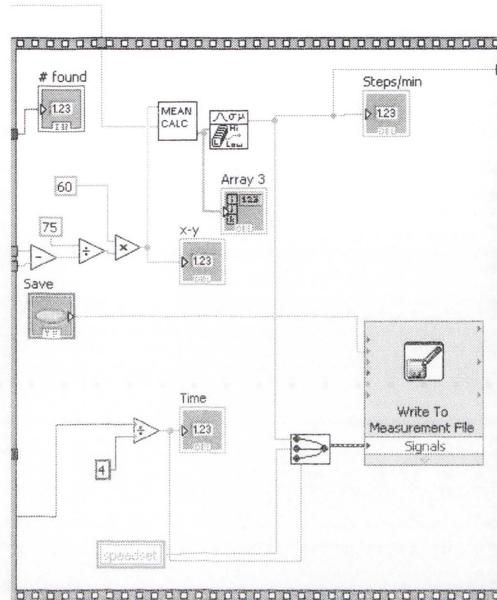


Figure 4.18 Mean calculator in step rate sensor

4.4.1. SR sensor accuracy tests

For the SISO and MIMO controllers, SR data is continuously sent from the SR sensor to the controller, to determine automatic treadmill settings. It is important to run an accuracy tests to examine whether the SR sensor is stable for the whole system.

The test is conducted with the test subject running on the treadmill for durations of 30 and 60 seconds, as well as speeds of 3, 5 and 7 km/h. The treadmill gradient was maintained at 2%. SR sensor accuracy tests are conducted by comparing the SR sensor readings to other methods of SR detection. Other methods use included pedometers and manual counting. Above all, these methods are counted the amount of steps over a set period of time. SR could easily be calculated by dividing the amount steps by the time elapsed. Three

pedometers are used in the test and are attached on the front, right and left of the test subject's body. The manual count is calculated by the treadmill operator. A total of six tests were conducted with the results shown below:

Table 4.1 Treadmill speed at 3km/h

Test Time	30 sec				
Average Step Rate Sensor reading (steps/sec)	Manual Count	PM Left	PM Front	PM Right	Average Error
2.67	2.73	2.63	2.67	2.77	1.14%

Test Time	60 sec				
Average Step Rate Sensor reading (steps/sec)	Manual Count	PM Left	PM Front	PM Right	Error
2.66	2.68	2.75	2.71	2.73	2.11%

Table 4.2 Treadmill speed at 5km/h

Test Time	30 sec				
Average Step Rate Sensor reading (steps/sec)	Manual Count	PM Left	PM Front	PM Right	Error
2.71	2.66	2.66	2.73	2.76	-0.30%

Test Time	60 sec				
Average Step Rate Sensor reading (steps/sec)	Manual Count	PM Left	PM Front	PM Right	Error
2.74	2.73	2.63	2.63	2.76	-2.00%

Table 4.3 Treadmill speed at 7 km/h

Test Time	30 sec				
Average Step Rate Sensor reading (steps/sec)	Manual Count	PM Left	PM Front	PM Right	Error
2.84	2.83	2.76	2.96	3.03	1.77%

Test Time	60 sec				
Average Step Rate Sensor reading (steps/sec)	Manual Count	PM Left	PM Front	PM Right	Error
2.8	2.78	2.75	2.81	2.86	-0.02%

From the results, above, it can be seen that the SR sensor is able to detect a similar SR to other detection methods. The highest error is 2.11%, errors found in the tests were very low, making the SR Sensor suitable for the purposes of this project. Meanwhile, for the validation of HR algorithm, POLAR HR monitor has also been tested to compare with the Alive ECG monitor's results. It is found that the difference is ± 4 bpm during moderate exercises, which is within the acceptable level for this study.

Compare with SR algorithm based on Kalman Filter, this SR algorithm in my thesis does not use the assumptions and the statistical information of the motion of human during exercises. There are also some other factors for exercise monitoring, to be considered, e.g., simplicity of algorithms, ease of implementation, flexibility of the control systems. It is recommended that the SR algorithm in my thesis is capable of being carried out in real time to identify SR rate in a feedback loop. The Kalman Filtering based method can be rather time consuming from computational point of view.

4.5. Summary

In this chapter, we proposed the Pan-Tomkins algorithm based on analysis of the slope,

amplitude and width of QRS complexes. This algorithm includes a series of filters and methods that perform filtering, derivation, squaring and integration. The Pan-Tomkins method was invented to reduce interference and noise in the ECG signal. The algorithm produced reliable ECG signal which would allow considerable flexibility and efficiency in changing the speed and gradient on the treadmill. The next part has demonstrated the process of calculating BPM by using the peak detector block in Labview. Mean value block is adopted to minimize the random signal errors from the HR monitor, faulty circuit connections and power supplies. By defining a 20% error margin, the BPM is able to increase consistently.

The last part of the chapter introduces the SR sensor in the Labview program. The SR is associated with walking and running speed in a certain degree. In this study, we observed that the human body has the tendency to slightly vary SR in order to save energy for a constant speed. Therefore, the reference SR is carefully selected and limited to a reachable value. In most of the Multi-variable control case, the major treadmill speed control is mainly depend on the reference of SR and measured SR. Meanwhile, the gradient of treadmill is adjusted gradually based on HR. It is recommended that the reference values of SR and HR should be considered based on exerciser's fitness level. To monitor the SR, sensor accuracy tests are conducted by comparing the SR sensor readings between pedometers and manual counting. Based on the accuracy test results, it is determined that the SR sensor provided reliable measurements for the experiment. These results show that the SR sensor is capable of being applied to the scenarios in the later chapter.

Chapter 5

Control configuration

As mentioned in Chapter 1 and Chapter 2, the treadmill exercise program is equipped with a set of actuators and therefore requires suitable controllers. The aim of the open loop response tests is to observe the control behaviour due to a change in speed or gradient. Based on the results, changes in control behaviour can be observed due to a step input, from which initial K_p and K_i values can be determined for the PI controller. The test subject is required to run for an initial period of time, until the variable being observed is stable. The K_p and K_i values allow us to determine relationships between the variables in a close loop control. After that, four independent SISO control closed loop experiments will be implemented. Section 5.1 presents the introduction of the PID control and describes the proposed concepts of the open loop control. Section 5.2 and Section 5.3 present the open loop experimental results of HR and SR. The control values of K_p and K_i are calculated in Section 5.4. Section 5.5 introduces the SISO Modelling Methodology. The experimental results for the HR and SR SISO control are shown in Section 5.6 and Section 5.7 and followed by a brief summary in Section 5.8.

5.1. PID control design introduction

With its three-term functionality covering treatment to both transient and steady state responses, proportional-integral-derivative (PID) control offers the simplest and yet most efficient solution to many real-world control problems. Since the invention of PID control in 1910 and the Ziegler–Nichols straightforward tuning methods in 1942, the popularity of PID control has grown tremendously. With advances in digital technology, the science of automatic control now offers a wide spectrum of choices for control schemes. However more than 90% of industrial controllers are still implemented based around PID algorithms, particularly at lowest levels. No other controllers match the simplicity, clear functionality, applicability, and ease of use offered by the PID controller. It has been evolving along with the progress of the technology and nowadays it is very often implemented in digital form rather than with pneumatic or electrical components (Astrom 1934).

The controller in our experiments is designed to allow an exerciser to maintain a pre-set HR that promotes cardiovascular development and ensures the safety of the exerciser.

The controller design aimed to achieve this by:

- Raising the HR or SR of the exerciser to the pre-set HR or SR level.
- Maintaining the HR and SR of the exerciser at the present level for the duration of the exercise session by adjusting the speed or gradient of the treadmill.
- Being robust enough to be able to operate with various individuals and at different pre-set HR and SR ranges without modification to the controller.

It is found that a first order model with transport delay is sufficient to get the starting proportional gain (K_p) and integral gains (K_i). The derivative gain (K_d) is not used as it is known that it can lead to large amounts of change in the output if small noise is present, and a derivative filter would lead to a less stable control effort.

The following list specifies the order in which the experiments are undertaken:

- 1) HR open loop response with speed
- 2) HR open loop response with gradient
- 3) SR open loop response with speed
- 4) SR open loop response with gradient

5.1.1. Open loop modelling

The following approach is applied to determine open loop models in this project. As explained earlier, it is concluded that a first order system with transport delay is acceptable in order to provide a starting point to start tuning the controller parameters. Moreover, modelling the system as a first order system with transport delay provides enough key information of how the plant reacts to a step change. It provides us with a basis to compare the different transient and steady state HR behaviour.

Procedure

- Both controlling variables (gradient and speed) are initially fixed at a predefined value.
- Manual control is performed at the predefined fixed values until the HR of the individual is stable.
- After the HR of the individual is stable, one of the controlling signals is switched manually to a step input while the other one remains fixed.

Having defined the maximum safe speed to be 7 km/h, step response is performed in order to determine the parameters of the process reaction. It is determined that a step response of 3 km/h would be used, as this would allow a proper reaction that could be analysed.

5.2. Open loop HR response

Two open loop response tests are conducted for HR with step inputs of speed and gradient. The wireless monitor is attached to the test subject using two ECG electrode pads. The two pads are attached in the top half of the chest and are approximately 3cm either side of the sternum. The VI used in the test is the SR sensor VI with manual speed and gradient control. The HR open loop tests are conducted for 4 mins or more, depending on the time it takes for the HR to be stabilised. The step change would occur once a stable initial SR is measured.

5.2.1. HR open loop response with speed

The step change introduced is from a treadmill speed setting of 3 km/h to 6 km/h and the treadmill gradient is maintained at 2%. The resulting graph from this test is shown below:

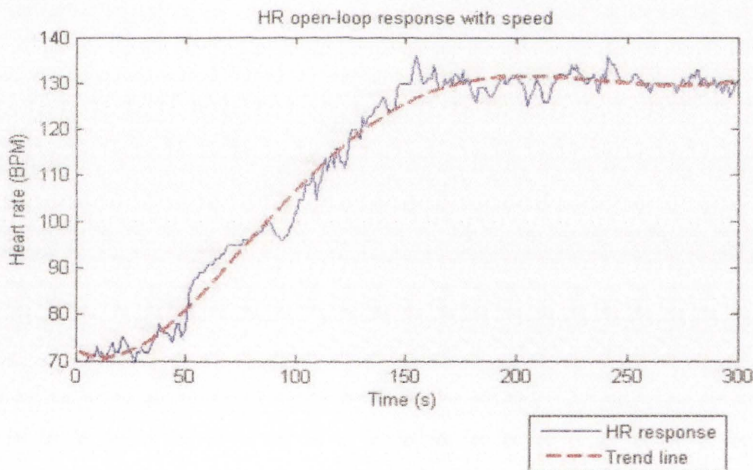


Figure 5.1 HR open-loop response with speed

In this test, the step change is inputted at the 50 seconds mark after HR initially stabilises at around 78 BPM. Afterwards the HR begins to rise steadily, until it stabilises at approximately 130 BPM at 160 seconds. The HR remains at approximately 130 BPM for the remainder of the test without too much fluctuation.

5.2.2. HR open loop response with gradient

The step change introduced is from treadmill gradient setting 2% to 12% and the treadmill speed is maintained at 4 km/h. The result is shown below:

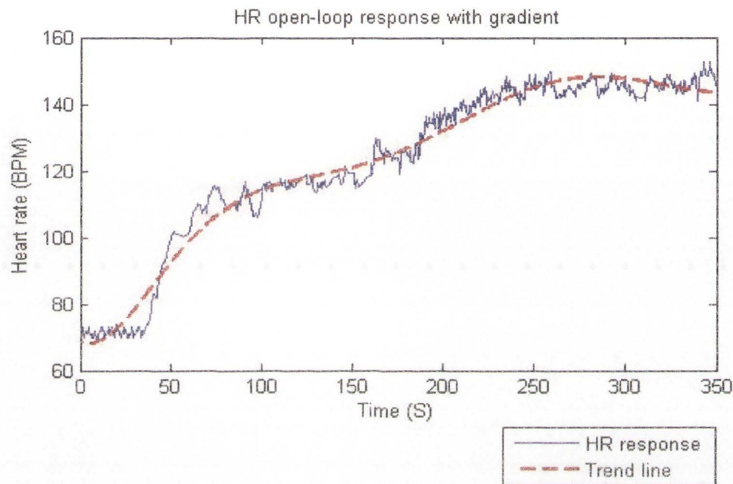


Figure 5.2 HR open-loop response with gradient

In this test, HR is allowed to stabilise initially at approximately 70 BPM before the step change is introduced at 48 seconds. Afterwards, the HR continues to rise steadily until it stabilises at the time of approximately 200 seconds. From this point until around 330 seconds, HR is maintained at 140 BPM and fluctuates around 5 BPM at this point for the remainder of the test.

5.2.3. Open loop HR response discussion

The results from open loop HR response indicate that the Labview designed controllers worked effectively to control the HR to the referenced level. For the different test subjects, the controller showed that it is able to obtain a minimum amount of overshoot, maintain

steady state error and operate within a certain range for rising time and settling time. It is observed however that for different subject and higher HR, the steady state fluctuated more around the reference rate than for lower HR. The measured results show that in most cases overshoot is kept to a minimum of no more than 5%. This is an important point to notice especially when dealing with the heart that the controller is able to maintain a relatively minimum overshoot and steady state error of no more than 2% so that the heart would not overly exert itself, especially for the case of angina pectoris where over exertion can lead to cardiac arrest.

5.3. Open loop SR response

Two open-loop response tests are conducted for SR with step inputs of speed and gradient. The VI used in the test is the SR sensor VI with manual speed and gradient control. The SR open loop tests are conducted for a period of approximately 2 mins, with the step change occurring on the 1 min mark.

5.3.1. SR open loop response with speed

The step change introduced is from a treadmill speed setting of 3 km/h to 6 km/h and the treadmill gradient is maintained at 2%. The graph for the test from which the PI controller values are determined, is shown below:

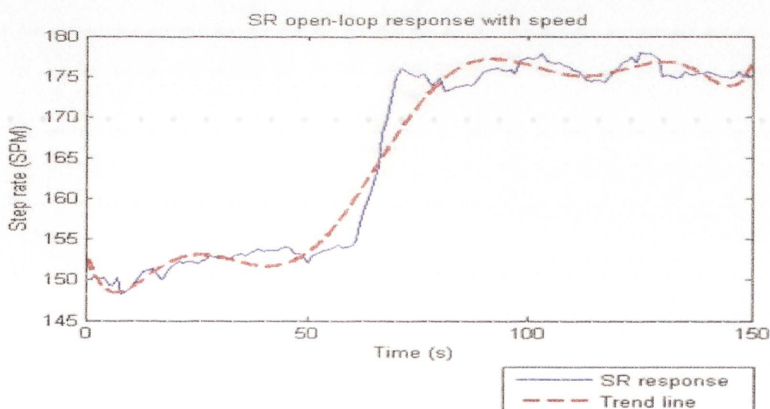


Figure 5.3 SR open-loop response with speed

From the Figure 5.3, it can be observed that when the treadmill speed is at 3 km/h the subject's SR is maintained between 170 and 175 SPM.

5.3.2. SR open loop response with gradient

The step change is from a treadmill gradient setting of 2% to 12% and the treadmill speed is maintained at 5 km/h. This would test the full range of gradient settings allowed for the test subject, as the test is conducted from the lower gradient limit to the upper limit. The graph for this test is shown below:

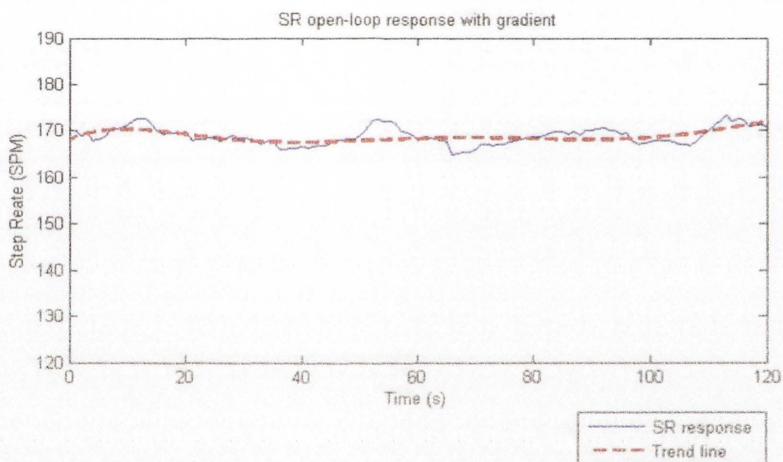


Figure 5.4 SR open-loop response with gradient

The step change is registered by the Labview VI at the beginning, but it can be seen from the graph that a change in SR did not occur. Throughout the test, the subject's SR is maintained between 165 and 175 SPM. From here, it can be suggested that SR is not affected by changes in treadmill gradient.

5.3.3. Open loop SR response discussion

As it is observed in the previous test, the subject's SR behaviour does not change when a step change is introduced. The step change is registered by the Labview VI at 63 seconds and despite this change, the SR is maintained between 168 and 175 SPM. The initial expectation for this test is for SR to decrease as treadmill gradient increased. This expectation can be compared to a runner running on a flat even surface then onto an inclined surface, such as a hill. When the exerciser gets to the hill, their SR slows down to compensate for the increased effort required to run up the inclined surface.

However, this expectation does not apply to treadmill exercise, as the speed of the treadmill is maintained, despite a change in gradient. Because the treadmill speed is maintained, the subject must also maintain their SR. As a result, the extra effort exerted by the exerciser, due to a change in gradient, is evident as an increase in HR.

In conclusion, this test demonstrates that SR is basically affected by the treadmill speed. The fact that SR is not influenced by gradient, that means if the controller is a MIMO system where one output is not affected by one of the inputs. This system characteristic will be utilised to design the MIMO controller.

5.4. Controller values

The K_p and K_i values are determined by analysing the open loop responses and applying the Ziegler-Nichols process reaction method. The following parameters are estimated from the open loop responses:

Table 5.1 Key open loop response parameters

Parameter	Description
T_i	The time at which the step input is introduced
T_r	The estimated time at which the system reacts to the step input
$T_{63\%}$	The time it takes the heart rate to reach 63% of its steady-state value from its initial value
Y_{ss}	The approximate steady-state heart rate
Y_o	The initial heart rate
$Y_{63\%}$	63% of the steady-state heart rate

Once these characteristics are obtained from the graph, the K_p and K_i values for the controllers are calculated using the following formulas:

Nichol-Ziegler Process Reaction Parameters

$$K = \frac{Y_{ss} - Y_o}{U_{ss} - U_o}$$

where is equal to the step change

$$\tau = T_{63\%} - T_r T_d = T_r - T_i R = \frac{K}{\tau}$$

Proportional and Integral Control Values

$$K_p = \frac{0.9}{RT_d}$$

$$K_i = \frac{0.27}{RT_d^2}$$

5.4.1. HR controller values

Taking HR open loop response with gradient as an example, the following Nichol-Ziegler process reaction parameters were estimated:

Parameter	Value
T_i	67s
T_r	78.5s
$T_{63\%}$	104.5s
Y_{ss}	131 BPM
Y_o	110 BPM
$Y_{63\%}$	123.23 BPM

From the parameters, the PI controller values are calculated for the HR SISO closed loop control with gradient:

Sampling time 10 sec

Kp	Ki
0.8	0.02

The same principle could be applied in HR open loop response with speed, the PI controller values are:

Sampling time 10 sec

Kp	Ki
0.02	0.005

5.4.2. SR controller values

Taking SR open loop response with speed as an example, the following Nichol-Ziegler process reaction parameters are estimated:

Parameter	Value
T_i	60.88s
T_r	63s
$T_{63\%}$	64.25s
Y_{ss}	176 SPM
Y_o	151 SPM
$Y_{63\%}$	166.75 SPM

From the parameters, the PI controller values are calculated for the SR SISO closed loop control with speed:

Sampling time 5 sec

Kp	Ki
0.551	0.023

The same principle could be applied in SR open loop response with gradient, the PI controller values are:

Sampling time 5 sec

Kp	Ki
0.262	0.011

5.5. SISO modelling methodology

Before implementing a MISO and MIMO controller, the objective is to implement four independent SISO control tests. Here, we take HR SISO closed loop control with speed as an example. From the open loop tests, initial controller gains are obtained in order to start observing the closed-loop feedback behaviour of the HR of the test subject. Suitable transient and steady state performance, while being driven by a stable control effort, are the objectives of feedback control. A block diagram of the system is shown in Figure 5.5:

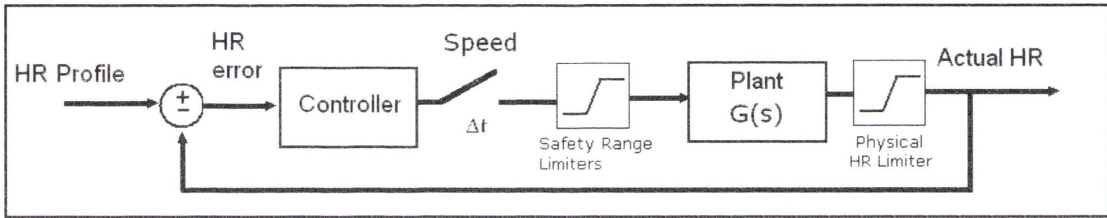


Figure 5.5 SISO PI closed loop control using speed as controlling signal

The original gains of the parameters are discretized using the equation presented in the literature review. The value of Δt is the time intervals to update the control effort. This is selected to be 3 seconds. This is long enough to allow the motor of the treadmill to speed up to its final set-speed before the next value is updated. This is the value used to discretize the controller gains.

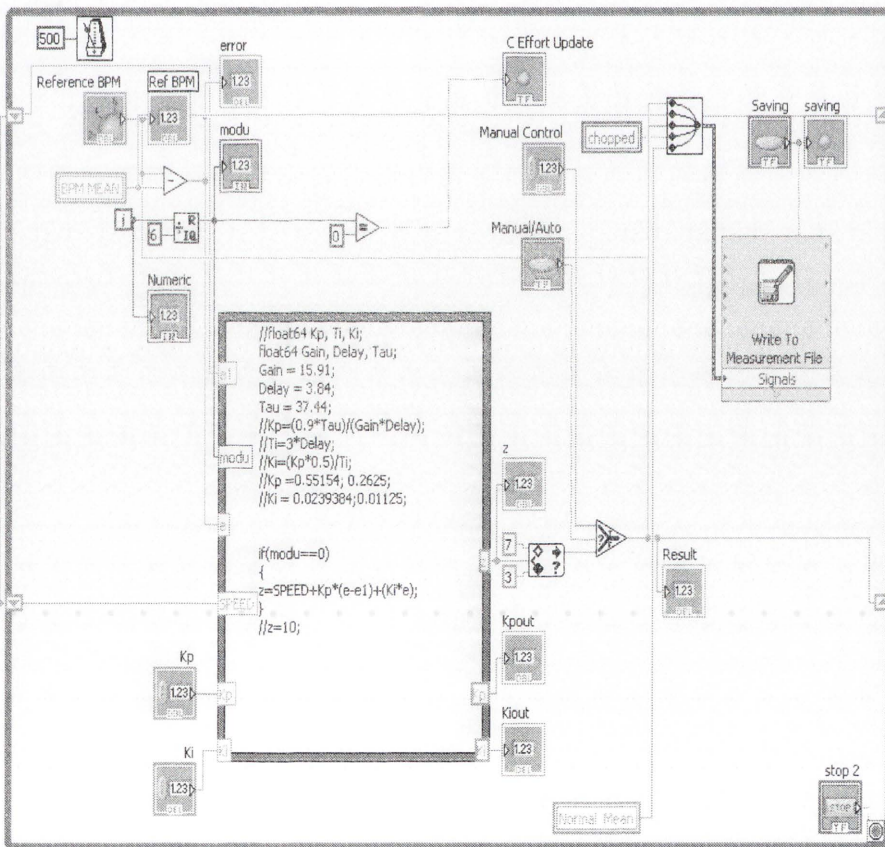


Figure 5.6 Implementation of SISO PI controller in Labview

The following list specifies the order in which the experiments were undertaken:

- 1) HR SISO control response with speed
- 2) HR SISO control response with gradient
- 3) SR SISO control response with speed
- 4) SR SISO control response with gradient

5.6. HR SISO control

The first SISO controller to be implemented, the target is to control the HR of the individual by varying the speed of the treadmill. The procedure is presented below.

HR SISO with speed control procedure:

- The reference input is chosen to be 135 BPM, a reference input that is neither too high nor too low in the HR range.
- The gradient of the treadmill is kept constant at 2%.
- The test subject starts jogging at the minimum speed of 3 km/h.

The next SISO controller is required to control the HR of the individual by varying the gradient of the treadmill. The procedure is presented below.

HR SISO with gradient control procedure:

- The reference input is chosen to be 135 BPM is the same as HR SISO with speed control.
- The speed of the treadmill is kept constant at 4.5 km/h (a suitable running speed around half of the maximum speed range).

- The test subject starts jogging at a gradient of 7% (the midpoint of gradient elevation).

5.6.1. HR SISO control with speed test results

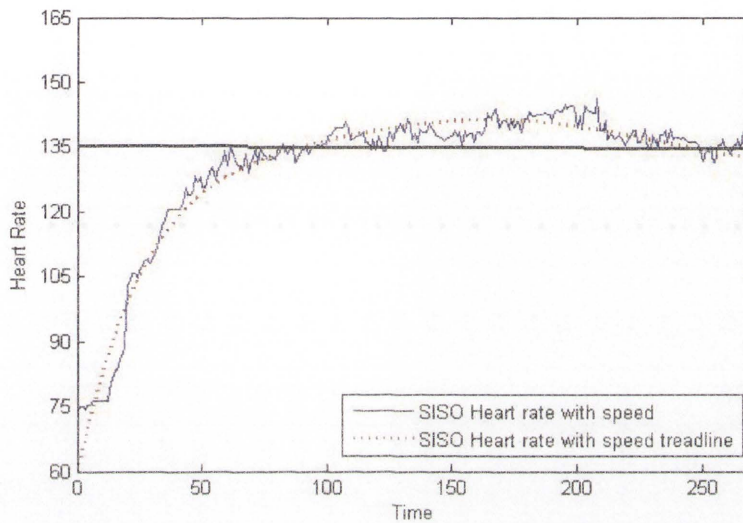


Figure 5.7 HR SISO control with speed control response

Table 5.2 Results of HR SISO control with speed

Controller Performance	Value
Rise Time	52s
5% Settling Time	225s
Overshoot	5.4%
Steady-State Error	+ 4.5BPM

5.6.2. HR SISO control with gradient test results

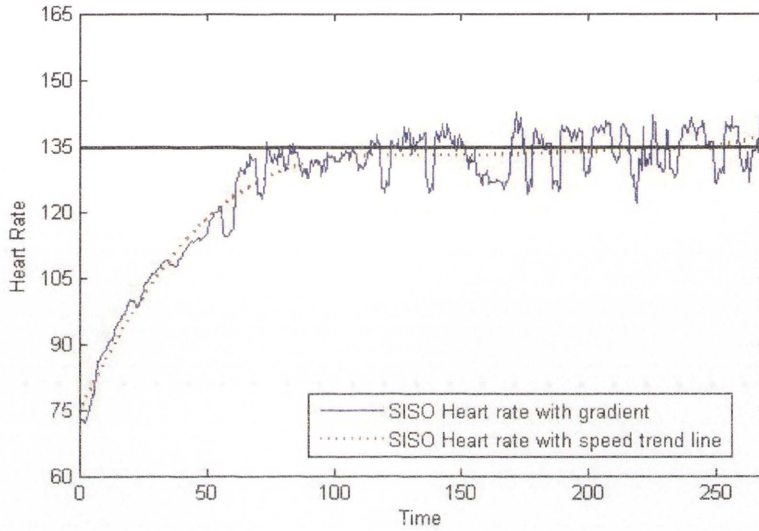


Figure 5.8 HR SISO control with gradient control response

Table 5.3 Results of HR SISO control with gradient

Controller Performance	Value
Rise Time	62.5s
5% Settling Time	107s
Overshoot	6.9%
Steady-State Error	+/- 5BPM

5.7. SR SISO control

The SR controller uses the treadmill speed to control the subject's SR during running. This test is started with the subject running at a set treadmill speed of 3 km/h until a stable SR is being detected. Once the sensor begins displaying stable readings, the SR controller is switched on to control the SR at 170 SPM. The tests will be operated for a duration that is long enough for the controller performance to be observed. For the next experiment, SR with gradient test, the constant speed of the treadmill is set at 4.5 km/h and the reference of the SR is 170 SPM. The initial gradient is setup at 7% while the subject is jogging on the treadmill.

5.7.1. SR SISO control with speed test results

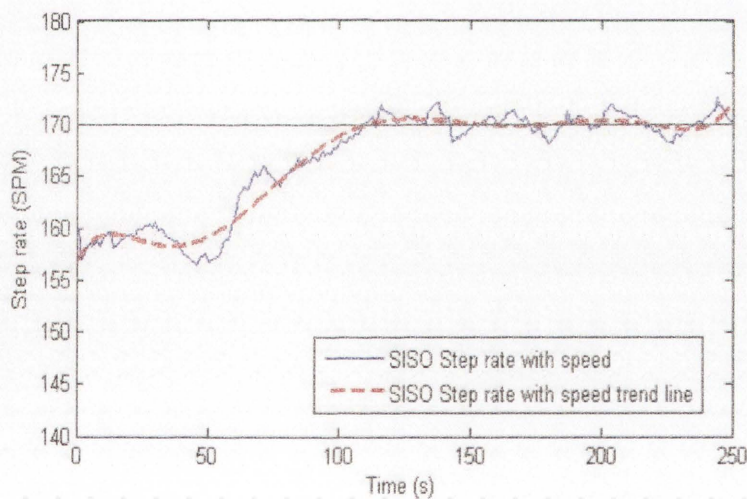


Figure 5.9 SR SISO control with speed control response

Table 5.4 Results of SR SISO control with speed

Controller Performance	Value
Rise Time	52.5s
2% Settling Time	106s
Overshoot	3.7%
Steady-State Error	+/- 6SPM

5.7.2. SR SISO control with gradient test results

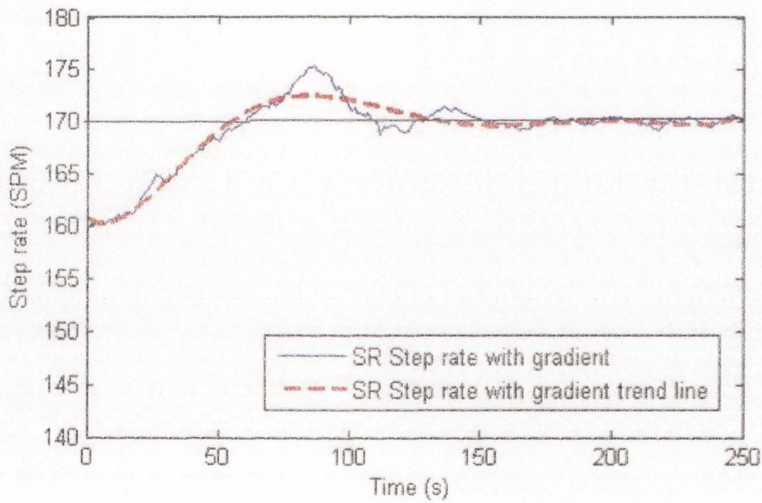


Figure 5.10 SR SISO control with gradient control response

Table 5.5 Results of SR SISO control with gradient

Controller Performance	Value
Rise Time	58s
2% Settling Time	126s
Overshoot	5.5%
Steady-State Error	+/- 5SPM

5.8. Summary

Based on the open loop experimental results shown above and using the Ziegler-Nichols tuning method, the initial PID gain coefficients are determined. By using the standard tuning rules for PID controllers, K_p and K_i values that have achieved acceptable control characteristics were determined. Throughout the HR open loop response experiment, the controller is demonstrated to be able to minimise overshoot, maintain steady state error at a stable level and have a consistent range for the rise time and settling time. SR open-loop response experiments have demonstrated that SR is basically affected by the treadmill speed and not influenced by gradient. Both of these values mean that acceptable K_p and K_i values can be obtained. With proper K_p and K_i values, reliable and efficient closed loop control responses can be achieved.

The SISO controller is designed to be simple, clear and easy to use. According to the control effort in our SISO HR and SR experiments, the graphs display that control effort does not change aggressively. From this, it can be assumed that SISO controllers are suitable for the component of the multivariable control systems. The HR and SR controller have been implemented to produce an acceptable controller response. Despite the existence of steady-

state error, it has been observed that the proposed controllers are able to maintain HR and SR close to the reference. This is achieved through the consistent performance of the SISO controller. An extension of this method to the multivariable systems will be presented in the next three chapters.

Chapter 6

MISO control methodology

In this chapter, two SISO control systems are incorporated to adjust either the treadmill speed or its gradient automatically. This setup makes it possible to achieve a desired HR. The purpose of this experiment is to apply a MISO control system by implementing a control algorithm which includes two PID controllers working simultaneously to track the desired HR profile. The performance of the MISO and SISO control systems are compared through the closed loop responses recorded during experimentation. On the other hand, different exercise zones with related HR reference setting are defined to test the efficiency of MISO control. This chapter is organised as follows. Section 6.1 introduces the MISO modelling methodology. Section 6.2 presents the results of the MISO control and Section 6.3 gives a comparison between SISO and MISO control. Section 6.4 tests the exercise zones by implementing the MISO control with different HR reference settings, followed by the summary in Section 6.5.

6.1. MISO control modelling

The idea of the MISO controller is to incorporate the two independent SISO controllers and work simultaneously to fast track HR profile. Figure 6.1 shows the block diagram of the MISO system.

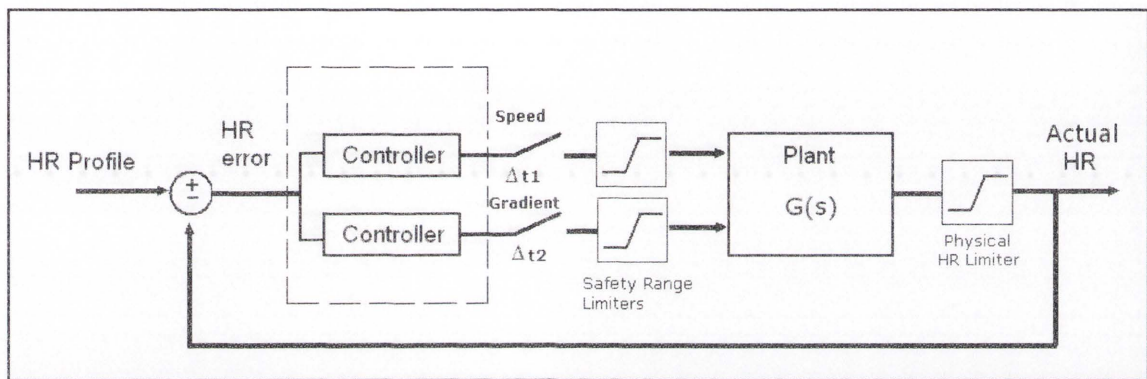


Figure 6.1 Block diagram of the MISO control system

The gains obtained in the SISO cases have been used and combined in the double PI controller. The values of Δt are the time intervals used to update the control effort. These update times are left at 3 seconds for the speed control effort, and 10 seconds for the gradient.

Procedure:

- The reference input is chosen to be 135 BPM, a reference input that is neither too high nor too low in the HR range.
- The speed of the treadmill starts at the minimum speed of 3 km/h.
- The test subject starts jogging at a mid-point gradient of 7%.

Implementation of the MISO controller in the Labview is similar to the SISO cases. After the HR error is computed, it is fed to a formula node where the two PI velocity form equations are implemented. Then, shift registers are used to pass previous values of error and control effort to the next iteration. The while loop is delayed by 0.5s to force each iteration to occur within this interval at all times. Two modules functions are used to signal when 3 and 10 seconds have elapsed in order to update the control efforts. The control efforts are limited by the Labview function to the desired safety ranges.

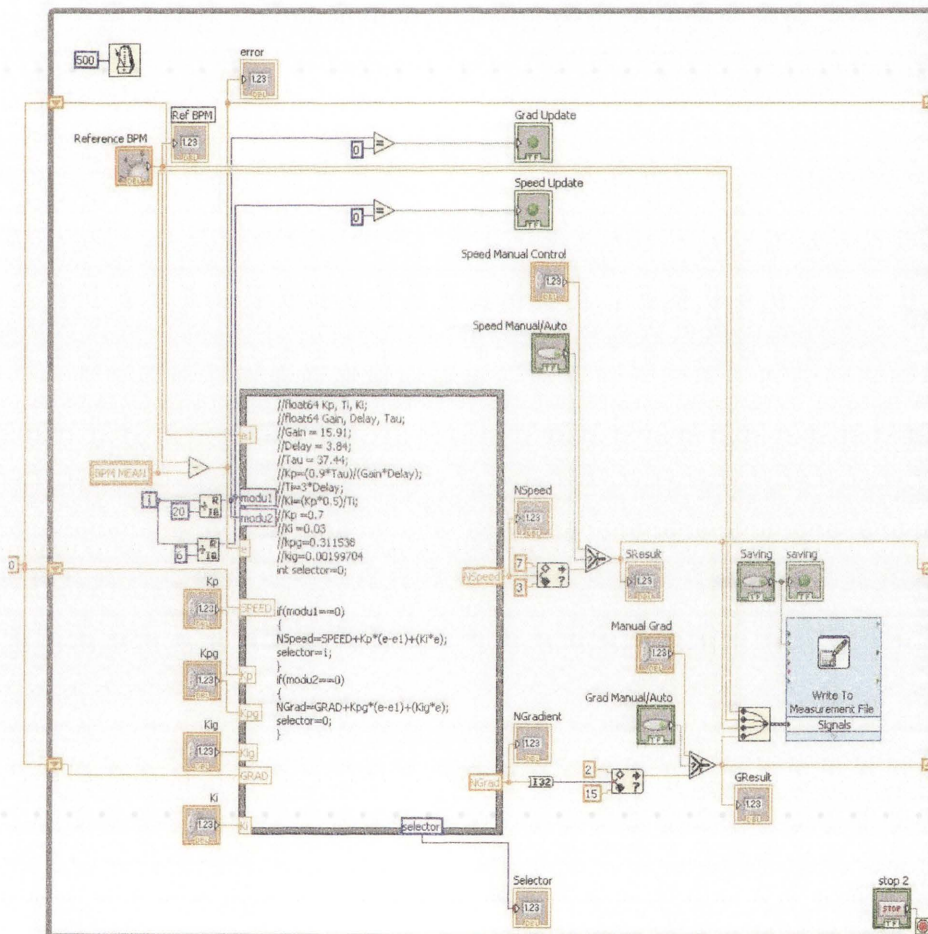


Figure 6.2 Implementation of MISO controller in Labview

6.2. MISO control test results

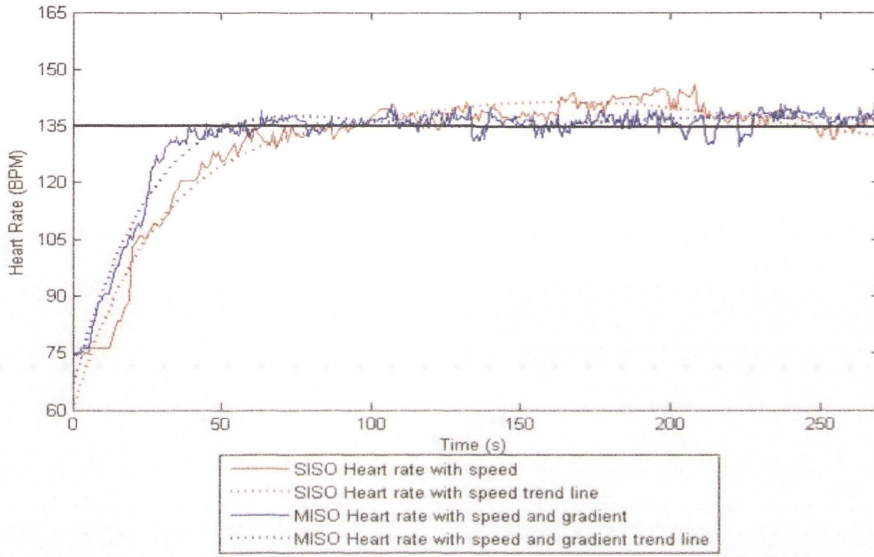


Figure 6.3 Comparison of SISO speed test with MISO control

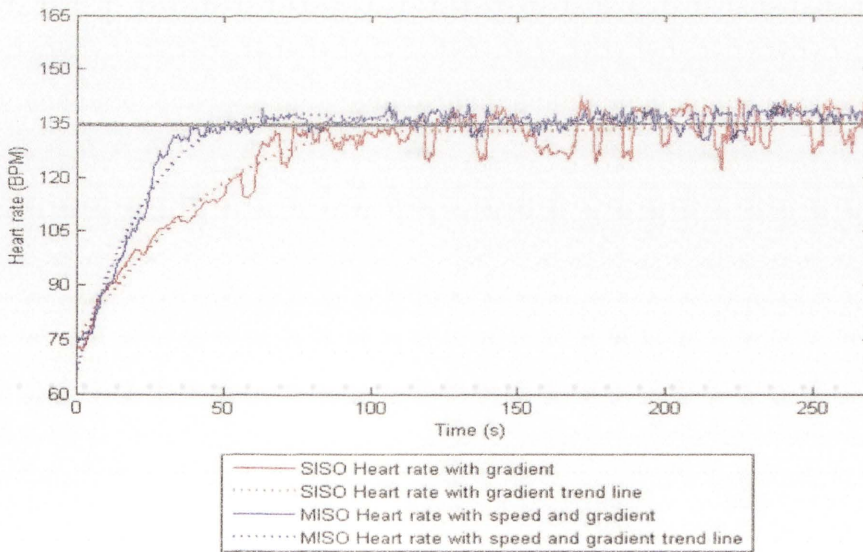


Figure 6.4 Comparison of SISO gradient test with MISO control

6.3. SISO control and MISO control comparison

Using the PID velocity form algorithm with the coefficients outlined in the previous section, the results of two closed loop SISO controllers and one MISO controller were depicted as follows:

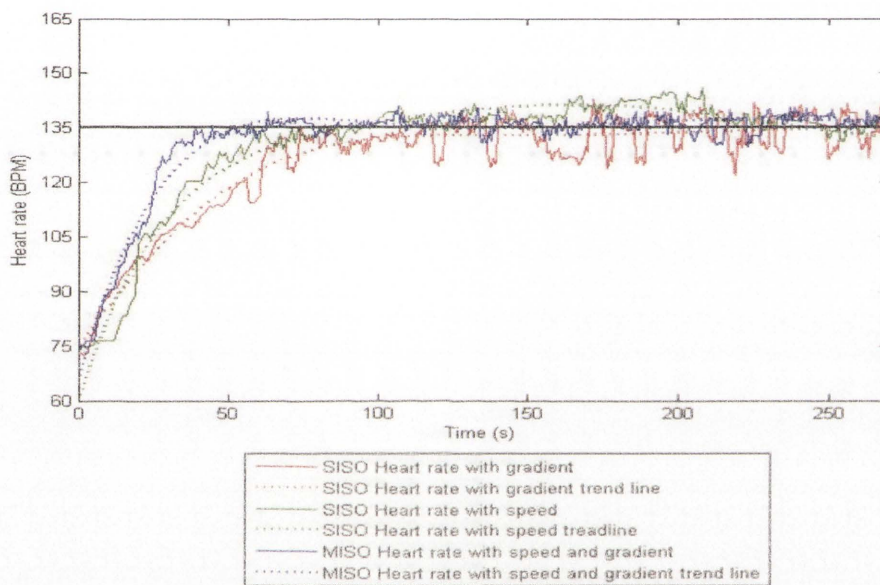


Figure 6.5 SISO and MISO control comparison

Table 6.1 SISO and MISO control comparison table

Description	SISO Speed	SISO Gradient	MISO
Maximum Percent Overshoot	5.4%	6.9%	2%
10-90% Rise Time	52 sec	62.5sec	46
5 % Settling Time	225 sec	107 sec	57s
Steady State Error	+/-4.5 BPMs	+/-5 BPMs	+/-3 BPM
Kps	0.02	NA	0.02
Kis	0.005	NA	0.005
Kpg	NA	0.8	0.8
Kig	NA	0.02	0.02

As we can estimate that after combining speed-input and gradient-input in the MISO control and comparing it with the two SISO controllers in Figure 6.5, the MISO controller has proved that it has faster initial rise time and stays closer to the reference HR during steady-state.

6.4. MISO control in exercise zones

Having selected the MISO control to conduct in this experiment because of its simplicity and stability. The objective of this section is to control the HR to follow a set reference within the exercise zones. The controller is configured to follow the reference setting. The parameters would be tuned to increase the control performance. The idea is to keep the HR within that zone exercise zone in order to maximise efficiency. Three exercisers are assigned to the tests.

Figure 6.6 below shows the exercise zones for the test subject participating in this experiment, whose characteristics were described in the literature review. Due to the physical limitation of the exerciser, the bottom three zones will be tested. This is because testing the aerobic hard core training zone and maximum effort zone require the test subject to have experience of athletes training background. It is not recommended for the regular test subject to stay for a long period of time in the strenuous exercise environment.

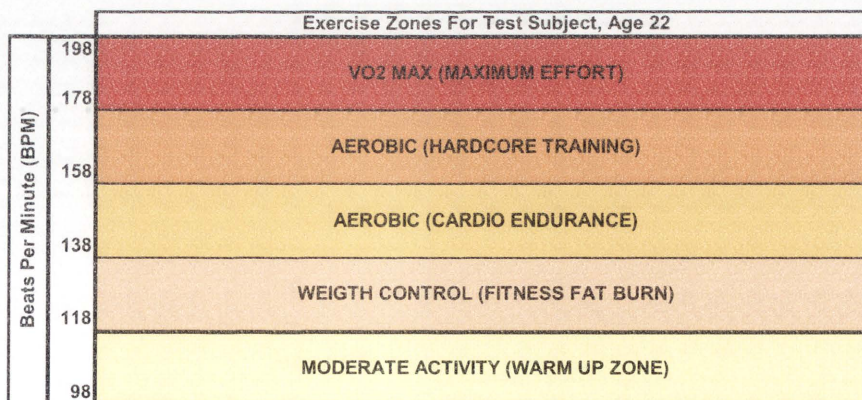


Figure 6.6 Exercise zones for different exercise purpose

6.4.1. Moderate activity exercise zone

The first zoning test is undertaken in moderate activity or warm-up zone. For our test subject, the limits of this zone are 98 - 128 BPM. The reference HR is chosen 108 BPM, which lies in the middle of the zone. The result is shown below:

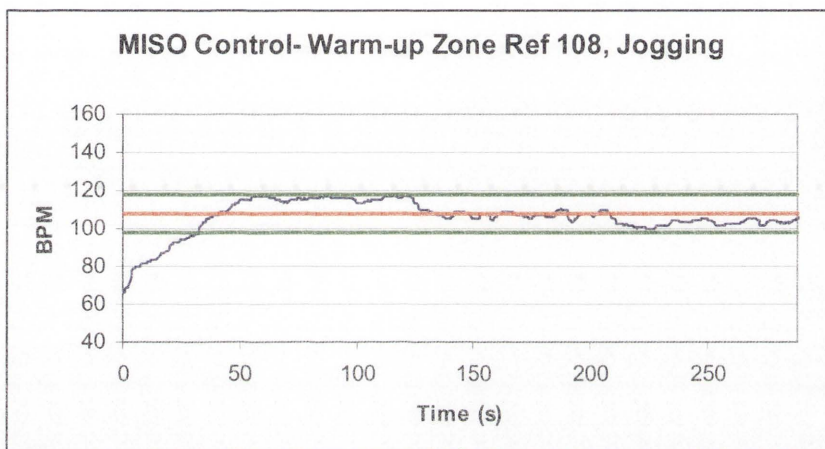


Figure 6.7 MISO control response in the warm up zone

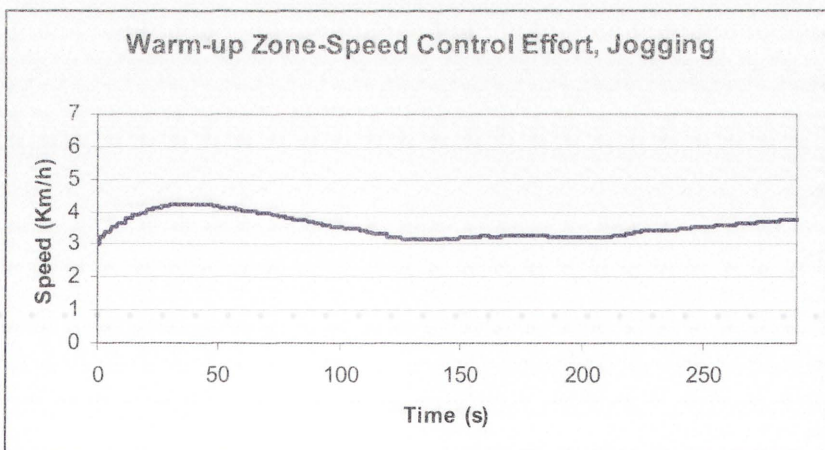


Figure 6.8 MISO control - speed control effort in the warm up zone

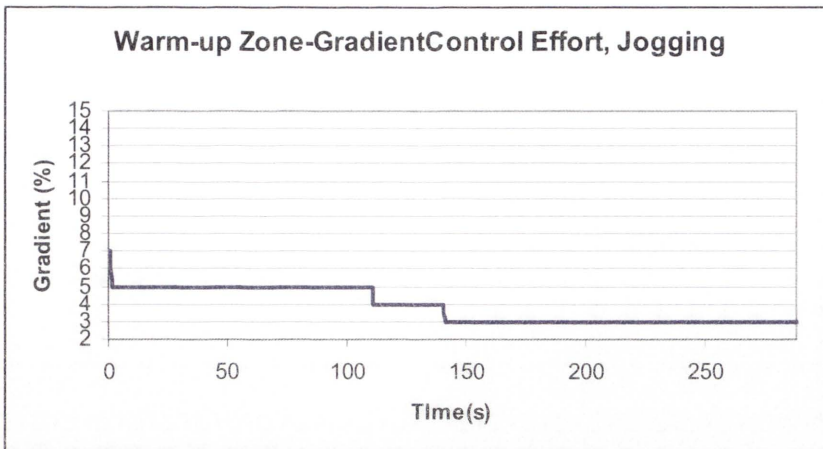


Figure 6.9 MISO control - gradient control effort in the warm up zone

Table 6.2 Performance results of MISO control in warm up zone

Maximum Percent Overshoot	9.4%
10-90% Rise Time	31 sec
5 % Settling Time	130 sec
Steady State Error	+3 BPMs
Kps	0.02
Kis	0.005
Kpg	0.8
Kig	0.02

6.4.2. Weight control exercise zone

The next zone to be tested is the weight control zone. For our test subject, the limits of this zone are 118 - 138 BPM. The reference HR that was chosen is 128 BPM, which lies in the middle of the zone. Several tests are performed with the subject jogging from the beginning. The result is shown in Figure 6.10:

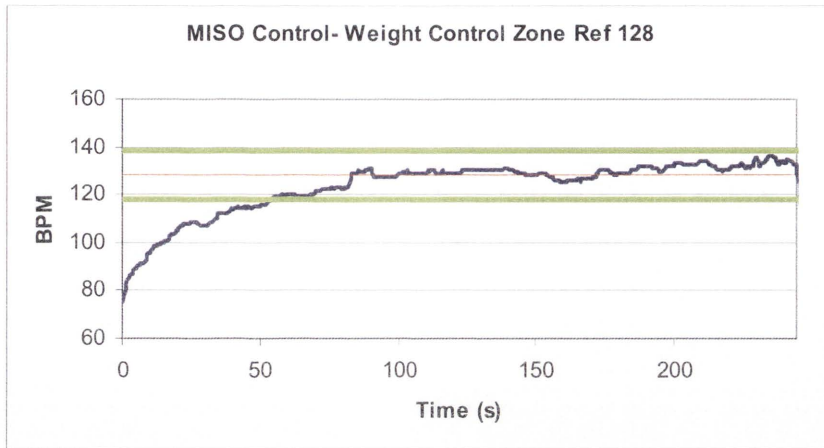


Figure 6.10 MISO control response in the weight control zone

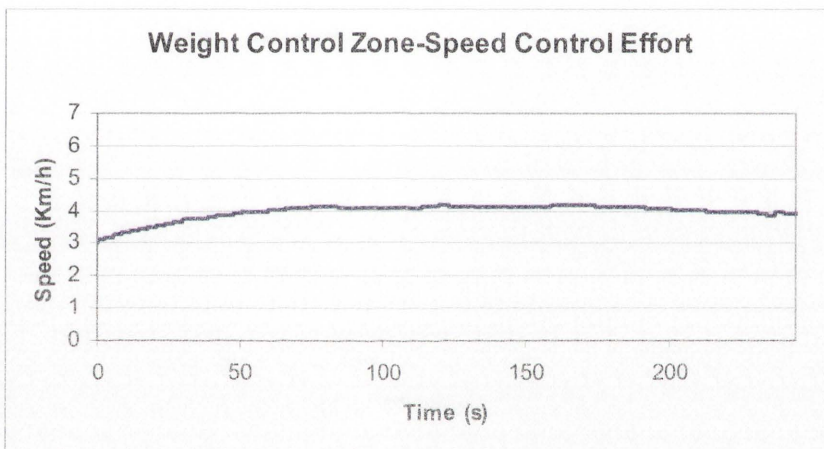


Figure 6.11 MISO control - speed control effort in the weight control zone

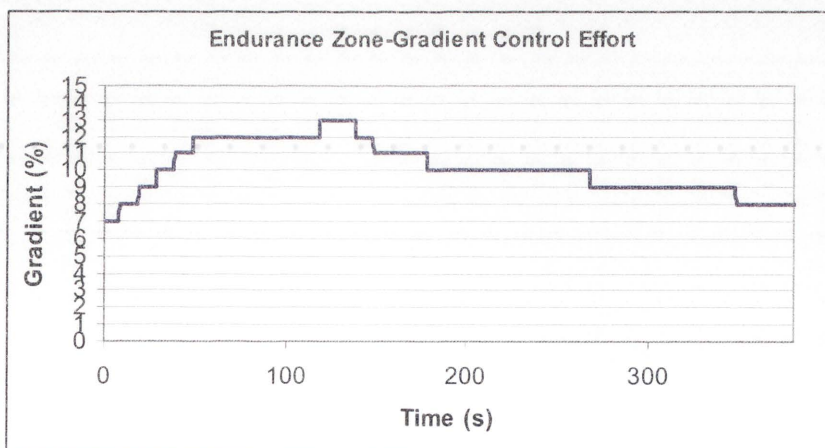


Figure 6.12 MISO control - gradient control effort in the weight control zone

Table 6.3 Performance results of MISO control in weight control exercise zone

Maximum Percent Overshoot	9.4%
10-90% Rise Time	31 sec
5 % Settling Time	130 sec
Steady State Error	+3 BPMs
Kps	0.02
Kis	0.005
Kpg	0.8
Kig	0.02

6.4.3. Aerobic cardio endurance exercise zone

The last zone to be tested is the aerobic cardio endurance zone. For our test subject, the limits of this zone are 138-158 BPM. The reference HR that is chosen is 145 BPM, which lies in the middle of the zone. Several tests are performed with the subject jogging from the beginning. The result is shown below:

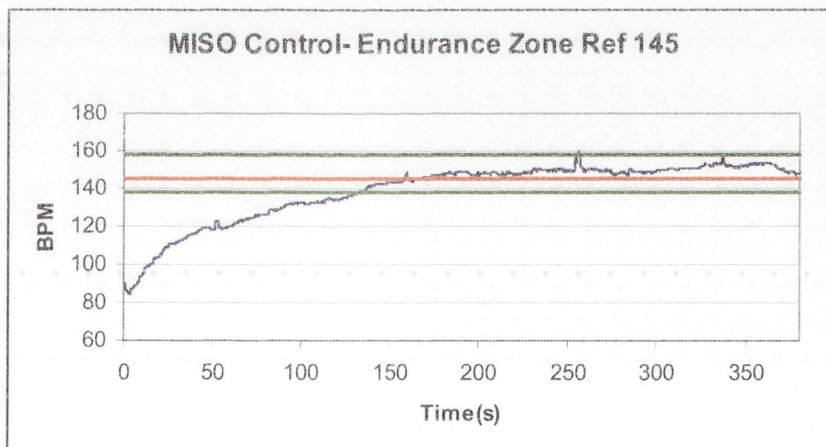


Figure 6.13 MISO control response in the cardio endurance exercise zone

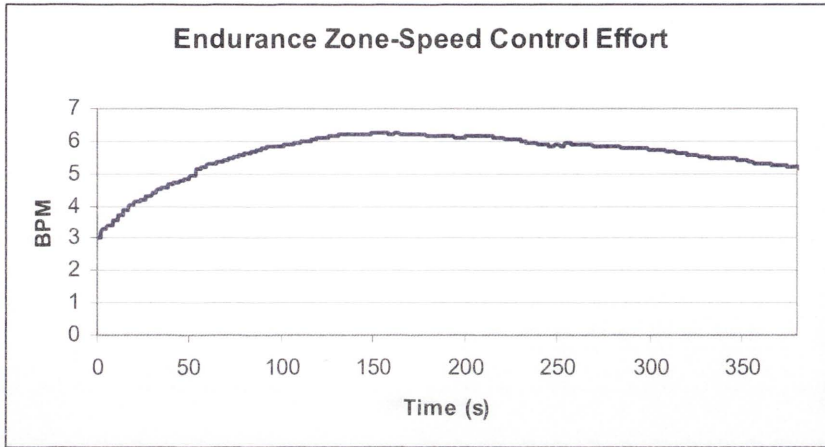


Figure 6.14 MISO control - speed control effort in the aerobic cardio endurance exercise zone

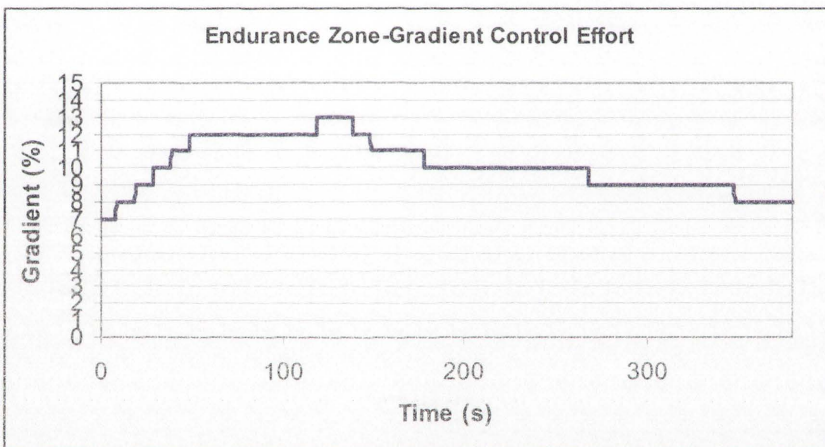


Figure 6.15 MISO control - gradient control effort in the aerobic cardio endurance exercise zone

Table 6.4 Performance results of MISO control in aerobic cardio endurance zone

Maximum Percent Overshoot	4.6%
10-90% Rise Time	146.5 sec
5 % Settling Time	172 sec
Steady State Error	-5 BPMs
Kps	0.02
Kis	0.005
Kpg	0.8
Kig	0.02

6.5. Summary

The main advantage of using MISO control in this experiment is improved HR control. This MISO controller configuration incorporates the key performance features of both the SISO controllers. By combining the SISO controllers together, the results show a short rise time, better steady-state stability and lower steady state error. As well as this, the MISO control reduced the control efforts required from both SISO controllers, which can improve the speed and gradient of the treadmill's ability to change more gradually. To the exerciser, this gradual change in speed and gradient allow their exercise to feel more comfortable and safer. Therefore, when implementing MISO control with speed and gradient as inputs, the controller performed effectively and robustly. It not only improves tracking performance but also prevents overshooting in the HR responses and allows HR to change in a more gradual and stable manner.

It is proved that MISO control in the treadmill exercise can improve the fitness by exercising in several different zones. By selecting different exercise zones to increase the cardiovascular fitness and vary the HR to the desired goals, it is found that this MISO control system can further improve the exercise effect and diversifies treadmill exercise protocols.

Chapter 7

MISO analysis

For HR regulation during treadmill exercises, it has been experimentally demonstrated that simultaneously adjusting both treadmill speed and gradient can achieve better tracking performance. Using two actuators and a multi-loop control structure for the control of a single output variable also has great potential to handle system failures so as to improve the reliability of treadmill based training and rehabilitation. This study provides theoretical analyses to show the benefits of using redundant actuators based on the examination of the steady state characteristics of HR response. This chapter extends nonlinear Decentralized Integral Controllability (DIC) analysis to the non-square process, and provides sufficient condition for HR tracking under multi-loop integral control. It is also experimentally explored HR response in steady state near walking-running transition zone. Simulation results indicate that simultaneously manipulating the gradient and speed can significantly improve the tracking performance in the walking-running transition zone.

This chapter is organised as follows. Section 7.1 gives a brief introduction to Decentralized Integral Controllability. Section 7.2 defines the Multi-loop Integral Controllability (MIC) for a Two-Input Single-Output (2ISO) nonlinear process explaining a sufficient MIC condition based on singular perturbation analysis. The MIC range as well as the transition zone for HR tracking will be presented in this section as well and followed by the summary in Section 7.3.

7.1. Introduction

A multi-loop PID controller based HR tracking system has been presented which simultaneously tuned both treadmill speed and gradient in closed loop, and achieved good performance in previous chapter. However, it is assumed that the HR response to treadmill exercise is in a linear range, and only linear modelling and control approaches were presented. The advantages of using both speed and gradient to regulate HR are therefore only valid in a certain linear response range. This chapter will theoretically analyse the advantage of using two manipulators in terms of nonlinearity near walking-running transition zone of treadmill exercise.

For most linear processes, the control of two correlated inputs and single output can be transferred as a SISO control problem by simply combining the two control inputs as one. However, in engineering practice, nonlinear systems with multiple control inputs are commonly encountered and sometimes it is not proper to combine them as a single input. Besides the process is investigated in this study, another example is the regulation of temperature of a container (such as a chemical reactor), which may apply multiple actuators (such as heaters and fans) to simultaneously control the temperature.

There are several advantages in practice for using multiple (redundant) actuators. Firstly, it can increase the non-saturation range. Real systems always have physical limitations and therefore have limited non-saturation range. If simultaneously execute multiple actuators, the output range can be extended. Secondly, it can increase the maximum gain of the actuator so that fast tracking or regulation of the manipulated variable can be achieved as shown experimentally in previous chapter.

Furthermore, from reliability point of view, redundancy of actuators can facilitate fault accommodation for the implementation of fault tolerant control strategies. For the regulation of HR, multi-loop integral controllers were developed in order to achieve zero steady state

tracking error. For multi-loop integral control of square process, Skogestad and Morari (Skogestad 1992) introduced the concept of Decentralized Integral Controllability (DIC) for evaluating the feasibility of a process to achieve Decentralized Unconditional Stability (DUS), a passive fault tolerant capability. DIC analysis determines whether a multivariable plant can be stabilized by multi-loop controllers, whether the controller can have integral action to achieve offset free control, and whether the closed-loop system will remain stable when any subset of loops is detuned or taken out of service (Yu 1990), (Campo 1994) and (Su 2004).

7.2. Multi-loop integral controllability

This chapter extended the Decentralized Integral Controllability (DIC) analysis for the nonlinear square process to this special non-square (a Two-Input Single-Output) process, and experimentally detected the HR range in which the Multi-loop Integral Controllability (MIC) is valid/invalid. Simulation study is provided to show that simultaneous manipulating of treadmill speed and gradient can significantly improve the tracking performance near walking-running transition zone.

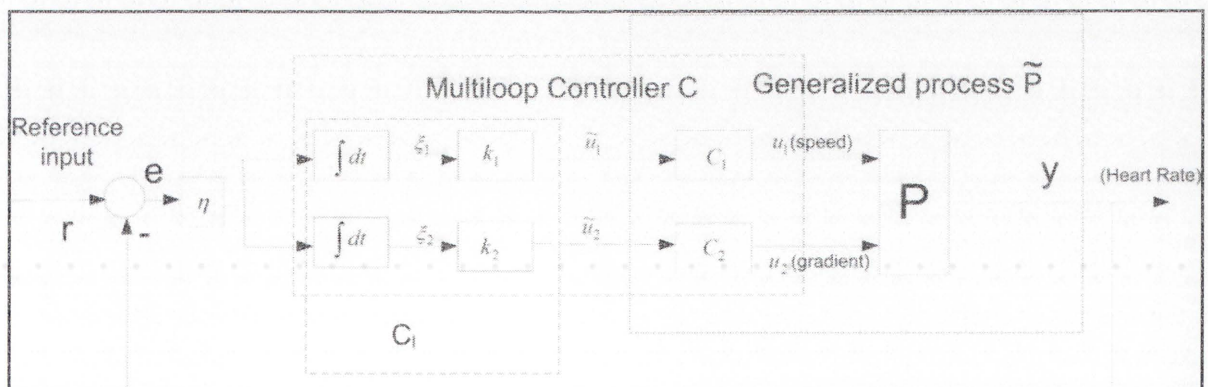


Figure 7.1 Multi-loop integral controllability for a 2ISO system.

7.2.1. Multi-loop integral controllability analysis for HR response

In the previous chapter, multi-loop PID controller has been designed for the regulation of HR response to treadmill exercise. Based on the configuration in previous chapter, we will introduce a definition of MIC for this special non-square process (2ISO), which is a direct extension of DIC concept from square processes to non-square processes.

As shown in Figure 7.1, we assume HR response can be described by the following extensive nonlinear state variable equations with an input vector $u \in \mathbb{R}^2$ and an output vector $y \in \mathbb{R}^1$:

$$R \begin{cases} \dot{x} = f(x, u) & x \in X \subset \mathbb{R}^n, u \in U \subset \mathbb{R}^2 \\ y = g(x, u) & y \in Y \subset \mathbb{R}^1. \end{cases} \quad (7.1)$$

It is assumed that the state $x(t)$ is uniquely determined by its initial value $x(0)$ and the input function $u(t)$. Another assumption made for convenience is that the system (7.1) has equilibrium at origin, that is, $f(0,0) = 0$, and $g(0,0) = 0$. If the equilibrium x_e is not at origin, a translation is needed by redefining the state x as $x - x_e$.

Definition 1 (Multi-loop Integral Controllability for nonlinear 2ISO processes) Consider the closed loop system depicted in Figure 7.1.

(i) For the nonlinear process R described by equation 7.1, if there exists a multi-loop integral controller C , such that the unforced closed loop system ($r = 0$) is Globally Asymptotically Stable (GAS) for the equilibrium $x = 0$.

(ii) Assume each individual loop is detuned independently by a factor k_i ($0 \leq k_i \leq 1$, $i = 1, 2$), and for each pair of multi-loop gain $\{k_1, k_2\}$ the closed loop system is still Asymptotically Stable (AS) for an equilibrium \tilde{x}_e (not necessarily $\tilde{x}_e = x = 0$), then the nonlinear process P is said to be Multi-loop Integral Controllable.

The stability with detuning factor $\{k_1, k_2\}$ for the square process is the so-called "decentralized unconditional stability". A closed-loop system which is decentralized unconditionally stable allows the gains of each controller subsystem to be modified independently by a factor in the range $[0, 1]$ (Su 2007).

It should be noted that for the non-square process under multi-loop integral control the equilibrium varies when the ratio of the detuning factor k_1 and k_2 is changed, which is different with the decentralized integral control for the square process.

In Figure 7.1, we assume the state equation of the general process \tilde{R} (which includes original process R and the two scalar nonintegral controllers c_1 and c_2) is modelled as below (with the same assumptions for process R in equation 7.1).

$$\tilde{R}: \begin{cases} \dot{x} &= f(x, \tilde{u}) \\ y &= g(x, \tilde{u}). \end{cases} \quad (7.2)$$

The state equation for the linear integral controller can be expressed as:

$$C_I: \begin{cases} \dot{\xi} = \begin{bmatrix} \dot{\xi}_1 \\ \dot{\xi}_2 \end{bmatrix} = \eta \begin{bmatrix} k_1 \\ k_2 \end{bmatrix} e = -\eta \begin{bmatrix} k_1 \\ k_2 \end{bmatrix} y \\ \tilde{u} = \xi. \end{cases} \quad (7.3)$$

Here, we assume the initial conditions of the two integrators in Figure 7.1 are zero. Then, it is easy to see that the above equation can be simplified as follows:

$$C_I: \begin{cases} \dot{\xi} = -\eta y = \eta e \\ \tilde{u} = [\tilde{u}_1 \ \tilde{u}_2]^T = [k_1 \ k_2]^T \xi. \end{cases} \quad (7.4)$$

Theorem 1 (Sufficient steady-state MIC conditions for nonlinear 2ISO processes)

Consider the closed loop system in Figure 7.1, and assume that the general process \tilde{R} and the linear part of the controller C_l are described by equation 7.2 and 7.4 respectively. If the following assumptions are satisfied:

(i) The equation $0 = f(x, \tilde{u})$ obtained by setting $\dot{x} = 0$ in equation 7.2 implicitly defines a unique C^2 function $x = h(\tilde{u})$ for $\tilde{u} \in \tilde{U} \subset \mathbb{R}^2$;

(ii) For any fixed $\tilde{u} \in \tilde{U} \subset \mathbb{R}^2$, the equilibrium $x = h(\tilde{u})$ of the system $\dot{x} = f(x, \tilde{u})$ is Globally Asymptotically Stable (GAS) and Locally Exponentially Stable (LES);

(iii) Denote $\tilde{u} = [\tilde{u}_1 \ \tilde{u}_2]^T = [k_1 \xi \quad k_2 \xi]^T$, and suppose the steady-state input output function of the general process \tilde{P} can be factorized as $g(h(\tilde{u}), \tilde{u}) = \psi(\tilde{u})(\tilde{u}_1 - \phi(\tilde{u}_2))$. Assume $\phi(\tilde{u}_2)$ is a unique C^2 function with $\frac{\partial \phi(\tilde{u}_2)}{\partial \tilde{u}_2} \leq \mu < 0$, and $\psi(\tilde{u}) \neq 0$ when $\tilde{u} \in \tilde{U} \subset \mathbb{R}^2$;

Further assume $k_1 \frac{\partial g(h(\tilde{u}), \tilde{u})}{\partial \tilde{u}_1} + k_2 \frac{\partial g(h(\tilde{u}), \tilde{u})}{\partial \tilde{u}_2} > \rho > 0$ (for some scalar $\rho > 0$) for in a neighborhood of $\tilde{u} = 0$, then there exists $\eta > 0$, such that the equilibriums (under different k_1 and k_2) are GAS. That is, if the two scalar controllers c_1 and c_2 can be found such that the generalized process \tilde{P} can satisfy Conditions i), ii) and iii), then the nonlinear 2ISO process is MIC.

Proof: We prove this theorem based on singular perturbation theory (Sepulchre 1996).

Consider the system of Figure 7.1 described by equations 7.2 and 7.4. In order to analyse the Lyapunov stability of the unforced closed loop $(\tilde{P}, -C_l)$, the input signal r is set to zero. The state equation for the closed loop $(\tilde{P}, -C_l)$ can be expressed as:

$$(\tilde{P}, -C_l): \begin{cases} \dot{x} &= f(x, [k_1 \xi, k_2 \xi]^T) \\ \dot{\xi} &= \eta e = -\eta y = -\eta g(x, \xi). \end{cases} \quad (7.5)$$

Equation 7.5 can be transformed into a standard singular perturbation form (Sepulchre 1996): Let $\tau = \eta(t - t_0)$, so that $\tau = 0$ at $t = t_0$. As $\frac{d\tau}{dt} = \eta$, we have:

$$(\tilde{P}, -C_l): \begin{cases} \eta \frac{d}{d\tau} x &= f(x, [k_1 \xi, k_2 \xi]^T) \\ \frac{d}{d\tau} \xi &= -g(x, \xi). \end{cases} \quad (7.6)$$

In order to be consistent with standard singular perturbation notation, we will for the moment use the notation \dot{x} to denote the derivative on the *slow* time scale τ when we analyse singular perturbation models.

Now, for the standard singular perturbation model (see equation 7.6), based on Condition a) and b), the verification of the following two conditions (the first two conditions of Theorem 3.18 in Seppulchre 1996) is straightforward:

(i) The equation $0 = f(x, \xi)$ obtained by setting $\eta = 0$ in equation 7.6 implicitly defines a unique C^2 function $x = h(\xi)$.

(ii) For any fixed $\xi \in P^m$, the equilibrium $x_e = h(\xi)$ of the subsystem $\dot{x} = f(x, \xi)$ is Globally Asymptotically Stable (GAS) (Seppulchre 1996) and Locally Exponentially Stable (LES).

We only need to prove Conclusion (iii) of Theorem 3.18 in (Sepulchre 1996), the stability (GAS and LES) of "slow time scale". That is, the following conclusion needs to be proved:

(iii) The equilibrium $\xi = 0$ of the reduced model (slow time scale) $\dot{\xi} = -g(h(\tilde{u}), \tilde{u})$ is GAS and LES. Where $\tilde{u} = [k_1 \xi \quad k_2 \xi]^T$.

To prove GAS, we select $V(\xi) = \frac{1}{2}(\tilde{u}_1 - \phi(\tilde{u}_2))^2 = \frac{1}{2}(k_1 \xi - \phi(k_2 \xi))^2$ as a Lyapunov function candidate for the "slow time scale" system. It can be seen that:

$$\begin{aligned}\dot{V}(\xi) &= (\tilde{u}_1 - \phi(\tilde{u}_2)) \cdot (k_1 - k_2 \frac{\partial}{\partial \tilde{u}_2} \phi(\tilde{u}_2)) (-g(h(\tilde{u}), \tilde{u})) \\ &= -\psi(\tilde{u}) (\tilde{u}_1 - \phi(\tilde{u}_2))^2 \cdot (k_1 - k_2 \frac{\partial}{\partial \tilde{u}_2} \phi(\tilde{u}_2))\end{aligned}\quad (7.7)$$

As $\psi(\tilde{u}) \neq 0$ when $\tilde{u} \in \tilde{Y} \subset \mathbb{P}^2$, it will be either always positive or negative:

1. When $\psi(\tilde{u})$ is positive and $\xi \neq 0$, it is easy to see that $\dot{V}(\xi) < 0$ as $(k_1 - k_2 \frac{\partial}{\partial \tilde{u}_2} \phi(\tilde{u}_2)) > 0$.
2. When $\psi(\tilde{u})$ is negative, we can change the sign of the general process \tilde{P} by simply changing the sign of the two scalar non-integral controllers c_1 and c_2 simultaneously. Then, the steady state function $g(h(\tilde{u}), \tilde{u})$ becomes $-g(h(\tilde{u}), \tilde{u})$. Thus, when $\xi \neq 0$

$$\begin{aligned}\dot{V}(\xi) &= (\tilde{u}_1 - \phi(\tilde{u}_2)) \cdot (k_1 - k_2 \frac{\partial}{\partial \tilde{u}_2} \phi(\tilde{u}_2)) (g(h(\tilde{u}), \tilde{u})) \\ &= \psi(\tilde{u}) (\tilde{u}_1 - \phi(\tilde{u}_2))^2 \cdot (k_1 - k_2 \frac{\partial}{\partial \tilde{u}_2} \phi(\tilde{u}_2)) < 0.\end{aligned}$$

This ensures the "slow time scale" system is GAS.

To prove Locally Exponential Stability (LES), we simply select $V_L(\xi) = \frac{1}{2} \xi^2$ as a Lyapunov function candidate for the "slow time scale". It can be seen that

$$\dot{V}_L(\xi) = -\xi g(h(\tilde{u}), \tilde{u}). \quad (7.8)$$

It is easy to check both $V_L(\xi)$ and $\dot{V}_L(\xi)$ will satisfy the requirements for LES given that

$$k_1 \frac{\partial g(h(\tilde{u}), \tilde{u})}{\partial \tilde{u}_1} + k_2 \frac{\partial g(h(\tilde{u}), \tilde{u})}{\partial \tilde{u}_2} > \rho > 0 \text{ for some scalar } \rho > 0 \text{ in a neighborhood of } \tilde{u} = 0.$$

Specifically, for $\dot{V}_L(\xi)$, in a neighborhood of $u' = 0$

$$\dot{V}_L(\xi) = -\xi g(h(\tilde{u}), \tilde{u}) \approx -[k_1 \frac{\partial g(h(\tilde{u}), \tilde{u})}{\partial \tilde{u}_1} + k_2 \frac{\partial g(h(\tilde{u}), \tilde{u})}{\partial \tilde{u}_2}] \xi^2.$$

Now, we consider two cases again:

1. For $\psi(\tilde{u}) > 0$ ($\psi(0) = q_1 > 0$) and $\xi \neq 0$, in a neighborhood of $\tilde{u} = 0$, we have

$$\begin{aligned}\dot{V}_L(\xi) &= -\xi g(h(\tilde{u}), \tilde{u}) = -\psi(\tilde{u})(\tilde{u}_1 - \phi(\tilde{u}_2))\xi \\ &\approx -\psi(0) \cdot (k_1 - k_2 \frac{\partial}{\partial \tilde{u}_2} \phi(\tilde{u}_2))\xi^2 < -\rho_{11}\xi^2,\end{aligned}$$

where ρ_{11} is a positive scalar.

2. For $\psi(\tilde{u}) < 0$ ($\psi(0) = q_2 < 0$), the sign of the general process \tilde{P} has been changed by changing the sign of the two scalar non-integral controllers c_1 and c_2 simultaneously. Then, in a neighborhood of $\tilde{u} = 0$, we have:

$$\dot{V}_L(\xi) \approx \psi(0) \cdot (k_1 - k_2 \frac{\partial}{\partial \tilde{u}_2} \phi(\tilde{u}_2))\xi^2 < -\rho_{12}\xi^2,$$

where ρ_{12} is a positive scalar.

Based on Definition 1, we can easily check that a necessary MIC condition for a 2ISO process is each single loop, a SISO system whose input is one of the inputs and output is the single output (with the other input fixed), is DIC respectively. For the HR regulation, the necessary condition is the speed-HR and gradient-HR loops are DIC respectively.

A sufficient DIC condition for a SISO system is its monotone increasing (or monotone decreasing) in steady state. It is easy to see the monotone increasing conditions for each loop

(i.e. $\varepsilon_{imax} \geq \frac{\partial}{\partial \tilde{u}_i} g(\tilde{u}_1, \tilde{u}_2) \geq \varepsilon_{imin} > 0$, $i=1,2$) are sufficient to ensure $0 > -\varepsilon \geq \frac{\partial}{\partial \tilde{u}_2} \phi(\tilde{u}_2)$. In fact,

from Condition iii) in Theorem 1, we can conclude that for the steady-state input output function of the general process \tilde{P} , $g(h(\tilde{u}), \tilde{u}) = 0$ implies that $\tilde{u}_1 = \phi(\tilde{u}_2)$. Then, we have

$g(h(\phi(\tilde{u}_2), \tilde{u}_2)) = 0$. Thus, $[\frac{\partial g}{\partial \tilde{u}_1} \frac{\partial \phi}{\partial \tilde{u}_2} k_2 + \frac{\partial g}{\partial \tilde{u}_2} k_2]\xi = 0$, and $\frac{\partial \phi}{\partial \tilde{u}_2} = -\frac{\partial g}{\partial \tilde{u}_2} / \frac{\partial g}{\partial \tilde{u}_1}$. Considering that

$\varepsilon_{imax} \geq \frac{\partial}{\partial \tilde{u}_i} g(\tilde{u}_1, \tilde{u}_2) \geq \varepsilon_{imin} > 0$, $i=1,2$, we have $0 > -\frac{\varepsilon_{2min}}{\varepsilon_{1max}} \geq \frac{\partial}{\partial \tilde{u}_2} \phi(\tilde{u}_2) \geq -\frac{\varepsilon_{2max}}{\varepsilon_{1min}}$.

For either purely walking (or purely running), it is not hard to see that the monotone increasing of speed or gradient respectively will lead to the monotone increasing in HR, i.e. each single loop is DIC in either walking zone or running zone. In the previous chapter, it is experimentally proved that in walking zone simultaneous manipulating both speed and gradient can achieve fast HR tracking.

However, due to the different motor patterns (Cappellini 2006) of walking and running, HR response in walking/running transition zone would be non-monotone. In the following part, experiments are designed and implemented to investigate the HR response to walking and running around transition speed.

7.2.2. Experiment design

The physical characteristics of all three participants are presented in Table 7.1.

Table 7.1 Subjects characteristics

Subject No.	Age (Year)	Height (cm)	Weight (Kg)
8	26	172	65
Mean \pm STD	\pm 2.5	\pm 3	\pm 5

All subjects are invited to exercise on a motor-controlled treadmill, and they all select 7 km/hour as the speed for which both walking and running are possible. Then, subject is asked to walk for 5 min at 7 km/h for a certain gradient and followed 7 min rest. This procedure is repeated for running as well as for different gradients. During experiments, HR response is recorded by the portable ECG monitor. The averaged steady state HR of the three subjects for both walking and running under different gradients is summarized in Table 7.2.

Table 7.2 HR response at steady state

Gradient (degree)	HR (bpm) Walking at 7 km/h	HR (bpm) Running at 7 km/h
0	108	124
15	121	145
25	136	170

From Table 7.2, it can be seen that for a certain gradient, the heart rate for running is more than 15% higher than that for walking with speed 7 km/h. During exercise, the subjects may switch between walking and running when the treadmill speed is around 7 km/h. So, we find out, for example, when gradient is around 15 degree, the transition zone for HR is between 121 bpm and 144 bpm. When the reference HR is in the transition zone, simultaneous manipulation of speed and gradient would be beneficial as shown in the following illustrative example by simulation.

7.3. Illustrative simulation study

Now, we provide simulation studies for the tracking of HR around transition zone. The reason why we use simulation rather than experiment is the fact that HR reflects not only the relative stress placed on the cardiopulmonary system due to activity, but it can also be elevated by emotional stress (Su 2009). In the experimental condition, it is rather difficult to well control emotional stress of the exercisers around transition zone. On the other hand, in the simulation study, the irrelevant stimuluses of HR can be totally removed so that we can see the transition effects during HR tracking more clearly.

First, we discuss the model of HR response to treadmill exercises which will be used in the following simulation studies. In the control of HR, paper (Su 2007) assumed the HR

response (vs. treadmill speed) can be described by a SISO Hammerstein model, i.e., a static nonlinear function followed by a linear dynamic system. In this study, both treadmill speed and gradient have been applied as control inputs. As shown in (Jamieson 2007), for different speed $v(t)$ and gradient $\theta(t)$, external exercise work rate on treadmill can be simply quantified as: $p(t) = mgv(t)\sin(\theta(t))$.

Therefore, the two control inputs (speed and gradient) together only manipulate one control input variable, external exercise work rate $p(t)$. In order to simplify the analysis of HR response to treadmill exercise, similarly we depict this 2ISO system as a special Hammerstein model as shown in Figure 7.2. In Figure 7.2, the linear dynamic part can be modelled as a first order SISO process: $G(s) = \frac{k}{Ts+1}$, with time constant $T = 35$ sec and steady state gain $k = 1$ as presented in (Su 2007).

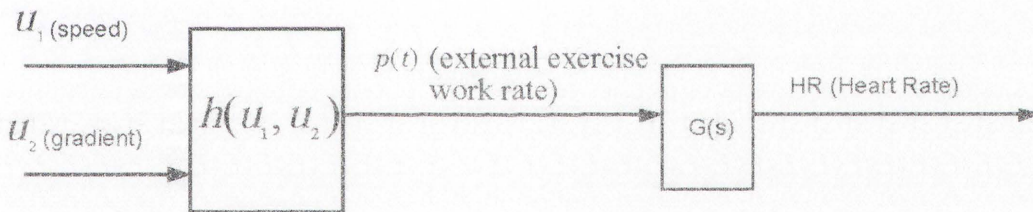


Figure 7.2 The 2ISO Hammerstein system

For purely walking or purely running exercises, according to $p(t) = mgv(t)\sin(\theta(t))$, the static nonlinearity $g(\tilde{u}_1, \tilde{u}_2)$ can be approximately modelled as $p(\tilde{u}_1, \tilde{u}_2) = k_h \tilde{u}_1 \sin(\tilde{u}_2) + p_0$, where p_0 is the Resting Energy Expenditure Rate. Near the transition zone, it will be much complicated. In order to simplify the simulation, we consider the following simple function: $p(\tilde{u}_1, \tilde{u}_2) = p(v, \alpha) = \kappa \cdot [av^3 + bv^2 + cv][\sin(\alpha) + \eta]$, where $\kappa = 0.3487$, $a = 21.3221$, $b = -3.0516$, $c = 0.1453$, and $\eta = 0.75$. When the gradient is fixed as 15 deg ($\alpha = 15$ deg) and assuming the resting HR is 75 bpm, the steady state relationship between treadmill speed and HR is plotted in Figure 7.3.

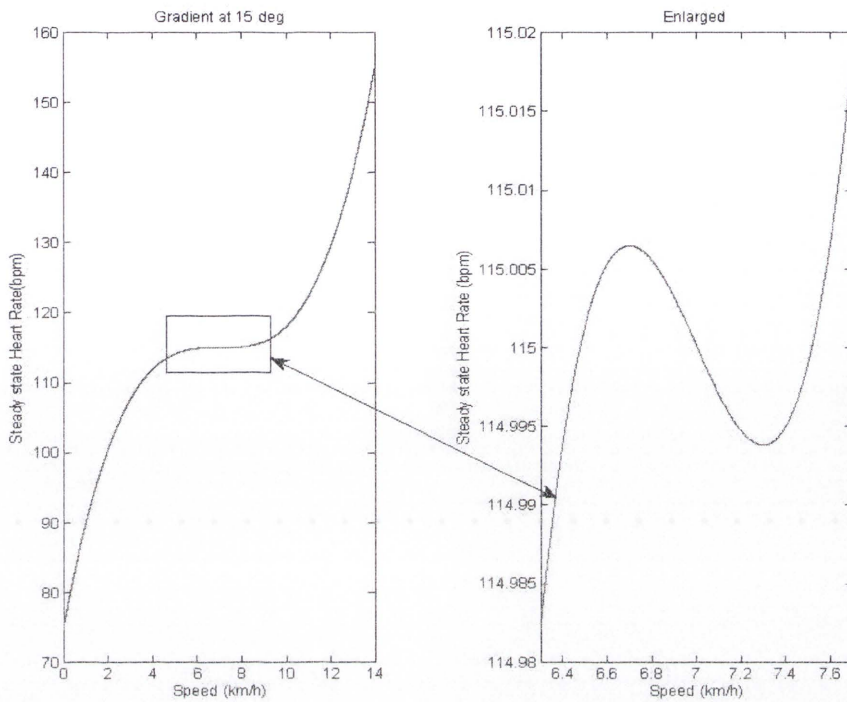


Figure 7.3 Steady state response of heart rate

It should be clarified the parameters of the static nonlinearity presented above is not identified based on experimental data. To achieve a more accurate model of static nonlinearity which includes the walking/running transition, extensive experimental data together with sophisticated modelling methods are required. In this study, our focus is not the modelling of HR response. We investigate the control approach which will handle HR tracking around walking/running zone. Therefore, we constructed a third order polynomial to describe the fluctuation of HR due to the transition of running and walking. During simulation, we added random noisy ($\sigma = 0.8$ bpm) to the HR sensor.

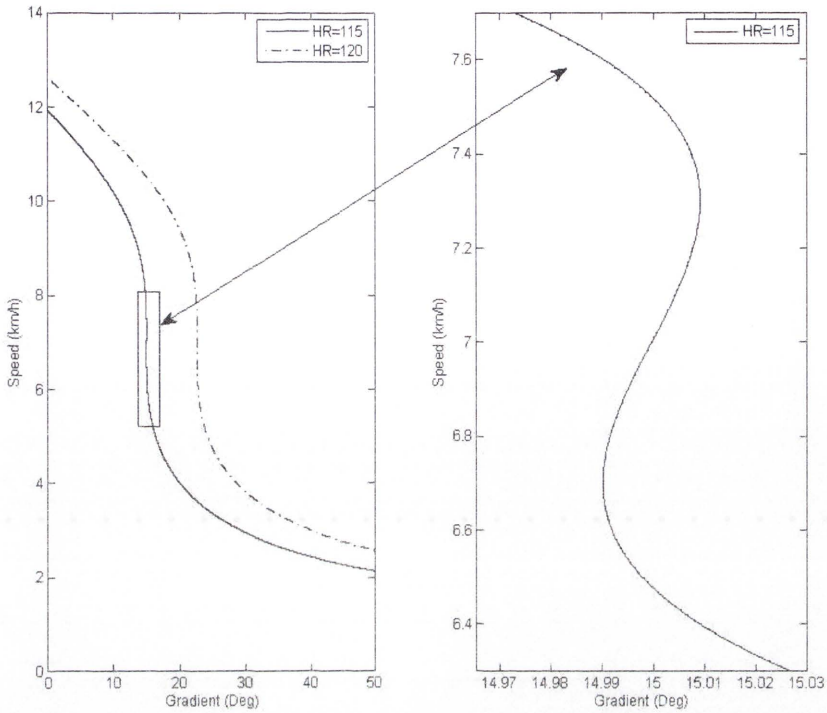


Figure 7.4 The function $u_1' = \phi(u_2')$

As it can be easily checked that $g(h(\tilde{u}), \tilde{u}) = p(\tilde{u}_1, \tilde{u}_2) = p(v, \alpha) = \kappa \cdot [av^3 + bv^2 + cv][\sin(\alpha) + \eta]$, when the HR reference is selected as r_0 , and simply choose $\psi(\tilde{u}) = 1$ (see Theorem 1), then $\tilde{u}_1 = \phi(\tilde{u}_2)$ can be determined analytically or numerically. For the selected HR reference r_0 (115 bpm and 120 bpm), we numerically calculated the function $\tilde{u}_1 = \phi(\tilde{u}_2)$ for each reference HR respectively. As shown in Figure 7.4, in the speed ranges (2 km/h - 6.6 km/h) and (7.4 km/h - 12 km/h), $\frac{\partial \phi(\tilde{u}_2)}{\partial \tilde{u}_2} < -\mu < 0$. However, in the speed range (6.6 km/h - 7.4 km/h), the condition $\frac{\partial \phi(\tilde{u}_2)}{\partial \tilde{u}_2} < -\mu < 0$ is not valid.

The above Hammerstein model has been implemented by using Matlab/Simulink. First, we fix treadmill gradient as $\alpha = 15$ deg, set the reference HR as 115 bpm, the initial speed as $v_0 = 6$ km/h, and select $\eta = 0.001$ and $k_1 = 0.5$ for the speed-HR loop integral controller. Figure 7.5 shows the simulation result for which only speed has been manipulated. From Figure 7.5 we can observe that although the regulated HR is quite close to reference HR, treadmill speed is swinging between 6.2 and 6.9 km/h.

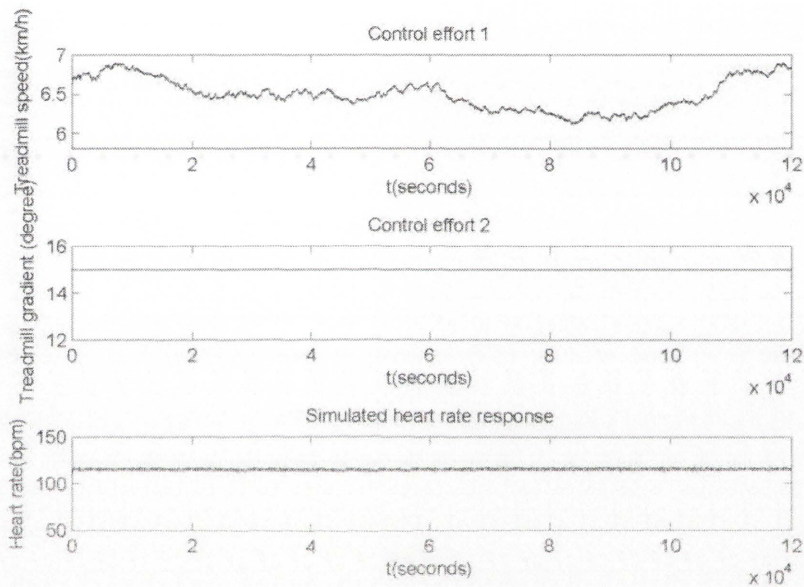


Figure 7.5 Simulation results - adjusting speed only

The speed fluctuation due to the transition of gaits may make the exerciser feel discomfort in real experimental settings. To address this problem, we simultaneously manipulate the gradient by using the gradient regulation loop (with $k_1 = 1$). Simulation result in Figure 7.6 shows the effectiveness of the multi-loop manipulation strategy (i.e. speed fluctuation is well suppressed around 6 km/h). Thus, this simulation study gives us a hint for the avoidance of the transition of motor patterns. That is to intensify the control of treadmill gradient near the transition zone by enlarging the loop gain for gradient-HR loop.

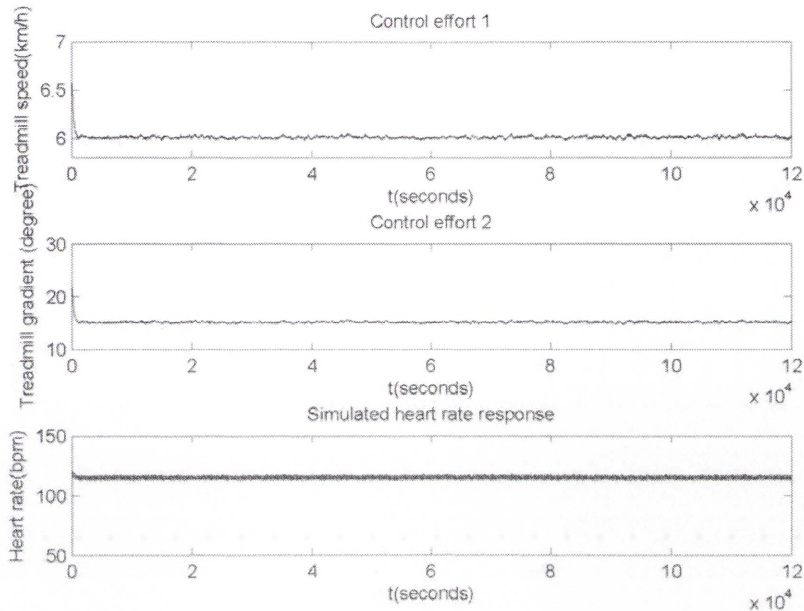


Figure 7.6 Simulation results - adjusting speed and gradient

It should also be noted that due to the closed loop system is Multi-loop Unconditional Stable, the stability of closed loop system is guaranteed for any integral gains $k_1 \in [0,1]$ and $k_2 \in [0,1]$.

7.4. Summary

This study investigates the benefits of using two controller inputs, the speed and gradient, for the regulation of heart rate during treadmill exercises. A main goal is to ensure zero offset tracking errors under faulty conditions. For this purpose, we extended the concept of nonlinear Decentralized Integral Controllability (DIC) to the MISO nonlinear process, and presented a sufficient condition which only needs to check the steady state input-output relationship of under-controlled processes. Based on the proposed condition, we investigate

the new defined Multi-loop Integral Controllability (MIC) for walking, running, and walking/running transition zones. Our simulation study showed that by simultaneously manipulating two control inputs, the automated control system can avoid the transition of motor patterns if the gains of the two multi-loop integral controllers are well tuned.

Chapter 8

MIMO control methodology

The final target in this thesis is for monitoring the proper HR and SR intensity in treadmill exercises, based on closed loop multivariable PID control of speed and gradient. In this scenario, two SISO controllers have been combined to form a MIMO system. Since it is a multiple-input and multiple output system, it is assumed that a MIMO system would outperform the SISO and MISO controllers. This is why investigating a MIMO setup would be of enormous interest in this thesis. The chapter is organized as follows. Section 8.1 introduces the MIMO modelling methodology. Section 8.2 presents the result of the MIMO control experiment. Section 8.3 is focused on aiming to improve the MIMO controller response, followed by the summary in Section 8.4.

8.1. MIMO control modelling

The objective of the MIMO controller is to control both the subject's HR and SR at the same level by varying the treadmill speed and gradient. For this test, the test subject is asked to run on the treadmill. Initially, treadmill speed and gradient are set to 3km/h and 2% respectively. Once stable readings are being obtained by both the HR and SR sensor, the MIMO controller would be switched on and readings from both sensors would be recorded. The reference HR and SR were both set to 160 BPM and 160 SPM respectively. The choosing of the reference value are required to be balanced between reachable values of HR and SR. It can be observed in the SISO closed-loop responses, SR could not go below 150SPM and it is difficult to get HR above 145BPM. In the end a reference value of 160 is chosen because at this SR it is possible that the subject's HR would be able to reach 160BPM with a high gradient.

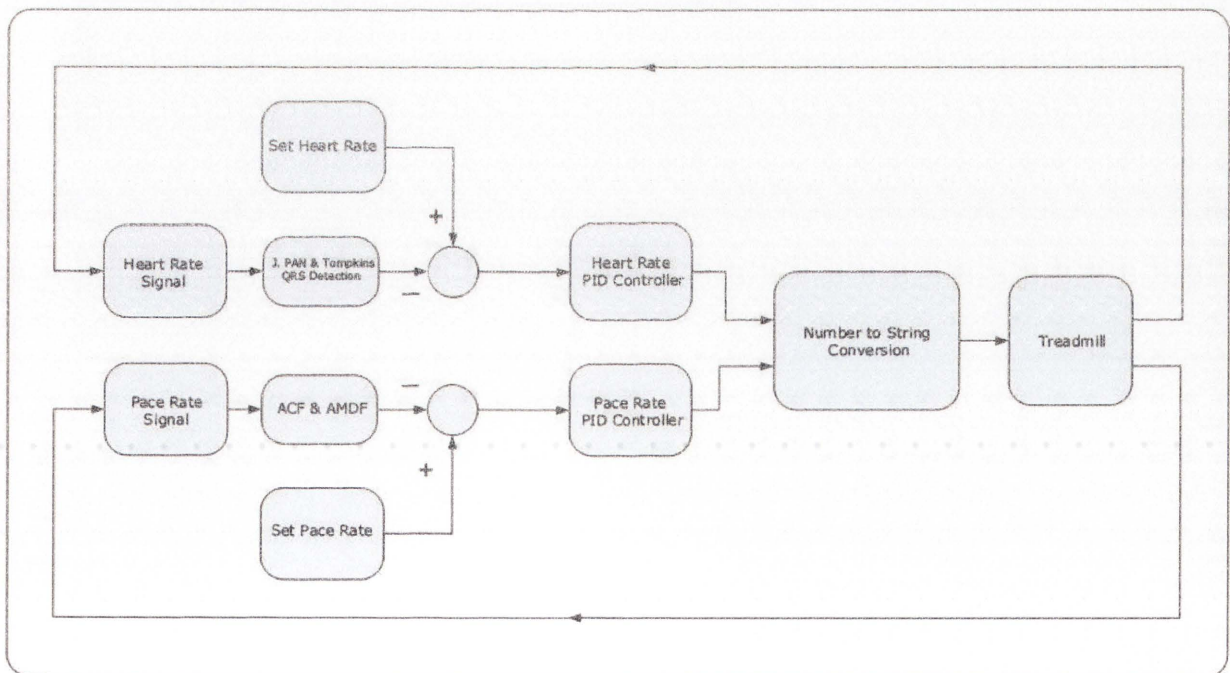


Figure 8.1 The structure of the MIMO control

The MIMO controller in the Labview is a combination of the HR controller and the SR controller. Because the two controllers have similar sections within the VI, e.g. treadmill operating system, these sections have been unified and can react with both controllers. Below are the various sections of the MIMO controller VI.

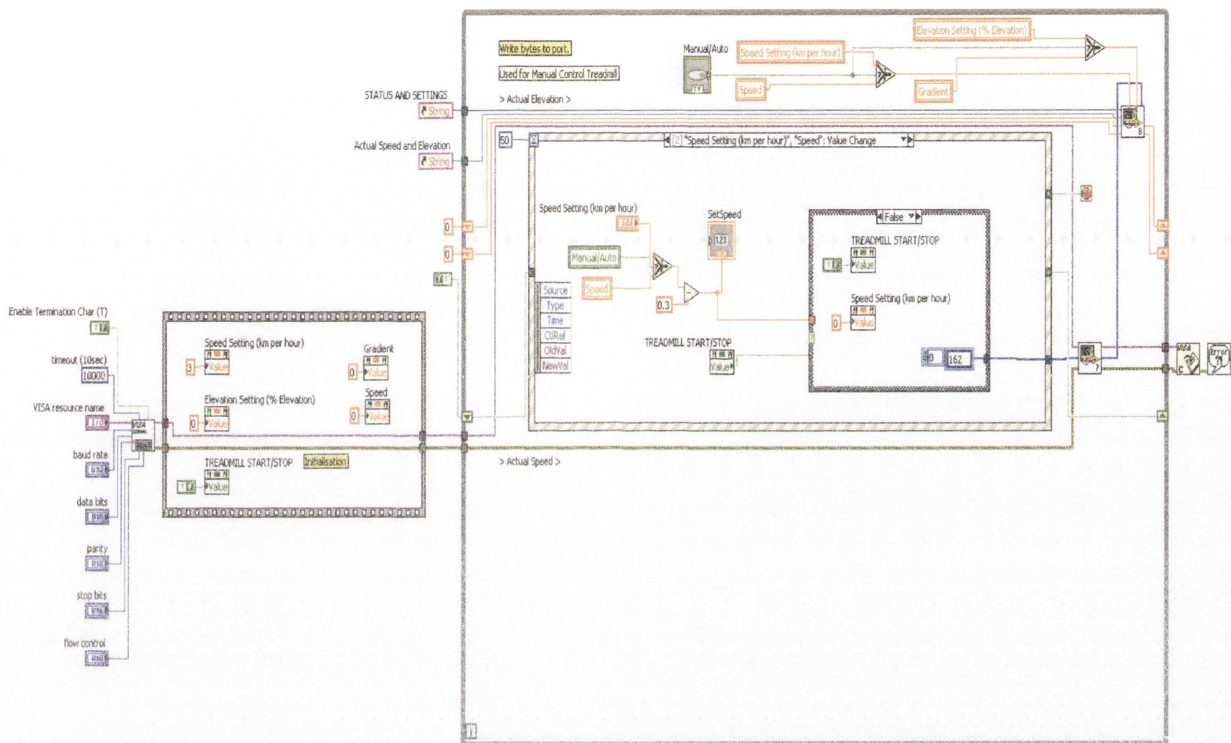


Figure 8.2 MIMO Control - treadmill operating system

The VI section above is the treadmill operating system of the MIMO controller. The initialisation block has been modified to include two variables, speed and gradient. These variables have now replaced result from the output of the HR controller and SR controller respectively.

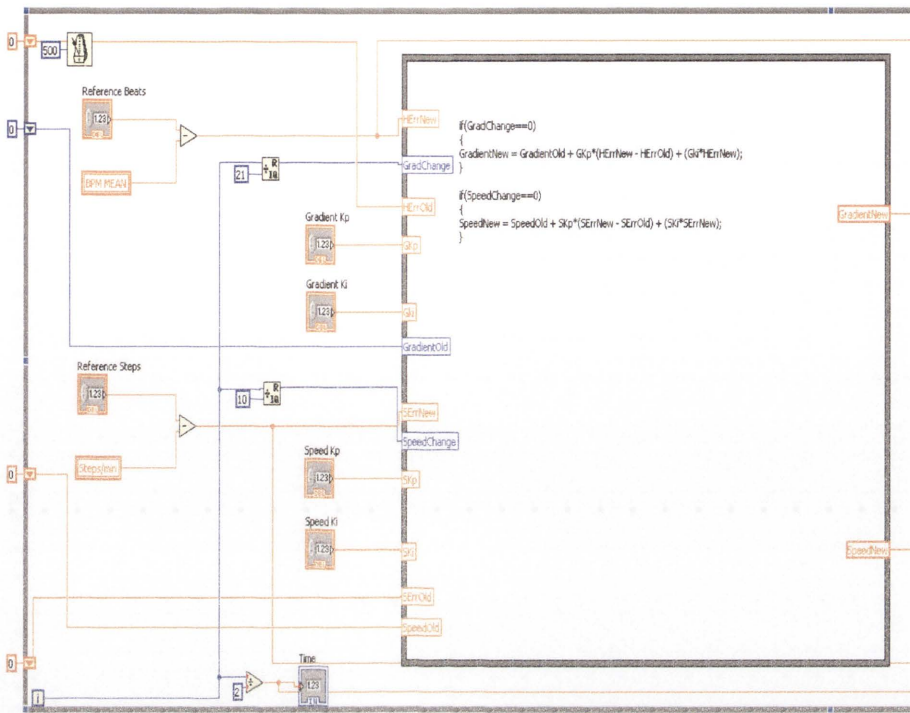


Figure 8.3 MIMO control - control algorithm

The figure above displays the first section of the MIMO control loop. This loop consists of the HR control algorithm and the SR control algorithm. Because both SISO control algorithms have different sampling times, an overall loop delay of 500ms is used. In order to create the required sampling periods for the algorithms, a count system is used to determine the elapsed time by counting loop iterations.

8.2. Test 1 results

The Kp and Ki values used in MIMO controller test 1 are identical to the ones used in the SISO controllers. The MIMO controller response and control effort of both the HR and SR controllers are shown in Figure 8.4:

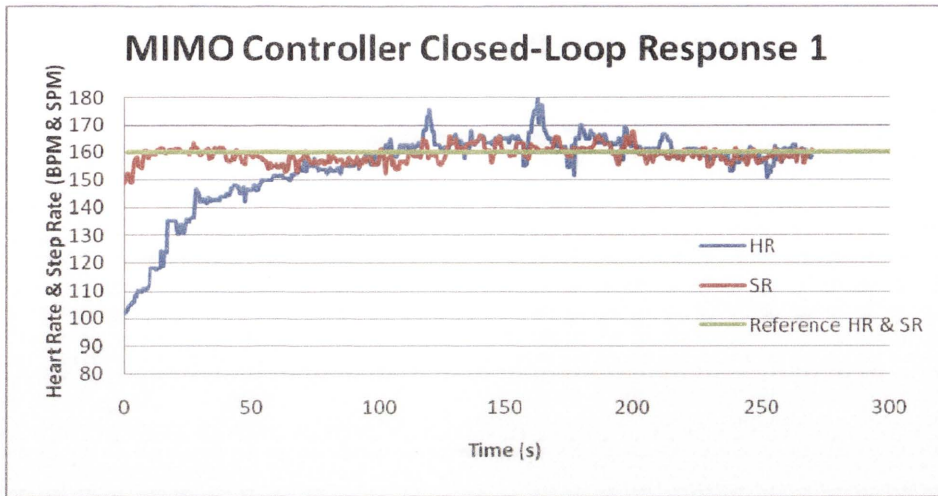


Figure 8.4 MIMO control test 1 - control response

Table 8.1 MIMO control test 1 HR controller performance

HR Controller Performance	Value
Rise Time	150s
5% Settling Time	180s
Overshoot	12.5%
Steady-State Error	+/- 10BPM

Table 8.2 MIMO control test 1 SR controller performance

SR Controller Performance	Value
Rise Time	27s
5% Settling Time	102.5s
Overshoot	4.7%
Steady-State Error	+/- 5SPM

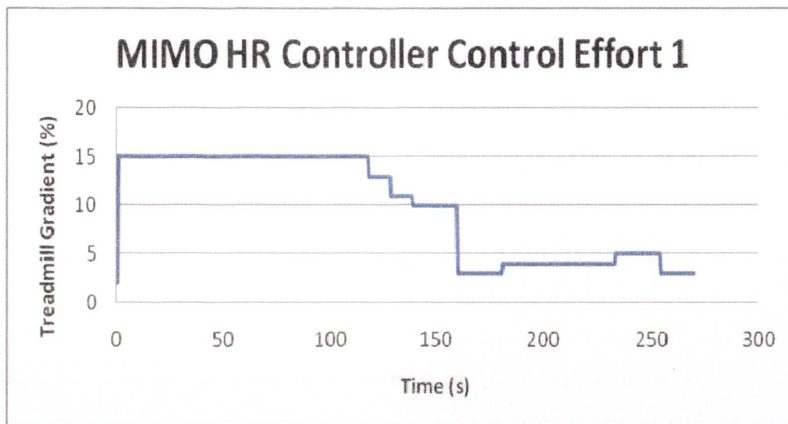


Figure 8.5 MIMO control test 1 - HR controller control effort

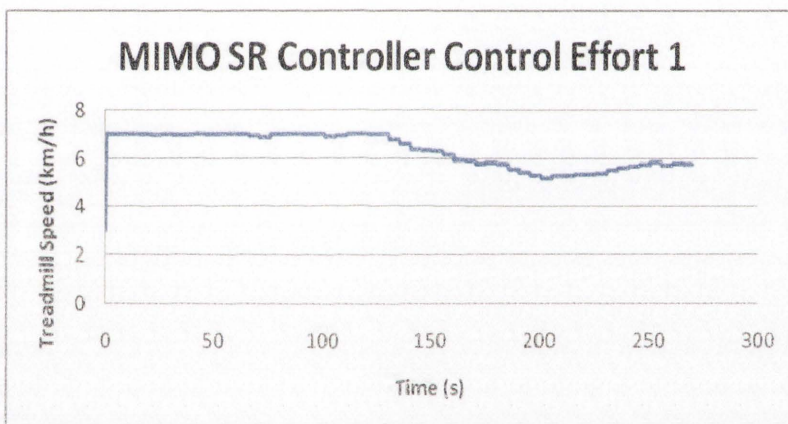


Figure 8.6 MIMO control test 1 - SR controller control effort

From the above graphs, it can be observed that the controller is able to control both HR and SR reasonably well. The initial response of the HR controller is very slow, with the rise time and 5% settling time of the HR controller occurring well after that of the SR controller. It can also be observed that overshoot and steady-state error are slightly high due to sudden rises and drops in HR.

With the SR controller, the response rises very quickly, but takes some time to settle due to some initial oscillation. However, overshoot is low and once the SR reaches steady state, the SR controller maintains it with minimum error.

Despite this reasonable controller response, some cause for concern is the fact that both control efforts saturate very early during the tests. It can be observed that both controllers immediately rise to their respective control limits until their control variables begin to settle. At this point in time, the control efforts drop before maintaining at a certain value.

8.3. Test 2 results

The second test is conducted to try and improve the MIMO controller response. A main issues observed in test 1 was the very slow HR controller response and saturated control efforts. It is preferred that the HR controller settles slower than the SR controller so that the effects of the SR controller on HR are considered by the HR controller. But in the first MIMO test, the HR controller response was very slow. Even though the SR controller settled before the HR controller, it would be better if the HR controller responded slightly faster. This would slightly improve the overall performance of the MIMO controller by allowing the MIMO controller to settle faster.

The saturation of the control efforts did not occur during the SISO tests, so it was unexpected that they would occur during the MIMO tests. Despite the fact that the controller limits are comfortable treadmill settings for the test subject, it is preferred that the controller does not immediately rise to its limits. An immediate limit rise is not an ideal controller characteristic.

After tuning the MIMO controller, the new K_p and K_i values are obtained for the HR and SR controllers. The Figure 8.7 displays the MIMO controller response and control efforts of the HR and SR controllers:

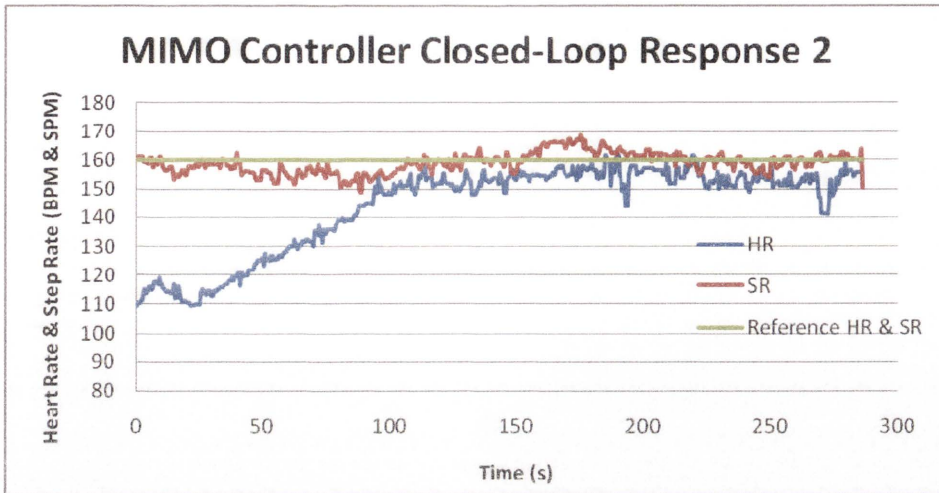


Figure 8.7 MIMO control test 2 - control response

Table 8.3 MIMO control test 2 HR controller performance

HR Controller Performance	Value
Rise Time	113s
5% Settling Time	61.5s
Overshoot	1%
Steady-State Error	+/- 10BPM

Table 8.4 MIMO control test 2 SR controller performance

SR Controller Performance	Value
Rise Time	176s
5% Settling Time	176.5s
Overshoot	5.4%
Steady-State Error	+/- 6SPM

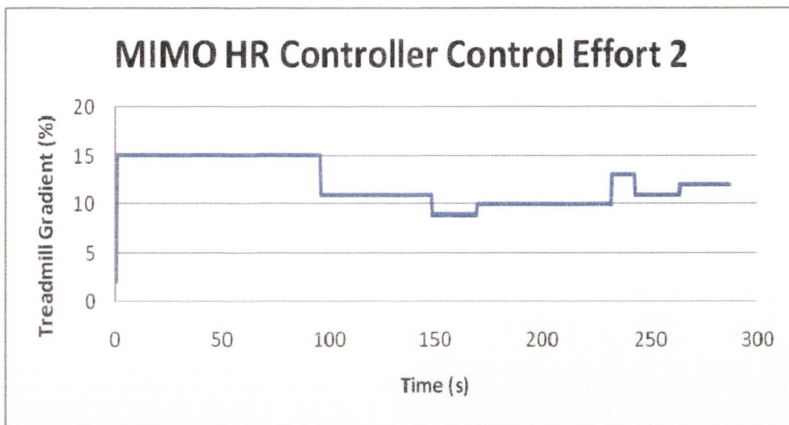


Figure 8.8 MIMO control test 2 - HR controller control effort

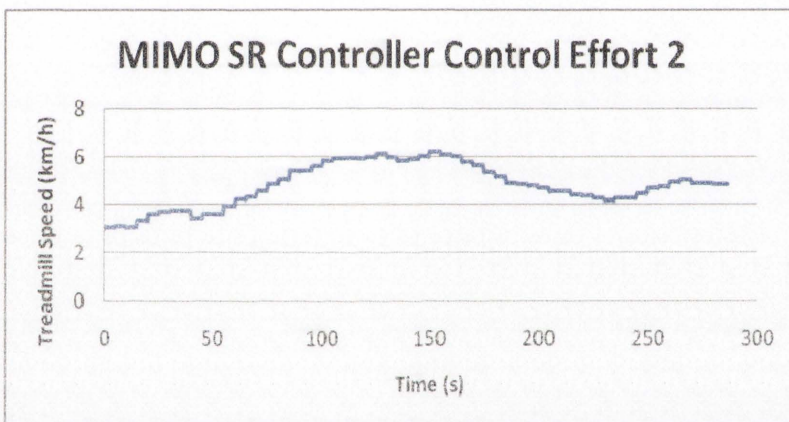


Figure 8.9 MIMO control test 2 - SR controller control effort

8.4. Summary

From the closed-loop response, it can be observed that the MIMO controller is able to maintain both HR and SR close to the reference value of 160. The HR controller responds faster than in test 1, with rise time and 5% settling time occurring earlier. There is also an

improvement in overshoot, but there is an increase in steady state error. The steady state value of HR is maintained at approximately 151 BPM.

Changes are also observed in the SR controller response. The rise time and 5% settling time have increased due to initial oscillation. Once SR does settle, it is controlled at the reference value reasonably well. As well as this, the overshoot and steady state error are fairly similar to that of test 1. The main improvement in test 2 is that the control effort of the SR controller does not saturate. The control effort, initially, increases slowly to 6km/h and varies slowly to control SR at steady state.

As mentioned previously, the main improvement in the MIMO controller is that the SR controller does not saturate. Despite this, the HR controller still saturates immediately during testing. Lower values of K_p and K_i in the second experiment were used in the controller where the control effort did not saturate. However it was found that this resulted in the controller being less responsive, reacting only when a large error was detected or after a substantial period of time.

In conclusion, both MIMO tests produced reasonable closed loop responses. Both controllers were able to eventually control HR and SR close to the reference value after a reasonable period of time. The main issue in test 1 was that the control efforts saturate immediately. As for test 2, steady state error increased as compared to test 1. As well as this, the HR controller settles before the SR controller. Even though the controller produced an acceptable performance in our current experiment, the concept is still in its infancy and improvements still need to be made.

Chapter 9

Conclusions and future work

This thesis investigates exercise intensity regulation for treadmill exercises. An automated treadmill system has been developed, which includes wireless portable ECG and TA sensors and a Labview based control module. Based on this automated system, efficient rate detection techniques have been developed by using the pitch estimation method. Several multi-loop integral control configurations have been proposed and implemented to regulate the HR and/or SR by manipulating treadmill speed and/or gradient. These control structures have been put into real time testing which includes SISO, MISO and MIMO control by using the established Labview module.

9.1. Conclusions

Firstly, this study developed efficient rate detection approaches for HR and SR based on pitch estimation method (Chapter 3, section 4). It is found that the re-usage or combination of ACF and AMDF are very effective for SR signals. Experimental results have shown that square ACF obtains a better result in contrast with AMDF, simple ACF and their combination. Simulation and experiments also show that the differential type algorithm is suitable for HR signal pre-processing. Furthermore, a real-time square wave matching method is developed to detect the rate of pre-processed signals. A SR sensor is implemented to extracted accelerometer data and calculated the amount of steps the exerciser takes per minute. An accuracy test is conducted to minimise the errors from the three pedometers.

Secondly, a HR detector is implemented in Labview by using the Pan - Tompkins QRS detection technique (Chapter 4). The HR sensor analyses the incoming ECG signal, filters the ECG signal and calculate the number of heart beats. A median average filter is used to smooth the output of the instantaneous HR values in order to provide with more stable HR information.

Thirdly, based on Ziegler-Nichols tuning method, the initial PID gain coefficients K_p and K_i values are obtained. By adopting the K_p and K_i values in the closed loop control experiment, four SISO control tests (Chapter 5) are designed and implemented for this study. They have been shown to be efficient in regulating both the HR and SR of an exerciser on the treadmill.

Finally, multivariable control such as that of a MISO controller (Chapter 6) and MIMO controller (Chapter 8) are implemented. The results have shown that the designed integral type controllers are able to automatically manipulate the treadmill's speed and gradient simultaneously to control HR and/or SR at the reference levels.

In order to ensure zero offset tracking errors under faulty conditions, this study extended the concept of the nonlinear Decentralized Integral Controllability (DIC) to the multiple input single output (MISO) nonlinear process, and presented a sufficient condition which only needs to check the steady state input-output relationship of under controlled processes. Based on the proposed condition, we investigate the new defined Multi-loop Integral Controllability (MIC) for walking, running, and walking/running transition zones (Chapter 7).

The MISO control system developed in this study can be implemented into the training program as the foundation for a regulated exercise (Chapter 6, section 4). This allows individuals to exercise at different levels such as promoting cardiovascular fitness by monitoring their HR and SR.

9.2. Direction for future research

The multivariable controllers developed in Labview for this study are robust and capable of efficiently manipulating the HR and SR of an exerciser to pre-set target values. However, for the entire concept of developing the multivariable controller to be complete, it requires further development in the following areas:

1. Further experimentation is required to better understand the SR and develop a more precise SR detection algorithm.
2. The Labview program could be improved by designing two profiles to gradually increase the HR and walking pace of the exerciser to the target level and then decrease the HR and walking pace towards the end of the exercise session.

3. The MIMO controller response should be improved so the control effort will not saturate casually. A better control model needs to be developed to make the whole system more stable.
4. The controller should be tested on individuals that have cardiovascular diseases and medical patients recovering from cardiovascular surgery, to assess its effectiveness in rehabilitation.
5. For the control zone, the sport athlete will be invited to test the maximum effort zone. Thus, more specific testings need to be conducted in different exercise zones. These test results need to be further analysed to achieve better outcome.

Bibliography

- ACSM (American College of Sports Medicine), 2000, ACSM. Position stand, physical activity, physical fitness, and hypertension, *Med Sci Sports Exerc*, vol. 25, no. 10, pp. i - x.
- Alive ECG user manual, 2006, Alive Technologies Pty Ltd.
- Ang, K. H., Chong, G. and Li, Y., 2005, PID control system analysis, design, and technology, *IEEE Transactions on Control Systems Technology*, vol. 13, pp. 559 - 576.
- Anonim, 2000, Describing the sequence of events in one heart beat ,
URL: <http://www.elliott-school.org.uk/departments/science/AS%20Biology/The%20cardiac%20cycle.ppt>, access by Feb 2010.
- Asano, Masakazu, Tanabe, Y., Watanabe, K., Genno, H., Nemoto, K., Nose, H. and Isawa M., 2005, Development of an Exercise Meter using Triaxial Acceleration, *International Conference of IEEE Engineering in Medicine and Biology Society*, vol. 4, pp. 3731 - 3734.
- Astrand, P. O., Cuddy, T. E., Saltin, B. and Stenberg, J., 1964, Cardiac output during submaximal and maximal work, *J. Appl. Physiol*, vol. 19, pp. 268 - 274.
- Astrom, K.J. and Hagglund, T., 1934, *PID controllers: Theory, Design, and Tuning*, Instrument Society of America, pp. 1 - 30.
- Bernotas, L., Crago, P., and Chizeck, H., 1986, "A discrete-time model of electrically stimulated muscle, *IEEE Trans. Biomed. Eng.* vol. 1, pp. 829–838.
- Borresen, J., Lambert, M., 2008, Autonomic Control of Heart Rate during and after Exercise Training Status, *Sports Medicine*, vol 38, pp 633 - 646.

- Bouchard, C. and Katzmarzyk, P. T., 1994, Physical activity and obesity, *Obesity reviews* an official journal of the International Association for the Study of Obesity, vol. 151 pp. 1732 - 1733.
- Campo, P. and Morari, M., 1994, Achievable closed-loop properties of systems under decentralized control: conditions involving the steady state gain, *IEEE transactions and automatic control*, vol. 5, pp. 932 - 943.
- Cappellini, R., Ivanenko, Y., Poppele, R. and Lacquaniti, F., 2006, Motor patterns in human walking and running, *Journal of Neurophysiology*, vol. 95, pp. 3426 - 3437.
- Chen, Mingqi, Lubecke, O. B., Lubecke, V. and Wang, X., 2005, Analog signal processing for heart rate extraction, *International Conference of IEEE Engineering in Medicine and Biology Society*, vol. 6, pp 6671-6674.
- Cheng, Teddy M, Savkin, A.V., Su, S., Celler, B. G. and Wang, L., 2008, A robust control design for heart rate tracking during exercise, *Conference Proceedings of the International Conference of IEEE Engineering in Medicine and Biology Society*, vol. 2008, pp. 2785 - 2788.
- Cheng, Teddy M, Savkin, A. V., Celler, B. G., Su, S. and Wang, L., 2008, Nonlinear modeling and control of human heart rate response during exercise with various work load intensities, *IEEE transactions on Biomedical engineering*, vol. 55, pp. 2499 - 2508.
- Clifford, G.D., Azuaje, F., McSharry, P., 2006, *Advanced Methods And Tools for ECG Data Analysis*, *Artech House Publishers*. pp. 11 - 14.
- Currie, G., Rafferty, D., Duncan, G., Bell, F. and Evans, A. L, 1992, Measurement of gait by accelerometer and walkway: A comparison study, *Med. Biol. Eng. Comput.*, vol. 30, pp. 669 - 670.
- Denniston, J. C., Maher, J. T., Reeves, J. T., Cruz, J. C., Cymerman, A. and Grover, R.F., 1976, Measurement of cardiac output by electrical impedance at rest and during exercise, *J. Appl. Physiol*, vol. 40, no. 1, pp. 91 - 95.

- Elia, M., Livesey, G., 1988, Theory and validity of indirect calorimetry during net lipid synthesis, *Am J Clin Nutr* ., vol. 47, no. 4, pp. 591 - 607.
- Eskinat, E., Johnson, S. and Luyben, W., 1991, Use of Hammerstein models in identification of nonlinear systems, *AIChE Journal*, vol. 37, pp. 255 - 268.
- Franklin, B.A., Bonzheim, K., Gordon, S., Timmis, G.C., 1998, 'Rehabilitation of cardiac patients in the the twenty-first century: Changing paradigms and perceptions', *Sports Sciences*, vol. 16, no. pp. 57 - 67.
- Freedman, M. E., Snider, G. L., Brostoff, P., Kimelblot, S., and Katz, L. N., 1955, Effects of training on response of cardiac output to muscular exercise in athletes, *J. Appl. Physiol*, vol. 8, no. 1, pp. 37-47.
- Gilman, M.B., 1996, The use of heart rate to monitor the intensity of endurance training, *International Journals of Sports Medicine* 21, vol. 2, pp. 73 - 79.
- Gilman, M.B. and Wells, C.L., 1993, The use of heart rate to monitor exercise intensity in relation to metabolic variables, *International Journals of Sports Medicine*, vol. 14, pp. 339 - 344.
- Harrison, Sandi, 2011, The first heart rate monitor invented,
URL:<http://www.livestrong.com/article/396827-the-first-heart-rate-monitor-invented/> accessed October 2011.
- Healthy People 2020, Physical Activity,
URL:<http://www.healthypeople.gov/2020/topicsobjectives2020/overview.aspx?topicid=33>, accessed October 2011.
- Heart Information Centre (HIC), 2011, Activity, Texas Heart Institute,
URL: <http://www.texasheartinstitute.org/HIC/anatomy/Anatomy.cfm>, access by October 2011.
- Hernandez, Oscar and Olvera, Edgar, 2009, Noise cancellation on ECG and heart rate signal using the undecimated wavelet transform, *International Conference on eHealth, Telemedicine and Social Medicine* pp. 142 - 150.

- Hiatt, W.R., Wolfel, E.E., Meier, R.H. and Regensteiner, J.G., 1994, Superiority of treadmill walking exercise versus strength training for patients with peripheral arterial disease, *Circulation*, vol. 90, pp. 1866 - 1874.
- Hui, L., Dai, B. and Wei, L., 2006, A pitch detection algorithm based on AMDF and ACF, MOE-Microsoft Key Laboratory of Multimedia Computing and Communication, vol. 1, pp. 377 - 380.
- Hu, F.B., Sigal, R.J., Rich-Edwards, J.W., et al, 2002, Walking compared with vigorous physical activity and risk of type 2 diabetes in women: a prospective study, *JAMA*. pp 282:1433-9
- Hunt, K. J., 2008, Treadmill Control Protocols for Arbitrary Work Rate Profiles Combining Simultaneous Nonlinear Changes in Speed and Angle, *Biomedical signal processing and control*, vol. 3, pp. 278 - 282.
- Holt, K.G., Hamill, J., Derrick, T.R., 1995, Shock attenuation and stride frequency during running, *Human Movement Science* vol. 14, pp. 45-60.
- Ibrahimi, Muhammed I, Mohd, M., Zahedi, E. and Tsuruoka, S., 2002, A comparison of abdominal ECG and Doppler ultrasound for fetal heart rate detection, *international journal of the Japan society of medical electronics and biological Engineering*, vol. 11, pp. 307 - 322.
- Imai, K., Sato, H., Hori, M., Kusuoka, H., Ozaki, H. and Yokoyama, H., et al., 1994, Vagally mediated heart rate recovery after exercise is accelerated in athletes but blunted in patients with chronic heart failure, *J Am Coll Cardiol.*, vol. 24, pp. 1529 - 1535
- Jamieson, L.P., Hunt, K.J. and Allan, D. B., 2007, A treadmill control protocol combining nonlinear, equally smooth increases in speed and gradient, *Med. Eng. Phys.* vol 2, pp. 221 - 225.
- Jeukendrup, A., Van Diemen, A., 1998, 'Heart rate monitoring during training and competition in cyclists', *Sports Sciences*, vol. 16, no. pp. 91 - 99.

- Jones, Shirley A., 2007, ECG success: exercises in ECG interpretation, © 2008 by F.A. Davis Company, pp. 13 - 28.
- Kahng, H. D. and Bae, K. S., 1994, Signal channel adaptive noise cancelation for enhancing noisy speech, International Symposium on Speech, Image Processing and Neural Network, vol. 3, pp. 1365 - 1340.
- King, C.N. and Mark, D.S., 1996, Exercise testing and prescription, Sports Medicine 21, vol. 5, pp. 326-336.
- Knobloch, K., Lichtenberg, A., Winterhalter, M., Rossner, D., Pichlmaier, M. and Philips, R., 2005, Non-invasive cardiac output determination by two-dimensional independent Doppler during and after cardiac surgery, *Ann Thorac Surg*, vol. 80, no. 4, pp. 1479 - 1483.
- Kraus, William E. and Keteyian, S.J., 2007, Cadiac rehabilitation, Copyright © 2007, Humana Press Inc, pp 225 - 228.
- Kumar, A., Dewan, L. and Singh, M., 2006, Real time monitoring system for ECG signal using virtual instrumentation, Wseas International conference on Biology and Biomedicine, vol. 3, pp. 142 - 146.
- Lambert, M.I, Mbambo, Z.H. and Gibson, A.C., 1998, Heart rate during training and competition for long-distance running, Sports Sciences, vol. 16, pp. 85 - 90.
- Lubans, D.R., Morgan, P. J., Collins, C.E., Boreham, C.A. and Calliste, R., 2009, The relationship between heart rate intensity and pedometer step counts in adolescents, Journal of Sports Sciences, vol. 27, pp. 591 - 597.
- Magosso, E. and Ursino, M., 2002, Cardiovascular response to dynamic aerobic exercise: a mathematical model. *Medical & Biological Engineering & Computing*, vol. 40, no. 6, pp. 660 - 674.
- Mary, Yamin-Garone, 2011, The most accurate heart rate monitors,
URL: <http://www.livestrong.com/article/392070-the-most-accurate-heart-rate-monitors/> accessed October 2011.

- Mathers, C., Vos, T. and Stevenson, C., 1999, The burden of disease and injury in Australia, © Australian Institute of Health and Welfare 1999, pp. 124 - 129.
- Mazenc, F., Malisoff, M., Querioz, M., 2011, Tracking control and robustness analysis for a nonlinear model of human heart rate during exercise, *Automatica*, pp. 968 -974.
- Mcgill, 2000, The EKG Waveform, Copyright © 1997-9 Molson Medical Informatics Project, URL: <http://sprojects.mmi.mcgill.ca/cardiophysio/NormalEKG.htm>, access by Dec 2010.
- Montoye, H.J., Washburn, R., Servais, S., Ertl, A., Webster, J.G. and Nagle, F. J., 1983, FA02-6, Estimation of energy expenditure by a portable accelerometer, *Medicine and Science in Sports and Exercise.*, vol. 15, no. 5, pp. 403 - 407.
- National Institute of Diabetes and Digestive and Kidney Diseases (NIDDK), 2010, Physical Activity and Weight Control, URL: <http://www.healthieryou.com/physact.html> accessed October 2011.
- Pan, Jiapu and Tompkins, W., 1985, A real-time QRS detection algorithm, *IEEE transactions on Biomedical Engineering*, vol. 32, pp. 230 - 236.
- Pavlatos, C., Dimopoulos, A., Manis, G. and Papakonstantinou, G., 2003, Hardware are implementation of pan & tompkins QRS detection algorithm, *International Conference of IEEE Engineering in Medicine and Biology Society*, vol. 2003, pp. 112 - 116.
- Popov, B., Sierra, G., Telfort, V., Agarwal, R., Lanzo, V., 2005, Estimation of respiratory rate and heart rate during treadmill tests using acoustic sensor, the *International Conference of IEEE Engineering in Medicine and Biology Society*, vol. 6, pp 5884-5887.
- Porszasz, J., Casaburi, R., Somfay, A., Woodhouse, L. and Whipp, B. J., 2003, A treadmill ramp protocol using simultaneous changes in speed and gradient, *Medicine & Science in Sports & Exercise*, vol. 35, pp. 1596 - 1603.

Rogers, C. D., 2011, The accuracy of treadmill heart rate monitors,

URL:<http://www.livestrong.com/article/329706-the-accuracy-of-treadmill-heart-rate-monitors/> accessed October 2011.

Rose, Lynne Haley, 2011, Treadmill & Heart rate,

URL: <http://www.livestrong.com/article/452994-treadmill-heart-rate/> accessed October 2011.

Saito, H. and Togawa, T., 1991, Treadmill control to regulate heart rate for exercise test, Rep. Inst. Med. Dent. Eng, vol. 25, pp. 65 - 72.

Saito, H. and Togawa, T., 1992, Treadmill control to realize linear increase of heart rate for exercise test, Rep. Inst. Med. Dent. Eng, vol. 26, pp. 63 - 68.

Saito, H. and Togawa, T., 1998, Open-loop control to achieve linear heart rate increase in the treadmill exercise test, Engineering in Medicine and Biology Society, vol. 5, pp. 2442-2443.

Sepulchre, R., Jankovic, M. and Kokotovic, P., 1996, Constructive Nonlinear Control, New York: Springer Verlag.

Skarlas, L. V., Beligiannis, G. N., Georgopoulos, E. F. and Adamopoulos, A. V., 2005, Intelligent modeling of the electrical activity of the human heart, International Journal of Signal processing, vol. 33, pp. 197 - 202. Skogestad, S., Morari, M., 1988, Variable selection for decentralized control, AIChE Annual Meeting, vol. 13, pp. 113 - 125.

Skogestad, S S. and Morari M., 1992, Variable selection for decentralized control, Modeling, Identification and Control, vol. 13, no. 2, pp. 113 - 125.

Stannard, S., and Thompson, M., 1998, Heart rate monitors: Coaches' friend or foe, Sports Coach, vol. 21, pp. 36 - 37.

- Stewart, S., Tikellis, G., Carrington, M., Walker, K. and O'Dea, K. 2008, Australia's Future Fat Bomb: A report on the long-term consequences of Australia's expanding waistline on cardiovascular disease. Preventive Cardiology at the Baker Heart Research Institute, pp. 6 - 27.
- Su, Steven, 2004, Analysis of decentralized integral controllability for nonlinear systems, *Computers & Chemical Engineering*, vol. 28, pp. 178 - 1787.
- Su, Steven, Wang, L., Celler, B. G., Ambikairajah, E. and Savkin, A., 2005, Estimation of walking energy expenditure by using support vector regression, *International Conference of IEEE Engineering in Medicine and Biology Society*, vol. 4, pp. 3526 - 3529.
- Su, Steven, Wang, L., Celler, B. G., Savkin, A. and Guo, Y., 2006, Modelling and Control for Heart Rate Regulation during Treadmill Exercise, *IEEE, EMBS Annual International Conference*, New York City vol. 1, pp. 4299 - 4302.
- Su, Steven, Wang, L., Celler, B. G., Savkin, A. and Guo, Y., 2007, Identification and Control for Heart Rate Regulation During Treadmill Exercise, *IEEE Transactions on Biomedical Engineering* vol. 54, pp. 1238 - 1246.
- Su, Steven W, Huang, S., Wang, L., Celler, B. G., Savkin, A. V., Guo, Y. and Cheng, T., 2007, Nonparametric Hammerstein model based model predictive control for heart rate regulation, *International Conference of IEEE Engineering in Medicine and Biology Society*, vol 2007, pp 2984 - 2987.
- Su, Steven W, Celler, B., Savkin, A., Nguyen, H., Cheng, T., Guo, Y. and Wang, L., 2009, Transient and steady state estimation of human oxygen uptake based on noninvasive portable sensor measurements, *Medical and Biological Engineering and Computing*, vol. 47, no. 10, pp. 1111 - 1117.
- Su, Steven, Huang, S., Wang, L., Celler, B. G., Savkin, A.V., Guo, Y. and Cheng, T.M. 2010, Optimizing heart rate regulation for safe exercise, *Ann. Biomed. Eng.*, vol. 38, pp. 758 - 768.

- Tan, L. and Karnjanadecha, M., 2003, Pitch Detection Algorithm: Autocorrelation Method and AMDF, the 3rd International Symposium on Communications and Information Technology, vol. 2, pp. 551 - 556.
- Tanasescu, M., Leitzmann, M.F., Rimm, E.B., Willett, W.C., Stampfer, M.J. and Hu, F.B., 2002, Exercise type and intensity in relation to coronary heart disease in men, JAMA, vol. 16, pp. 1994 - 2000.
- Thadani, U. and Parker, J. O, 1978, Hemodynamics at rest and during supine and sitting bicycle exercise in normal subjects, Am. J. Cardiol, vol. 41, no. 1, pp. 52 - 59.
- Uduehi, D., Ordys, A. and Grimble, M. J, 2002, Multivariable PID controller design using online generalised predictive control optimisation, the 2002 IEEE International conference on Control Applications, vol. 2, pp. 213 - 217.
- Vehkaoja, A., Verho, J., Comert, A., Aydogan, B., Perhonen, M., Lekkala, J. and Jalttunen, J., 2008, System for ECG and heart rate monitoring during group training, the International Conference of IEEE Engineering in Medicine and Biology Society, vol. 2008, pp. 4832 - 4835.
- Weng, K., Turk, B., Dolores, L., Nguyen, T. N., Celler, B. G., Su, S.W. and Nguyen, H. T., 2010, Fast tracking of a given heart rate profile in treadmill exercise, Engineering in Medicine and Biology Society, vol. 25, pp. 69 - 72.
- Yu, C. and Fan, M., 1990, Decentralized integral controllability d-stability, Chemical engineering science, vol. i, pp. 3299 - 3309.